Université Mohamed Boudiaf - M'sila

FACULTE DE TECHNOLOGIE

DEPARTEMENT DE GENIE ELECTRIQUE

Numéro de série : ……

Numéro d'inscription : …….

Thèse

Présentée pour l'obtention du diplôme de

DOCTORAT TROISIEME CYCLE

Filière : Electrotechnique
Spécialité : Réseaux Electriques

THEME

Contribution à l'étude du comportement des isolateurs de haute tension pollués par différentes méthodes

Présenté par

Oussama GHERMOUL

Soutenue le : 07/03/2024

Devant le jury composé de :

Nom & Prénom	Grade	Etablissement	Qualité
CHOUDER Aissa	Professeur	Université de M'sila	Président
BENGUESMIA Hani	Maitre de conférences 'A'	Université de M'sila	Encadreur
BENYETTOU Loutfi	Professeur	Université de M'sila	Co-encadreur
BELHOUCHET Khaled	Maitre de conférences 'A'	Université de M'sila	Examinateur
M'ZIOU Nassima	Professeur	Université de Boumerdès	Examinateur
MOKHNACHE Leïla	Professeur	ENS des Energies Renouvelables, de l'Environnement et du Développement Durable de Batna	Examinateur

Année universitaire: 2023/2024

University of Mohamed Boudiaf - M'sila

FACULTY OF TECHNOLOGY

DEPARTEMENT OF ELECTRICAL ENGINEERING

Serial number : ……

Registration number : …….

Thesis

Presented for obtaining the diploma of

THIRD CYCLE DOCTORATE

Sector: Electrotechnics
Specialty: Electrical Networks

THEME

Contribution to the study of the behavior of high voltage polluted insulators by different methods

Presented by

Oussama GHERMOUL

Defended on : 07/03/2024

Before the jury composed of :

Last & first names	Grade	Establishment	Quality
CHOUDER Aissa	Professor	University of M’sila	President
BENGUESMIA Hani	Associate Professor 'A'	University of M’sila	Superviser
BENYETTOU Loutfi	Professor	University of M’sila	Co-superviser
BELHOUCHET Khaled	Associate Professor 'A'	University of M’sila	Examiner
M’ZIOU Nassima	Professor	University of Boumerdes	Examiner
MOKHNACHE Leïla	Professor	HNS of Renewable Energies, Environment & Sustainable Development of Batna	Examiner

University year: 2023/2024

Acknowledgment

In the first place, we thank God Allah, who gave us the courage, patience, strength and serenity and the will to do this modest work during all these years of study.

The success of any project depends largely on the encouragement and guidelines of many others. We take this opportunity to express our gratitude to the people who have been instrumental in the successful completion of this project.

In the second place, I would like to express my profound appreciation to my main advisor, Dr. Hani Benguesmia, for his tremendous help, knowledgeable counsel, and consistent commitment during the whole study process.

Dr. Benguesmia's vast experience and dedication to my academic development have greatly influenced the direction my thesis has taken. His support and guidance have had a genuine, long-lasting influence. Additionally, I would like to express my gratitude to my co-advisor, Dr. Loutfi Benyettou, for his invaluable assistance with this study. The advice and ideas from

Dr. Benyettou have been much valued.

Every advisor has contributed a distinct viewpoint to our project, and I am appreciative of the chance to gain from their combined experience.

I extend my sincere appreciation to Dr. Aissa Chouder, the President of the jury from the university of M'sila, Dr. Leila Mokhneche from the Higher National School of Renewable Energies, Environment & Sustainable Development, Dr. Nassima M'ziou from the University of Boumerdes and Dr. Khaled Belhouchet from the University of M'sila, for kindly supervising and directing this thesis's review process. Their contribution to maintaining the academic integrity and caliber of this work is much appreciated.

Dedications

To my dearest Father,

Your unwavering support, wisdom, and love have been my guiding light throughout my life's journey. I dedicate my achievements to you and hope to continue making you proud.

To my beloved Mother,

Your kindness, strength, and boundless love have been my constant inspiration. My journey would have been incomplete without your love and guidance. I dedicate my success to you.

To my cherished Family,

You have been my rock, my joy, and my source of endless encouragement. I dedicate my accomplishments to our shared dreams and the values you have instilled in me.

To my treasured Friends,

Your laughter, your presence, and your unwavering friendship have added immeasurable richness to my life. I dedicate my achievements to the bonds we have nurtured.

To Akram Kadjadja and Moulay Abdessalam,

Your support has meant the world to me, and I dedicate my success to our friendship.

With love and gratitude,

Ghermoul Oussama

ملخص

عوازل الجهد العالي هي أجزاء أساسية من النقل الكهربائي التي توفر إمدادات ثابتة من الطاقة. توفر هذه الأجزاء الحيوية وظائف مزدوجة تتمثل في الدعم الميكانيكي لمكونات الجهد العالي وتوفير العزل الكهربائي المهم. تواجه العوازل مجموعة متنوعة من الصعوبات، حيث تشكل الومضات الكهربائية المرتبطة بالتلوث مصدر قلق كبير. في المقام الأول مسافة التسرب هي ما يميز كل سلسلة عازل من بين عوامل أخرى. تتأثر هذه المسافة بمستوى الجهد المستخدم. في مجملها، تركز هذه الأطروحة على الإجهاد الكهربائي على العوازل و تستخدم هذه الأطروحة ثلاث طرق مختلفة لمحاولة تعزيز فهم العوازل بالإضافة إلى عمل نموذج تنبؤي لجهد وميض العازل L1512. نحن نستفيد من استخدام عمليات المحاكاة، ونستخدم COMSOL Multiphysics للاستفادة الكاملة من عمليات المحاكاة ثنائية وثلاثية الأبعاد. هذا لمعرفة توزيعات الإمكانات الكهربائية والمجال الكهربائي داخل وحول سلسلة العازل L1512 التي تتكون من 1 إلى 5 سلاسل عازلة للمحاكاة ثنائية الأبعاد و10 سلسلة عوازل للمحاكاة ثلاثية الأبعاد. يهدف هذا إلى تحسين تصميم العوازل بالإضافة إلى تقديم اقتراح حول المكان الذي يجب أن يوضع فيه العازل. بعد ذلك تم استخدام منهجية سطح الاستجابة (RSM) لبناء نموذج موثوق للتنبؤ بجهد الوميض، والذي تم تصميمه خصيصًا للعازل L1512. يركز النهج الذي نستخدمه على التصميم المركب المركزي الذي يأخذ مستويات التوصيل والتلوث كعوامل ويتم عمل نموذجين. الأول ينتج نتائج جيدة باتباع منهجية رياضية تقليدية. يؤكد النموذج الثاني على إمكانيات RSM في هذه الحالة بشكل أكبر من خلال تصميم مخصص. يوضح هذا النهج المنهجي أنه أداة موثوقة للمهندسين، مما يوفر التوازن بين احتياجات البيانات ودقة النموذج. وأخيرًا، تم تسليط الضوء على استخدام الشبكات العصبية الاصطناعية (ANNs) في الفصل الأخير. تم تصنيع هذه الشبكات باستخدام MATLAB للتنبؤ بجهد الوميض للعازل L1512.

الكلمات المفتاحية: عازل، التلوث، المجال الكهربائي، الجهد الكهربائي، العنصر المحدود، RSM ، ANN ،

Abstract

High voltage insulators are essential parts of electrical transmission that provide a steady supply of power. These vital parts provide double functions of mechanically supporting high voltage components and supplying crucial electrical insulation. Insulators encounter a variety of difficulties, with pollution-related flashovers being a major worry. Primarily the leaking distance is what distinguishes each insulator chain among other factors. This distance is influenced by the voltage level being used. In its entirety, this thesis focuses on the electric stress on insulators and uses three different methods to try to enhance the understanding of the insulators as well as making a prediction model for the 1512L insulator flashover voltage. We take advantage of the use of simulations, employing COMSOL Multiphysics to fully utilize two and three dimensional simulations. This is to see the distributions of the electric potential and electric field within and around the 1512L insulator chain consisting of 1 to 5 insulator chains for the 2D simulation and 10 insulators chain for the 3D simulation. This is made more towards the enhancement of the insulators design as well as give a suggestion of where the region the insulator should be placed. After that the response surface methodology (RSM) was used to build a reliable flashover voltage prediction model that is tailored for the 1512L insulator. The approach we employ focuses on a central composite design that takes conductivity and pollution levels as factors and two models are made. The first produces good results by following a conventional mathematical methodology. The second model emphasizes the possibilities of RSM in this situation even more through a customized design. This methodical approach demonstrates to be a reliable tool for engineers, providing a balance between data needs and model accuracy. Lastly usage of artificial neural networks (ANNs) is highlighted in the final chapter. These networks are made using MATLAB for predicting the flashover voltage of the 1512L insulator.

Keywords: Insulator, Pollution, Electric field, Electrical potential, Finite Element, RSM, ANN,

Résumé

Les isolateurs haute tension sont des éléments essentiels de la transmission électrique qui fournissent une alimentation électrique constante. Ces pièces vitales assurent une double fonction de support mécanique des composants haute tension et de fourniture d'une isolation électrique cruciale. Les calorifugeurs rencontrent diverses difficultés, les contournements liés à la pollution constituant une préoccupation majeure. C'est principalement la distance de fuite qui distingue chaque chaîne d'isolateurs, entre autres facteurs. Cette distance est influencée par le niveau de tension utilisé. Dans son intégralité, cette thèse se concentre sur la contrainte électrique sur les isolateurs et utilise trois méthodes différentes pour tenter d'améliorer la compréhension des isolateurs ainsi que pour créer un modèle de prédiction de la tension de contournement de l'isolateur 1512L. Nous profitons de l'utilisation de simulations, en utilisant COMSOL Multiphysics pour utiliser pleinement les simulations bidimensionnelles et tridimensionnelles. Il s'agit de voir les distributions du potentiel électrique et du champ électrique à l'intérieur et autour de la chaîne d'isolateurs 1512L composée de 1 à 5 chaînes d'isolateurs pour la simulation 2D et de 10 chaînes d'isolateurs pour la simulation 3D. Ceci vise davantage à améliorer la conception des isolateurs et à donner une suggestion sur l'endroit où l'isolant doit être placé. Ensuite, la méthodologie de surface de réponse (RSM) a été utilisée pour créer un modèle de prédiction de tension de contournement fiable, adapté à l'isolateur 1512L. L'approche que nous utilisons se concentre sur une conception composite centrale qui prend la conductivité et les niveaux de pollution comme facteurs et deux modèles sont créés. Le premier produit de bons résultats en suivant une méthodologie mathématique conventionnelle. Le deuxième modèle souligne encore davantage les possibilités du RSM dans cette situation grâce à une conception personnalisée. Cette approche méthodique se révèle être un outil fiable pour les ingénieurs, offrant un équilibre entre les besoins en données et la précision du modèle. Enfin, l'utilisation des réseaux de neurones artificiels (ANN) est mise en évidence dans le dernier chapitre. Ces réseaux sont réalisés à l'aide de MATLAB pour prédire la tension de contournement de l'isolant 1512L.

Mots clés: Isolant, Pollution, Champ électrique, Potentiel électrique, Éléments Finis, RSM, ANN,

List of Abbreviations and Symbols

List of abbreviations and symbols

L	Level of pollution
σ	Conductivity (mS/cm2)
FEM	Finite Element Method
DC	Direct current
V	Electric potential
E	Electric field
ε	Absolute permittivity
ε_0	Permittivity of free space
ε_r	Relative permittivity
ρ	The charge density
D	Displacement vector
DOE	Design of Experiments
RSM	Response surface methodology
CCD	Central Composite Design
CCC	Central Composite Circumscribed
CCI	Central Composite Inscribed
CCF	Central Composite Face centered
BBD	Box-behnken Design
k	Number of factors
ANOVA	Analysis Of Variance
R^2	The coefficient of determination
S	The residuals standard deviation
SS_{Error}	The sum of squares of the error
SS_{Total}	The total sum of squares
U_p	The predicted flashover voltage
V_{L-L}	Line voltage

C	Voltage supported by one insulator
ANN	Artificial Neural Network
FNN	Feedforward Neural Network
RNN	Recurrent Neural Networks
CNN	Convolutional Neural Networks
ReLU	Rectified Linear Unit function
MAE	Mean absolute error
MSE	Mean squared error
R	The coefficient of correlation

List of figures and tables

List of Figures & tables

List of tables

Table of Contents

Table of Contents

Chapter IV: Artificial Neural Network

GENERALE INTRODUCTION

General introduction

In high-voltage overhead electrical energy transmission networks, insulators play a crucial role. These parts maintain the system mechanically and provide crucial electrical insulation, ensuring the steady flow of electrical energy.

The performance and weather resistance of insulators have been improved over time through manufacturing innovations. Insulators are essential to preserving a consistent energy supply because disruptions are a big worry. They play a crucial part in establishing electrical insulation between grounded and high voltage components, which highlights their importance for the dependability of the electrical energy transmission system [1].

Additionally, the high-voltage overhead wires, which traverse a variety of areas and climates and carry electrical energy, expose these systems to a number of challenges, most notably the problem of insulator pollution. Pollution on insulators poses a serious risk to both the reliability and quality of energy, thus it must be carefully taken into account while designing and sizing transportation networks. The buildup of pollutants, whether they come from industrial, urban, coastal, or desert sources, can impair the effectiveness of insulation and raise the possibility of electrical system disturbances. All things considered, insulators are crucial to the efficiency and dependability of high-voltage transmission lines [2].

The many types of pollution are significantly influenced by the location of electrical installations. Dry contaminants typically cause few problems. However, these deposits become conductive when they come into contact with moisture, allowing leakage currents to flow and causing the localized drying of pollution layers [3]–[5]. Local arcs may start because of this change that causes the change potential distribution. Depending on the electrical circumstances, the effects of these discharges might range from surface degradation to insulator flashover, causing short circuits and electrical disruptions [6].

Numerous management techniques are used to fight the negative impacts of pollution, including washing of insulators and applying hydrophobic coatings. Although these maintenance activities are efficient, they are expensive and logistically difficult.

In this context, various mathematical flashover models have been developed [7], [8]. Most of these models are based on the simple Obenaus model, which consists of putting in series with an

arc of length ‘x’ a resistor, which simulates the pollution layer. However, the mathematical treatment of these different models requires the use of simplifying hypotheses: one-dimensional geometry, uniform resistivity, for example...etc. They therefore only allow us to identify the broad outlines of the behavior of insulators under pollution. When it comes to evaluating the performance of different insulators, it is essential to carry out tests.

This thesis inevitably begins with an in-depth review of high voltage insulators, an essential part of electrical power systems, with a focus on how well they operate in harsh environments. In order to comprehend the significance of high voltage insulators in the area of power transmission, we carefully review the prior research at the outset of this academic investigation. In this procedure, we examine several insulator types and forms and the challenges they face. Pollution, which comes in a variety of forms and has a considerable impact on how well insulators function, is one of the main challenges. This information serves as a strong foundation for the chapters that follow, in which we explain how insulators are essential for preserving the stability of power systems.

Next, we enter the field of computer simulations, where we will create a simulated testing environment to investigate the behavior of insulators using the capabilities of COMSOL Multiphysics. We investigate scenarios in two and three dimensions, concentrating especially on the electrostatic components.

This makes it easier for us to picture how the electric potential and electric field distributed throughout the surface of the insulator. Here, we try to understand the behavior of insulators in various settings. This should assist in the improvement of the design of the insulator and helps in the identification the conditions that the insulator performs best under.

The thesis then shifts to a more mathematical discourse and explores the Response Surface Methodology (RSM) especially the Central Composite Design (CCD) . Our focus is specifically on the 1512L insulator, which is widely used in Algeria's desert regions. An accurate prediction of flashover voltage is the main goal. The result of this research is the development of a mathematical model specifically designed for the precise prediction of flashover voltage, improving prediction accuracy by effectively utilizing CCD techniques.

In last chapter, we explore the field of artificial intelligence with a focus on Artificial Neural Networks (ANNs). We will begin by going through the various ANN types and the technical terminology that is associated to their operation. We will then employ MATLAB, a program that has the useful "net fitting app" feature. Similar to the chapter before, we will use this tool to develop a specific ANN model. To predict the flashover voltage of the 1512L insulator. There will be two models as well to compare them with previous.

Finally, we present a general conclusion of this work and the outlook suggested by this study.

CHAPTER I

State of the art: Insulators and Pollution

I.1.Introduction

High voltage insulators are used to separate the high voltage part from the ground or any other metallic part that exist in the environment other than the high voltage part itself. With no changes to the shape structure or conditions of the insulator, the insulator would hold for the voltage it is designed for with no problems [9].

The use of overhead line insulators is widespread and includes high-voltage transmission, rural electrification, and urban power distribution. Suspension, post, and strain insulators are just a few examples of how their designs change to meet the unique requirements of various settings. Together, they all contribute to the complex work of energy transport.

However, as they travel across many environments, insulators run against a powerful problem: pollution. Despite their toughness, the insulators are vulnerable to the slow buildup of impurities from industrial activities waste to salts, dust, and different environmental pollutants [10]. The insulators' surface is compromised by this pollution, changing their electrical properties and raising the possibility of flashovers, which could disrupt the power supply. Pollution is such a problem because it causes premature aging and performance degradation of the insulator [11].

In this chapter, an in depth study about pollution and its types along with the insulators and their types are defined as well as the various methods used to counter the problem insulators may encounter on their service.

I.2.High voltage insulators

High voltage insulators, also called insulating chains, are devices used in high voltage power lines to insulate electrical conductors and equipment. They are designed to withstand high voltages, typically above 1000 volts, and to prevent leakage current and unwanted electrical discharge. They are used in electricity transmission and distribution systems, such as high-voltage overhead lines, transformers and substations.

In the design of high voltage insulators, several insulating rings are stacked and connected together by metal rods. Insulating rings are used to create an electrical barrier between the high voltage conductor and the supporting structure in order to prevent the passage of electrical current. The metal rods ensure the mechanical rigidity of the insulator.

Insulators usually have two functioning role:

I.2.1.A mechanical role:

The high voltage insulator plays a mechanical role by carrying the electrical conductor. The pin and the cap, attached to the conductor and support structure respectively, support the conductor and allows it to remain at an adequate distance from the tower or support structure, thus ensuring the mechanical safety of the system.

I.2.2.An electrical role:

High voltage insulators play an essential electrical role in electricity transmission systems. Their main function is to provide effective electrical insulation between high voltage conductors and supporting structures, such as towers.

I.3.Pollution

Pollution is a problem that has many consequences on the insulators life and its efficiency. The accumulation of pollution on insulators can create a conductive layer which facilitates the circulation of leakage currents, thus creating electrical arcs and partial discharges. This can lead to power outages, short circuits and negative impacts on electrical equipment. Pollutions can be classified from its source or through its severity into many types so we get the following sets

I.3.1.Classification due to its source

Pollution classification due to its source could be made by what environment they are generated at. We get the following major sources

I.3.1.1.Naturel pollution

Naturel pollution refers to pollution that comes from nature so we can say that it is the highest found pollution in all the types mentioned here. Below are some of the sources that produce this harmful pollution for the insulator

- **Marine pollution**

Like the name suggests marine pollution is the pollution that comes from sea or any body of water which would in most cases be the sea and would target the overhead lines that are close. The droplets of salty water are carried with the wind to the insulator, once the insulator is wet the conductivity of the surface will be elevated and so the voltage that the insulator can support drops drastically [12].

Land pollution and desert pollution

Land and desert pollution can be said to be of the same source since both are not from the sea with the difference that the desert pollution is less moisturized. In land the pollution can be in the form of dirt or any other material found with fog and rain it becomes more moisturized and can cause severe damage to the insulator. The desert is more temperature high than any other place so the sand can be stacked on the insulator with no way of cleaning it which is carried by the sand whirlwinds [13].

I.3.1.2.Industrial pollution

The more an overhead line is close to an industrial zone it is more exposed to the industrial residue in the form of smoke and other residual forms. The flashover voltage then depends on the material the industries produce because metallic and plastic substances do not have the same conductivities [14].

I.3.1.3.Mixed pollution

This pollution is a combination of two or more pollutions of different sources for example industrial and marine pollution and it is generally the most dangerous pollution for the insulator [15].

I.3.2.Classification of pollution due to its severity

The following classification is made due to the severity of the site. Considerable efforts have been made to classify it quantitatively. According to M.Mohamed [16] it is classified as follows

Table I.1. Classification of pollution due to its severity

Pollution level and rate	Description of the environment
Light <0.06 mg/cm^2	Areas with low industrial zones or housing but frequently subject to winds and/or rains. Naturel regions such as mountainous regions or agricultural regions.

Medium <0.20 mg/cm^2	✚ Areas with industries that do not produce particularly polluting fumes and/or with an average density of dwellings equipped with heating installations. ✚ Areas exposed to the sea wind, but not too close to the coast. ✚ Areas with high density of dwellings and/or industries but frequently subjected to winds and/or rainfall.
Heavy <0.60 mg/cm^2	✚ Areas near the sea, or exposed to relatively strong winds from the sea. ✚ Areas with high density of industries and suburbs of large cities with high density of polluting heating installations residue.
Very heavy >0.60 mg/cm^2	✚ Generally, rare areas that are very close to the coast and exposed to spray, very strong sea winds and pollutants. ✚ Desert areas characterized by long periods without rain, exposed to strong winds carrying sand and salt and subject to regular condensation. ✚ Generally small areas, subject to conductive dust and industrial fumes producing particularly thick conductive deposits. ✚ Any of the above when mixed would be classified as very heavy for instance, industries situated in the desert.

I.4.Process of insulator flashover

Humidified pollution, whether natural or industrial, causes a major problem for insulators and generates electric arcs on their surfaces. These arcs can develop and cause flashover. The flashover of a polluted insulator is a phenomenon of dielectric breakdown by the establishment of an electric discharge between its ends, caused by the humidification of the pollution deposit on its surface. It manifests itself by an electric arc in the surrounding air between the two conductive parts; the damage is superficial because of the thermal energy released by the arc.

Insulator flashover happens in four different steps leading to the insulator service ending and is as follows [17], [18]

✚ **Deposition of pollution layer:** Initially, a solid layer composed of salts and insoluble materials forms on the surface of the insulators. However, in the case of marine pollution, the pollution comes in the form of sea spray.

- **Wetting of the pollution layer:** The pollution layer becomes moist due to ambient humidity or precipitation, which results in the dissolution of pollutants present in the deposit. This creates an electrolyte, allowing an electric current to flow.
- **Appearance of dry bands and local discharges:** When the current circulates through the layer of humidified pollution, dry bands are formed due to the Joule effect heating resulting from the circulation of the current. These dry bands are areas of high electrical resistance. As a result, local discharges, also called partial arcing, can occur.
- **Insulator flashover:** It occurs when the electric arc propagates along the surface of the insulator, which can lead to gradual propagation of local discharges and ultimately to complete short-circuiting of the insulator.

I.5.Type of insulator

Insulators are divided and classified into different types due to the material they are made as the following arrangements:

I.5.1.Due to their materials

Insulator classification can be made by their insulating material type. The major insulator types used in transmission lines are:

I.5.1.1.Glass insulators

Glass insulators are widely used especially for overhead lines of high and medium voltages due to its low manufacturing cost and their long lifetime. At first glass, insulators were made using normal glass that is both lower in electrical and mechanical properties meaning that it supports lower voltages and is easily breakable compared to toughened glass. After toughened glass was discovered, glass insulators naturally were made out of it. It can support 5 to 6 times the amount normal glass can support both electrically and mechanically [19].

I.5.1.2.Porcelain insulators

Porcelain is a widely known term for high quality ceramic since porcelain is less absorbent than ceramic it can easily withstand more moisture and harsher weather envirenments. With the increase in the quality of insulator comes a significant increase in the production cost [19].

For insulators intended for places where there are very high mechanical stresses, ceramics with very fine grains are preferably used. Ceramics are often found in substations: support insulators, voltage transformers, power transformer crossing terminals [15].

I.5.1.3.Composite insulators

Also called synthetic insulators are insulators that consist of a core made of fiberglass impregnated with resin, giving the insulator its mechanical strength, and an envelope made of synthetic insulating materials.

These insulators benefit from being extremely lightweight and having a strong mechanical resistance. They can be employed in extremely bad pollution circumstances and have good hydrophobic qualities. These insulators age as a result of the many stressors they are exposed to, including electrical, mechanical, atmospheric, etc., which is a drawback in their application [20].

I.5.2.Other classification for the insulators

This classification is more of like a naming for insulators and how they are used in the electric power system

I.5.2.1.Disc insulators

Disc insulator are the type of insulators, which are used mainly for transmission lines. As their name suggests they are made in the shape of a disc and they are usually used in the form of a chain depending on the service voltage. Disc insulators are also called cap and pin insulators. They are made of three different parts namely the cap, pin, insulation part and the patching part

Figure I.1: Cap and pin insulator.

- **Cap and pin:** are the parts made of a metallic material and are responsible for the connection between the pole and the high voltage cable
- **Insulation part:** the insulation part refers to the material actually responsible for the electric separation between the pole and the cable. It is mainly made of toughened glass or porcelain.

Patching part: this part is the one responsible for holding the entire insulator together. While its main job is to hold it together, it still is an insulating material and contributes to the electric insulation.

I.5.2.2. Suspension insulators

These kinds of insulators are typically employed as conductor carrying insulators to safeguard the overhead power lines. In towers, the suspension insulator is frequently made of porcelain or glass materials. They have a string form because several insulators are connected in series [21].

It carries a power conductor at its lowest end and is hinged to the tower's cross arm. When a higher voltage of roughly above 33 kV is needed, these insulators are used.

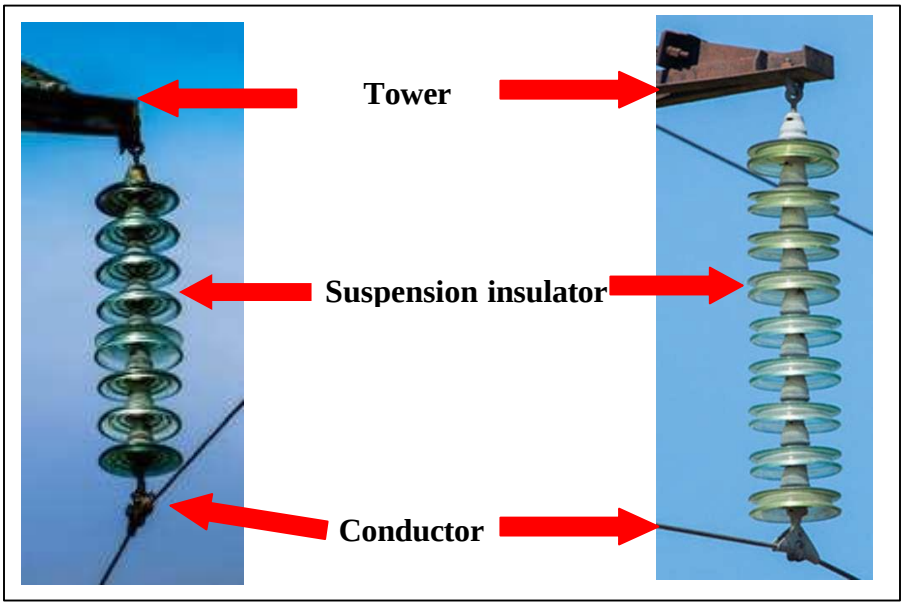

Figure I.2: Suspension insulator string.

I.5.2.3. Pin insulators

Power distribution lines are where you will typically find pin insulators [22]. It is a piece of equipment that shields a wire from external supports like a pin (a wooden or metal dowel) on a utility pole. It is a single-layer shape constructed of porcelain or glass, two non-conducting materials.

Depending on the voltage application, one or more pin insulators can be used on a physical support. The pin insulator is made of a material with a high mechanical strength and can withstand voltages of up to 11 kV. These can be set up either vertically or horizontally.

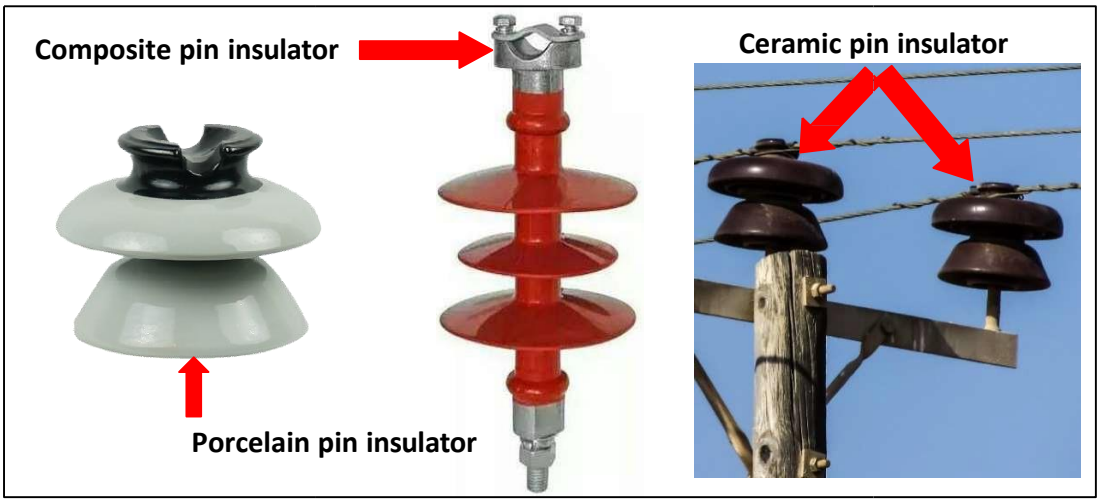

Figure I.3: Pin insulators.

I.5.2.4.Post insulators

Insulators are essential to the safe and stable distribution of electricity generated at power plants.

- Post insulator are closely similar to pin type insulator only they are more suitable for high voltage insulation in substations or generating substations. These are used because they make sure that the electricity produced in power plants is distributed in a secure and reliable manner.
- Post insulators can handle electricity up to 1100KV and are constructed of ceramic material or a single piece of composite material (silicone rubber). Due to its superior mechanical qualities, it is frequently used to safeguard transformers, switchgear, and other connected equipment.

Figure I.4: Post insulators.

I.5.2.5.Shackle insulators

Shackle insulators, which are employed in low voltage distribution systems, are typically modest in size. This kind of insulator can be positioned either vertically or horizontally. This insulator can be connected using a metal strip.

It has a tapered hole that more evenly distributes the load force, lowering the possibility of fracture if fully loaded. After underground cables for distribution became widely used, the use of these insulators has declined recently.

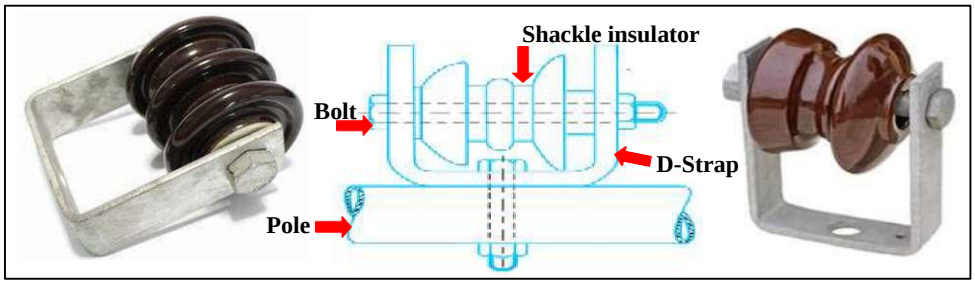

Figure I.5: Shackle insulator.

I.5.2.6.Long rod insulators

In order to isolate the transmission lines, the long rod insulators are typically hinged on steel towers. They also serve as protection mechanisms by safely supplying power. Long rod insulators typically consist of several insulators depending on the usage and demand.

These are porcelain rods with metal end fittings and a weather shelter on the outside. Employing this kind of insulator has the benefit that it can be used in tension and suspension positions.

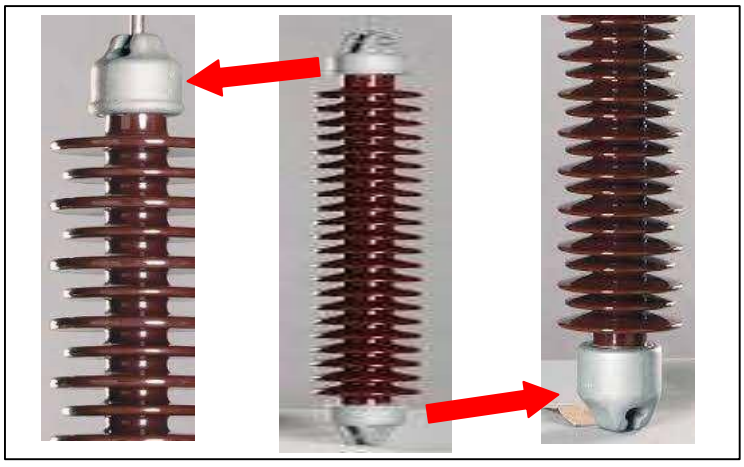

Figure I.6: Long rod insulator.

I.5.2.7.Stay insulators

This particular low voltage insulator combines a stay wire or main grip to counterbalance and fasten dead-end poles. These rectangular insulators come in smaller sizes than other varieties and have a rectangular shape. They are used in low voltage distribution lines [23].

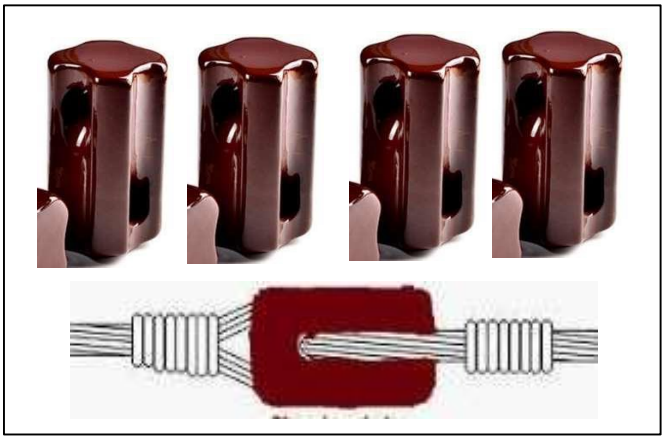

Figure I.7: Stay insulators.

These insulators can be positioned between the ground and the line conductor. Additionally, they serve as safeguards against sudden voltage changes or malfunctions that occur suddenly. When the poles collapse to the ground or when the stay wires unexpectedly snap from an increased mechanical load, the significance of these insulators is evident.

I.5.2.8.Strain insulators

These particular insulators are made to function while being subjected to mechanical stress in order to endure the stretching of a hung electrical wire or cable. As it is utilized to support radio antennae and overhead power lines, it is comparable to a suspension insulator.

Figure I.8: Strain insulators.

To electrically isolate two wire lengths from one another while keeping a mechanical connection, a strain insulator is placed between them. Alternatively, utilized to handle the pull of the wire to support while electrically insulating it when a wire connects a pole or tower.

I.5.3.Profile of insulator

These insulator profiles are made for disc type insulators and are for alternating voltage of overhead transmission lines with a rated voltage greater than 1000 V with ceramic or glass insulating materials [24].

I.5.3.1.Standard profile

Due to their flatness, the evenly spaced internal grooves, and the length of the creepage distance that exceeds the standard request, the shape and dimensions are in compliance with international standardization (CEI 305 1978). This style is popular in areas with moderate pollution.

Figure I.9: Standard profile.

I.5.3.2.Aerodynamic profile

Due to the air movement, with the interior grooves are completely eliminated, which decreases the accumulation of pollutants on the lower surface. This design is especially useful in desert regions where self-washing by rain is rare.

Figure I.10: Aerodynamic profile.

I.5.3.3.Anti-fog profile

The spacing between the rings is wider than the standard profile, which simplifies manual washing if necessary and allows for effective cleaning in wind or rain. In cases of extreme pollution, the distance also prevents arcing between adjacent rings.

Figure I.11: Anti-fog profile.

I.5.3.4.Spherical profile

The lack of internal grooves and the spherical shape with a long leakage length make hand washing simple and effective for these types of profiles.

Figure I.12: Spherical profile.

I.5.3.5.Two-alternating and three alternating profiles

The figure bellow shows the three alternating profile and the two alternating profile is very similar the only difference is that the two alternating profile does not have the middle rib on the outer side of the glass. With a leakage distance equivalent to that of the anti-fog profile. The elimination of sub-ribs the inside of the glass reduces pollution, promotes self-cleaning and facilitates manual cleaning when needed.

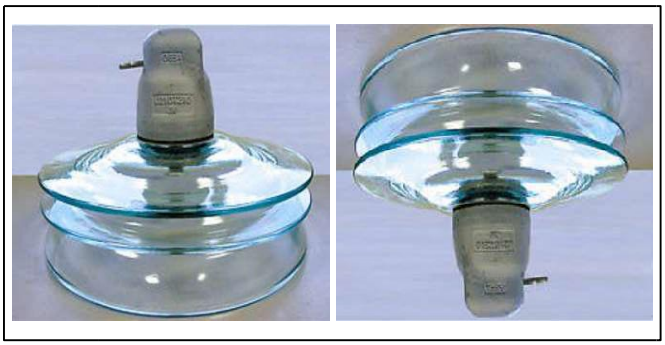

Figure I.13: Three alternating profile.

I.6.Choice of insulators

Insulators account for a very modest percentage [25], in the price of a medium voltage overhead line; however, they are an essential element on which operational safety, quality, reliability and continuity of service depend on. The importance of their role is apparent above all from the difficult to quantify cost of any service interruption of which they may possibly be the cause. It is therefore essential to choose them with discernment based on the electrical and mechanical constraints they must withstand.

The insulators best suited to a given environment are those which retain the lowest rate of pollutant deposits, i.e. the insulators which have the best self-cleaning properties. Thus the shape and profile of the insulators now appear as a criterion of choice for the selection of insulators under pollution.

Even when well chosen, insulation is still not safe from an incident. The severity of pollution at a site can change; the initially correct sizing of the insulators may then become insufficient, hence the need to be able to protect existing installations against possible new sources of pollution.

Almost permanently, the insulator is subjected to well-defined electrical and mechanical constraints according to the intrinsic characteristics of the line, but which may accidentally become very high for particular environmental conditions.

It is moreover the knowledge of these so-called accidental constraints, which makes it possible to choose the most suitable equipment.

Among the constraints affecting the proper functioning of insulators we cite pollution. Indeed, this constitutes a serious problem for the insulation of high-voltage structures, which must be taken

into account when sizing the insulation of high-voltage lines. This is due to the formation of more or less conductive layers on the surface of the insulator. These layers can cause a considerable reduction in the surface resistivity of the insulating surfaces and consequently a reduction in the withstand voltage of the insulators.

I.7.Flashover prevention

To prevent flashover on the surface of high voltage insulators, there are a few steps to take:

I.7.1.Continuous monitoring

Through continuous monitoring, flashover and potential failures can be quickly detected before they cause significant damage. Monitoring systems can measure and monitor insulator parameters such as current, voltage, partial discharges and temperature, which can indicate abnormal variations and provide early warnings of any potential problems. Using the collected data and proper analysis, adequate measures can be taken to repair or replace faulty insulators, before they cause serious electrical accidents. Additionally, regular maintenance work and preventive repairs can be planned to ensure the proper functioning and safety of the electrical system.

I.7.2.Visual inspection

Allows you to identify possible defects or visible problems such as cracks, fractures, deformations or other damage. It can also be used to detect the accumulation of dust, pollution or other substances that could impact the performance of the insulator. The visual inspection process requires examining the insulator surface by direct observation, using assistive tools such as magnifying glasses or thermal cameras to detect minor details or defects [26].

I.7.3.Repair of defects

Repair of faults on high voltage insulators refers to the actions taken to correct any damage or fault identified on the insulator. When an insulator shows signs of deterioration, such as cracks, chips, deformation. It is essential to repair them quickly to preserve the performance of the insulator.

Repair of faults on high voltage insulators may vary depending on the nature and extent of the damage. In some cases, it may be necessary to completely replace the damaged insulator with a

new one. In other cases, targeted repairs can be made to restore the functionality of the insulator [27].

I.7.4.Use of hydrophobic coatings

Hydrophobic coatings are materials specially designed to repel water and reduce the formation of water droplets or films on the surface of insulators. These coatings create a protective barrier that prevents water from accumulating and causing insulation problems. When high voltage insulators are exposed to humid conditions, such as rain, dew or condensation, hydrophobic coatings prevent water from settling and forming a conductive path. This reduces the risk of electrical flashovers and partial discharges. Additionally, hydrophobic coatings can also repel contaminants such as dust, salt or air pollutants, which may otherwise accumulate on the surface of insulators. This helps keep the insulator clean and preserves its electrical performance [28].

I.7.5.Regular cleaning

Regular cleaning of electrical insulators is essential to maintain their performance and avoid potential problems such as electrical flashovers, partial discharges and risk of failure.

It is essential to implement a regular maintenance program and follow appropriate cleaning protocols to ensure the reliability and durability of H.T. insulators [28], [29].

One other method that is very effective is the usage of leakage distance extenders. These extenders increase the leakage distance of the insulator minimizing the leakage current and the probability of flashover however this method is very costly and only used when the other methods fall short [30].

I.8.Insulator characteristics

In the following, a definition of some of the most important characteristics of high voltage insulators are presented.

I.8.1.Leakage distance

Can also be referred to as the creepage distance, which is the shortest distance between the high voltage point of the insulator to the ground connected point of it along its surface.

I.8.2.Dry arcing distance

Refer to the shortest distance from the high voltage point of the insulator to the ground connected point of it through the air of the insulator.

I.8.3.Perforation distance

Refer to the distance from the high voltage point of the insulator to the ground connected point of it through the core of the insulator.

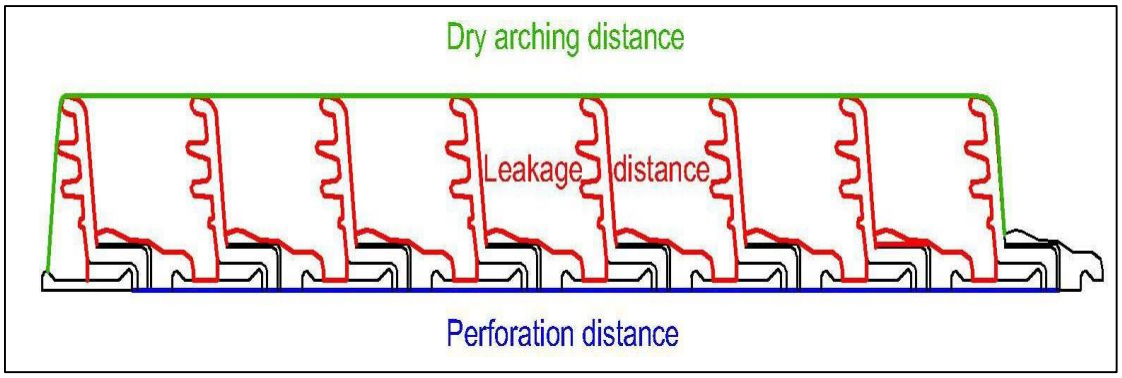

Figure I.14: Dry arching, Leakage and perforation distances.

I.8.4.Withstand voltage

This is the highest voltage level that the insulator can withstand without causing a disruptive discharge.

I.8.5.Flashover voltage

The flashover voltage is the lowest voltage level at which all arcs join the two electrodes together causing the current to flow freely from the high voltage electrode to the ground electrode.

I.8.6.Leakage current

It is a low amplitude current, circulating through the polluting layer along the surface of the insulator, its intensity becomes significant when approaching the flashover voltage. It depends on several factors such as the nature of the polluting layer and the length of the leakage line. The leakage current may take a different route through the perforation distance especially when the number of insulators in the chain is low and the pollution is non-existent.

I.9.Previous literature

When speaking about previous literature in the field of high voltage insulators it can be very demanding to cover everything since it is a very vast subject of research. However, even with vastness and verity of the studies not just in dry and clean case studies but also in work that additionally considers consequences from pollution, ice, and water droplets, transmission lines, towers, and ground wires are not taken into account in the electric field calculations. There hasn't been any investigation on comprehensive models that contain all of the relevant factors together [31], [32].

Ouchen [25] simulated the electric field in the uniform and non-uniform cases of pollution on 3 insulator chain. For the uniform case where the pollution covers the entire insulator, he used four cases, clean and three different conductivity values cases. He found that the maximum field values does not occur at triple junction parts; instead, it may occur on the outside of the glass shell. In the non-uniform case, the insulators are polluted in three different cases, pollution on the top side, on the bottom side and fully polluted except for the region around the pin of each insulator to resemble a dry band. He found that the formation of the dry band in the lower zone of the chain of insulators causes an intense electric field. The dielectric breakdown voltage of the air can be reached between two points on the insulating surface, leading to the initiation of an electric arc, which short-circuits part of the creepage distance.

Bo Zhang et al [32] simulated a 330kV transmission tower including the composite insulators using both the charge simulation method and boundary element method. He found that the method allows for the modeling of extremely complicated geometry as well as the investigation of the impacts of different hardware components, such as tower configurations and grading devices, on the electric fields surrounding the tower and composite insulators.

On the other hand Cui and Ramesh [33] used the experimental approach. To see the electric field distribution of different kinds of insulators they used an electric field measurement probe which is based on the Pockels electro-optic effect. Using six different insulators two different cases were observed the first is where the whole insulator is polluted the second case is where the lower surface of the sheds is polluted. They made a logarithmic regression model for the prediction of their flashover voltage. After predicting the flashover voltage for a 115 kV composite insulator with a clean surface a good agreement was observed

To predict the flashover voltage of insulators Bessedik and Hadi [34] used the least squares support vector machine coupled with the particle swarm optimization. The model uses the diameter of the insulator, the leakage distance, the insulator height and the conductivity to output the critical flashover voltage. The results showed a good prediction ability of the flashover voltage for insulators that are not used for the training stage. According to them, all necessary geometric variables utilized in different types of insulators might be easily and correctly standardized. Then, for various contaminated insulators, the suggested method may be more useful to predict the critical flashover voltage.

On the other hand Stefenon et al [35] used computer vision techniques such as binarization with threshold, threshold with Otsu, Sobel edge detector, adaptive binarization with threshold, Canny edge and Riddler–Calvard techniques detection for the extraction of contamination characteristics of polluted insulators and a neural network used for the classification of these conditions. They reported that the proposed model is more accurate then well-established models such as support-vector machine (SVM), k-nearest neighbor (k-NN), and ensemble learning methods.

I.10.Conclusion

A thorough discussion of high voltage transmission line insulators and the crucial elements affecting their performance has been given in this chapter. It is impossible to exaggerate the role that insulators play in guaranteeing the steady operation of electrical power systems. In order to maintain a reliable and effective power supply, it is essential to comprehend the many types of insulators, the effects of pollution, and the ways to prevent flashover.

In conclusion, this chapter has identified the complex interactions between variables that have an impact on high voltage transmission line insulators. It is obvious that insulator design and upkeep will change as technology and research develop in order to meet the rising demands of our electrical power systems. Power utilities and engineers may make wise judgments to ensure the reliable and efficient transmission of electricity, even under difficult environmental conditions.

The simulation of insulator potential and field distributions under various conditions will be covered in the following chapter, along with an explanation of how the potential and field distribution affect the insulator under various contaminated conditions.

CHAPTER II

2D and 3D Simulations

II.1.Introduction

The introduction of simulation has had a profound impact on how we approach complex systems in the constantly changing world of engineering and technology. This digital solver has assumed a particularly important role in the area of high voltage insulators for overhead lines. The complex models and algorithms come together to provide a fresh perspective on the behavior and traits of high voltage insulators. The most intricate details of real-world occurrences may be recreated and manipulated using simulations, which give researchers a way to study electric fields and potentials in insulators in unprecedented depth [36].

The idea of electric field distribution is crucial to this investigation. Electric fields within insulators are crucial in determining their behavior and reaction to electrical stresses [37]. Through visualization and analysis of how these electric fields interact with the many geometrical features of insulator design, simulations provide a way to identify stress points, potential flaws, and areas of optimal performance. While understanding the equilibrium and stability of insulators relies heavily on electric potential distribution, although not as important as the electric field distribution [38]. The gradients and variations in electric potential can be shown through simulations, allowing us to identify any potential weak points or regions subject to excessive voltage stress if they exist.

In this chapter multiple simulation have been done. Using comsol Multiphysics a two and three dimensions (2D/3D) simulation were made. The 2D simulation considers the increase of insulator number in an insulator string from 1 to 5 insulators under a uniform type pollution.

The 3D simulation considers the shape and position of the pollution to try and define the properties and environments that the insulators excel in.

II.2.COMSOL Multiphysics

COMSOL Multiphysics is renowned for its extraordinary versatility in modeling and simulating complex physical systems with interconnected phenomena spanning many physics domains. It offers a unified environment for the simulation of complicated systems involving interactions between several physical processes, such as electrical, mechanical, thermal, fluid flow, and chemical reactions. The user-friendly interface of COMSOL Multiphysics is one of its best qualities. The software provides an easy-to-use graphical user interface that makes it simpler to build up simulations. Through a streamlined workflow, this

method enables users, whether they are novices or seasoned professionals, to easily generate, modify, and visualize models.

The Finite Element Method (FEM) is the numerical method used by COMSOL Multiphysics. When working with complex geometries [39], FEM is especially useful since it breaks these sophisticated structures into smaller, easier-to-manage parts.

This division enables very precise approximations of partial differential equation solutions, ensuring accuracy and flexibility to unique geometries [40].

Each specified physics module in the COMSOL library is devoted to modeling a different physical phenomenon. These modules cover a wide range of topics, such as acoustics, fluid dynamics, electromagnetics, heat transfer, and structural mechanics. When necessary, users can easily combine and modify these components to build complex Multiphysics models.

II.3.Modeling Insulators in COMSOL

The study chosen for this model is the stationary study, which is a study that does not depend on any variable such as time or position or any such variable meaning that it does not change as the simulation progresses.

For the physics, it is the electrostatics physics. For this, we need to speak about certain things, which revolve around previous works and some thoughts that come to us. Previous researchers and engineers used conductivity as a main property to study flashover and leakage current and such terms for insulators but that is unnecessary for our physics and the only needed material property is the relative permittivity since we are studying the potential and field distribution. Additionally, conductivity is a property that may define many materials or many conditions, which the pollution is in, whether it is moisturized or dry, and the same can be said for the relative permittivity. Each material has a relative permittivity that it is defined by and it can change depending on the state the pollution is in or if it is mixed with others.

For the 2D simulation the modeled insulators and insulator chains are shown in figure II.1 below

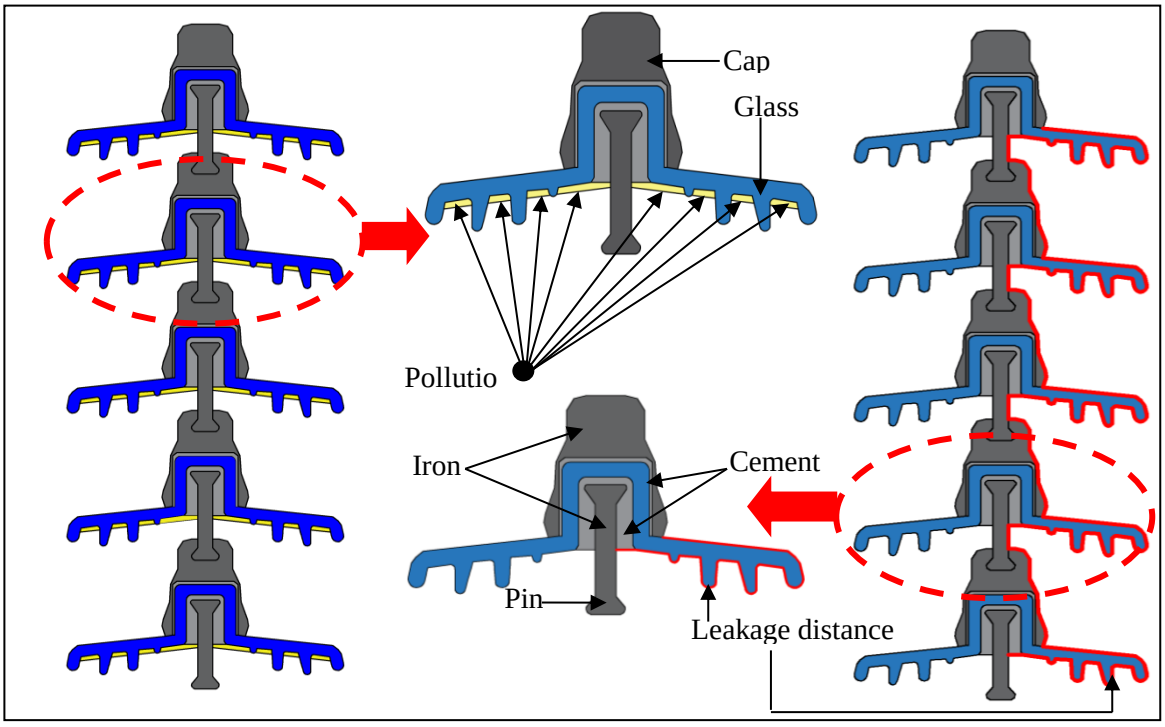

Figure II.1: Insulator with and without pollution.

The dielectric constant used for the pollution is a high enough value to induce changes in the distributions and is taken from previous researches [41]. The first priority in designing insulators is to create a shape for the insulating material that can withstand different pollution environments.

High field values indicate possible arc-starting locations; in other words, these are the locations where the highest probabilities of the arcs would originate. Only the relative permittivity is required in COMSOL for electrostatic physics to calculate the potential and field distributions, so the relative permittivity will be examined.

For the 3D simulation the modeled insulator chain and the pollution types are shown in figure 2 and figure 3 and figure 4 respectively below

The droplet shapes may refer to water droplets in other words rainy conditions while the surface shape may refer to less rain and with high values of permittivity, we can refer them to industrial zones of metallic substances for instance.

The metallic substance will be in the form of powder meaning their values drop compared to the original value due to the existence of air particles between them.

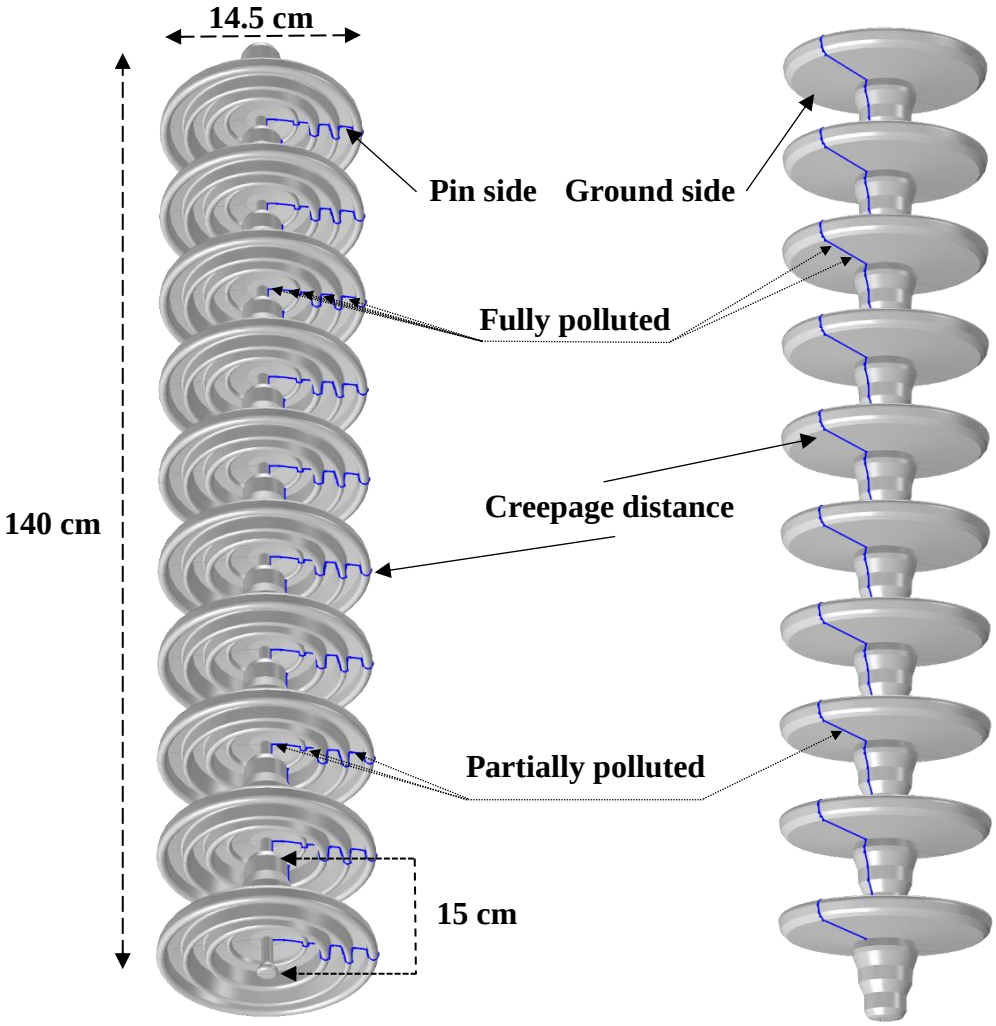

Figure II.2: A detailed description of the model studied

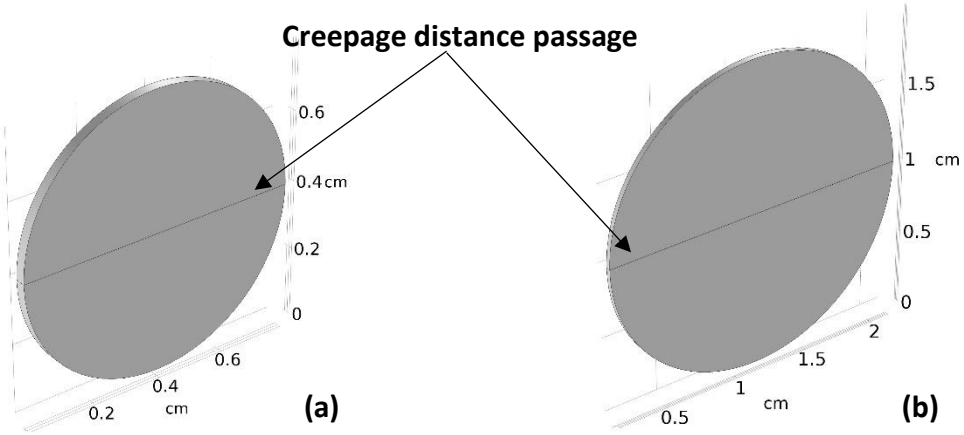

Figure II.3: Surface shape of pollution on the (a) pin side and on the (b) ground side

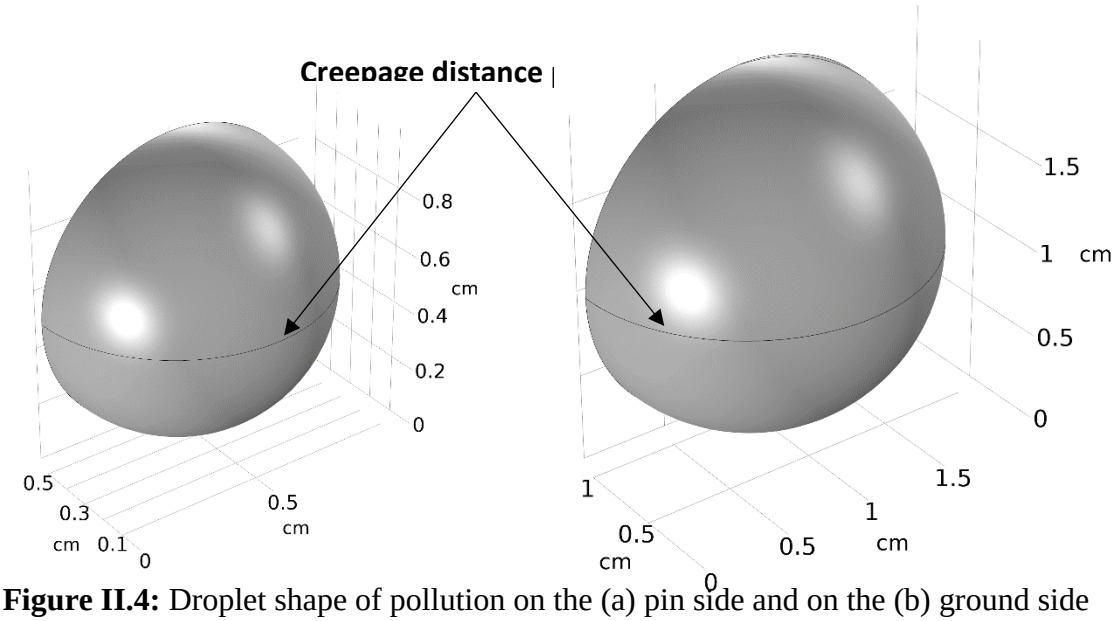

Figure II.4: Droplet shape of pollution on the (a) pin side and on the (b) ground side

Additionally the material properties needed for the simulations are presented in table II.1 below

Table II.1. the model material properties

Material	Relative permittivity (ε_r)
Iron	10^6
Glass	4.2
Cement	5.9
Air	1.0006
Pollution	80

II.4.The equations used

COMSOL Multiphysics calculates the electric potential allows the calculation of the electric field through the following equation [42], [43]:

$$E = -\nabla V \quad \text{(II.1)}$$

Maxwell's equation:

$$\nabla \cdot D = \rho \quad \text{(II.2)}$$

$$D = \varepsilon E \quad \text{(II.3)}$$

$$\nabla \cdot \varepsilon E = \rho \quad \text{(II.4)}$$

We get Poisson's equation as follows:

$$\nabla \varepsilon \cdot \nabla V = -\rho \tag{II.5}$$

Laplace's equation takes the following shape when the space charges are ignored:

$$\nabla \varepsilon \cdot \nabla V = 0 \tag{II.6}$$

II.5.2D simulation

Two boundaries are established for the models; the pin will always serve as the location of the electric potential and a value of 25 kV of voltage will be added with each insulator added to the chain. The last insulator's cap, which serves as the ground, forms the second boundary.

The software's default mesh, which is typically suitable for thin and intricate issues that may arise due to small geometry shapes, is used to create the majority of generated meshes in general. However, the software also offers other meshing choices, such as a mapped mesh or a free quad mesh. Other meshing options may therefore be better for it based on the geometry that is being meshed. In figures II.5 to II.7, the default meshing option, free triangular mesh, was used to create our mesh. This mesh is suitable for the small geometries that surround the small edges of the geometry, which are depicted in the figures below as black spots but are actually small triangular shapes. The mesh always has a triangular form despite being smaller in size near the edges and in tiny areas of the insulator.

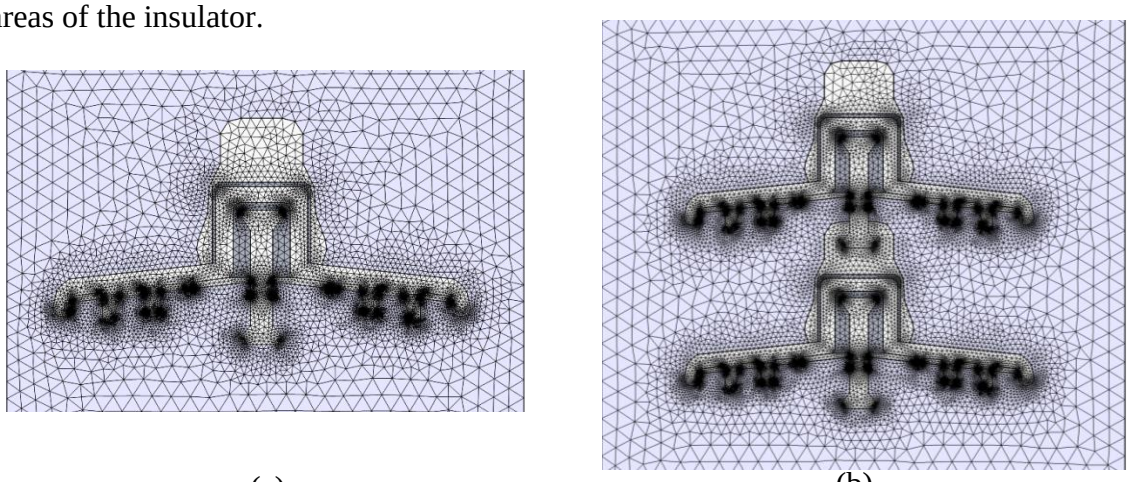

(a) (b)

Figure II.5: Geometry mesh by triangles for (a) one insulator, (b) two insulators.

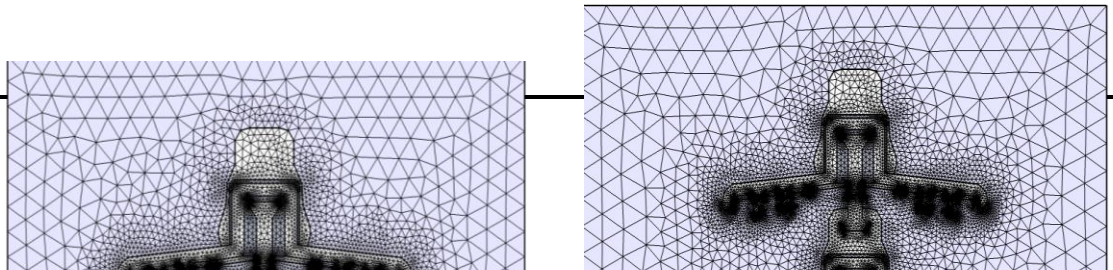

Figure II.6: Geometry mesh by triangles for (a) three insulator, (b) four insulators.

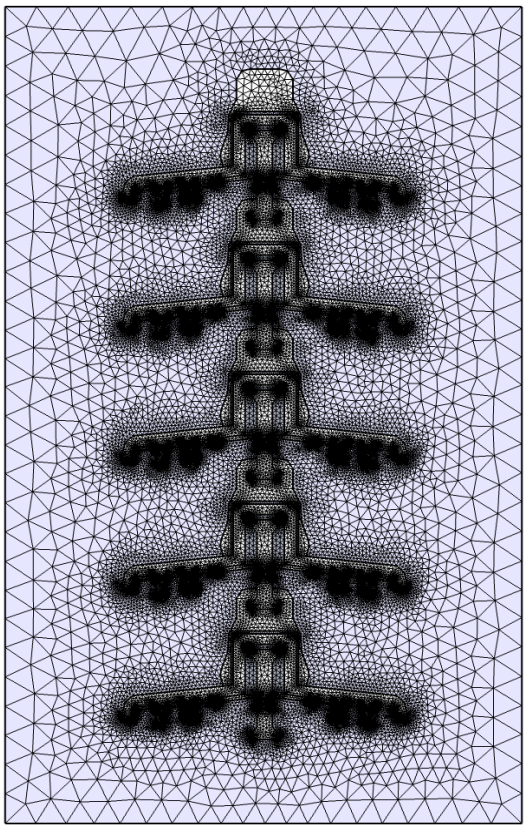

Figure II.7: Geometry mesh by triangles for five insulators.

II.6.Results and discussion

For each of the cases under investigation, the contour plot for the electric potential distribution within and around the insulator is created. The same is done for the electric field, with the addition of a streamline plot that depicts the direction of the field lines. In order to see the differences between the clean and polluted insulators in the various scenarios under study, the potential and field distributions along the leaking distance shown in figure 1 are also shown.

II.6.1.Electric potential distribution

Figures 8 to 12 display the equipotential lines and potential distribution for five different scenarios of the insulators string surface in the clean state.

These findings show that the absence of contour lines in the cap and pin of each chain's insulator is caused by the absence of any obstructions to the electric potential in the chain's metal components. Contrary to that, the glass surface and both cement sections experience the most significant alterations. This is because the electric potential is concentrated along the chain's center, which is also its shortest path. However, there is a great deal of fluctuation in the potential values due to the existence of the many materials impeding it. The color of the contour lines in these obstructive materials varies in a way that indicates a decline with each distance from the potential pin to the ground cap, showing that the potential decreases as each insulator is added to the chain.

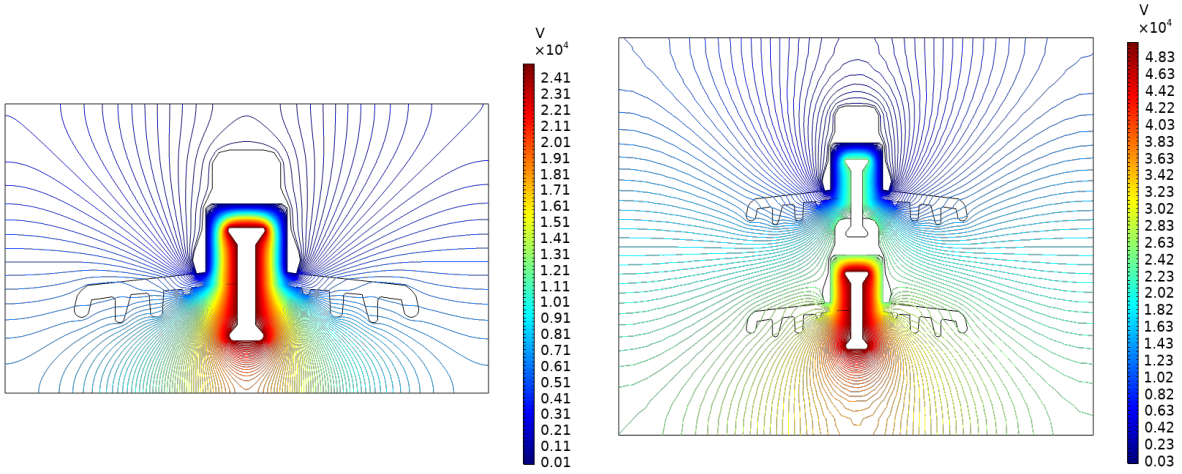

(a) (b)

Figure II.8: Potential distribution in the clean state for: (a) one insulator, (b) two insulator.

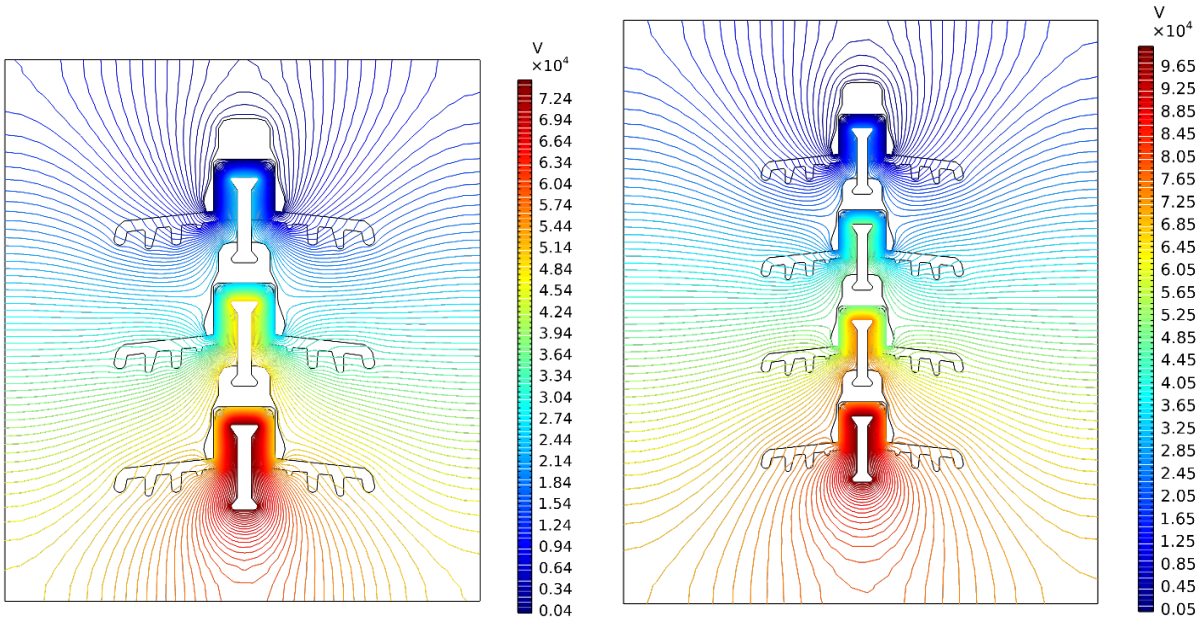

(a) (b)

Figure II.9: Potential distribution in the clean state for (a) three insulators, (b) four insulators.

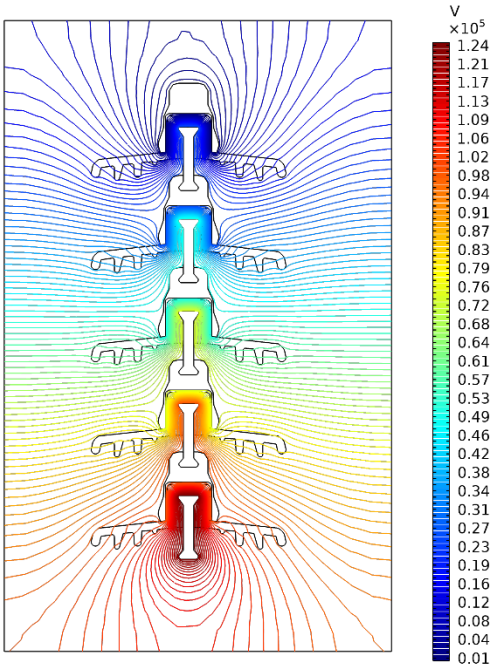

Figure II.10: Potential distribution in the clean state for five insulators.

The images below show how the electric potential varies for each element of the insulators string (five examples) as a function of the leakage distance.

Figures 13 to 17 shows that in all circumstances, the potential value is significantly higher in the presence of pollution than it is in the absence.

As we add more insulators to the chain, as shown in previously mentioned figures, the potential at the end of the chain decreases until it reaches the values determined from the chain's clean state.

It is also clear from figure 15 to figure 17 that the electric potential begins to develop in a predictable manner, making it possible to anticipate the potential surrounding the chain of six insulators. As can be observed, the presence of pollution in this manner only affects the distribution's value from the side on which it is stationed, not its shape considerably (pin side in this case).

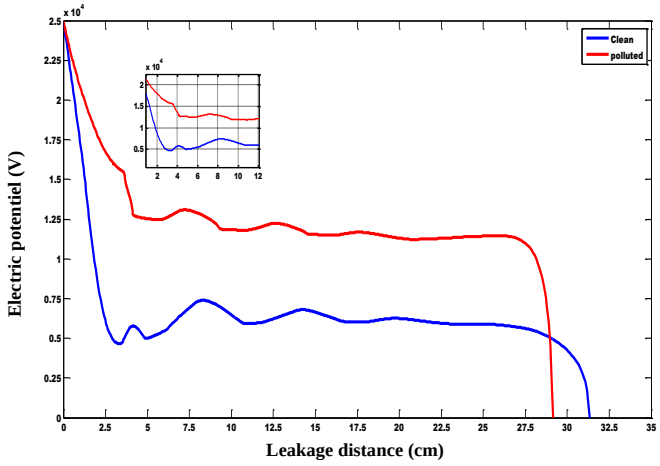

Figure II.11: Electric potential-leakage distance across one insulators.

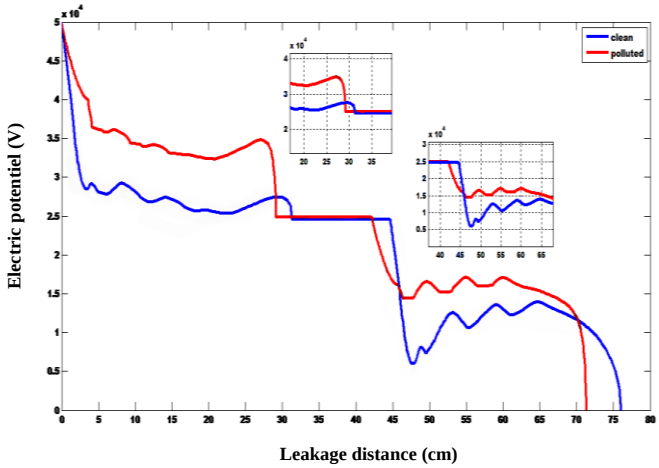

Figure II.12: Electric potential-leakage distance across two insulators.

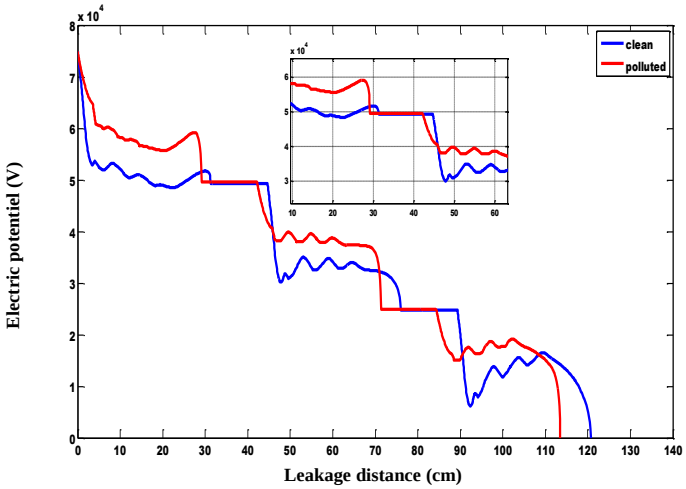

Figure II.13: Electric potential-leakage distance across three insulators.

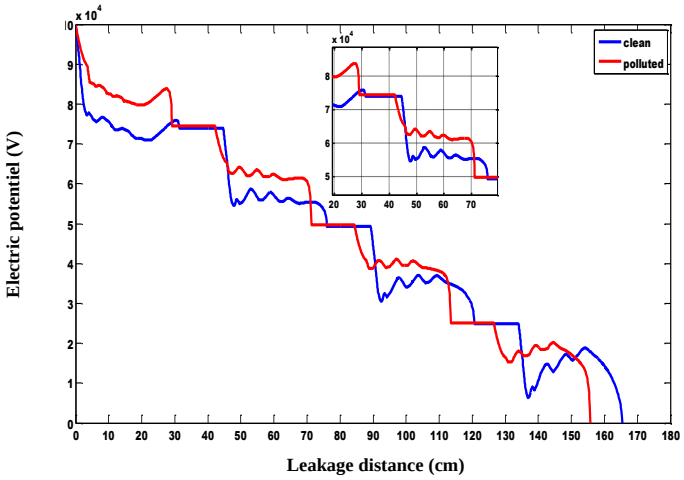

Figure II.14: Electric potential-leakage distance across four insulators.

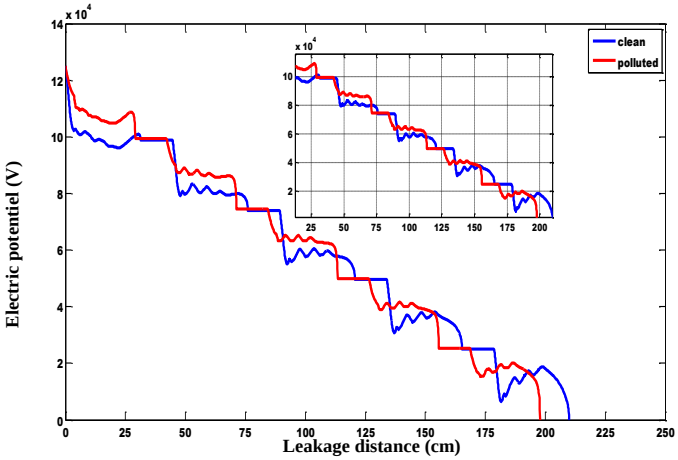

Figure II.15: Electric potential-leakage distance across five insulators.

II.6.2.Electric field distribution

The first-importance factors in the architecture, sizing, quality, and dependability are the performances of the insulators deployed in contaminated areas. Insulator for high voltage, It is crucial to understand the mechanisms leading to flashover under pollution in order to monitor the effectiveness of a structure's insulation.

In five distinct situations of the insulators string surface in the clean state, the electric field distribution and equipotential lines are shown in the figures 18 to 22 along with electric field vectors.

The aforementioned contour and streamline figures demonstrate how the electric field is focused on the upper and bottom sides of the pin and cap, respectively, where they make contact with the glass. While occasionally breaking the line when it enters the glass, as seen in the streamlines.

The distribution of the electric field is the same whether the contour or streamline plots are used, despite the difference in the number of insulators. Similar to the potential, each insulator's center, located between the pin and the cap, is where the field varies the most.

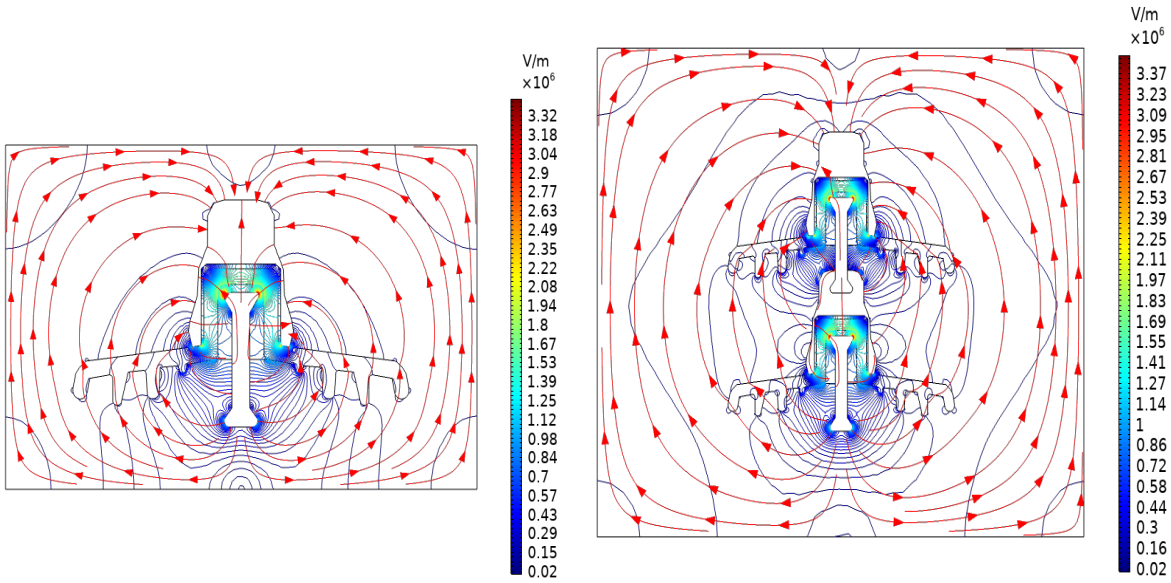

(a) (b)

Figure II.16: Electric field distribution and streamlines in the clean state for: (a) one insulator, (b) two insulator.

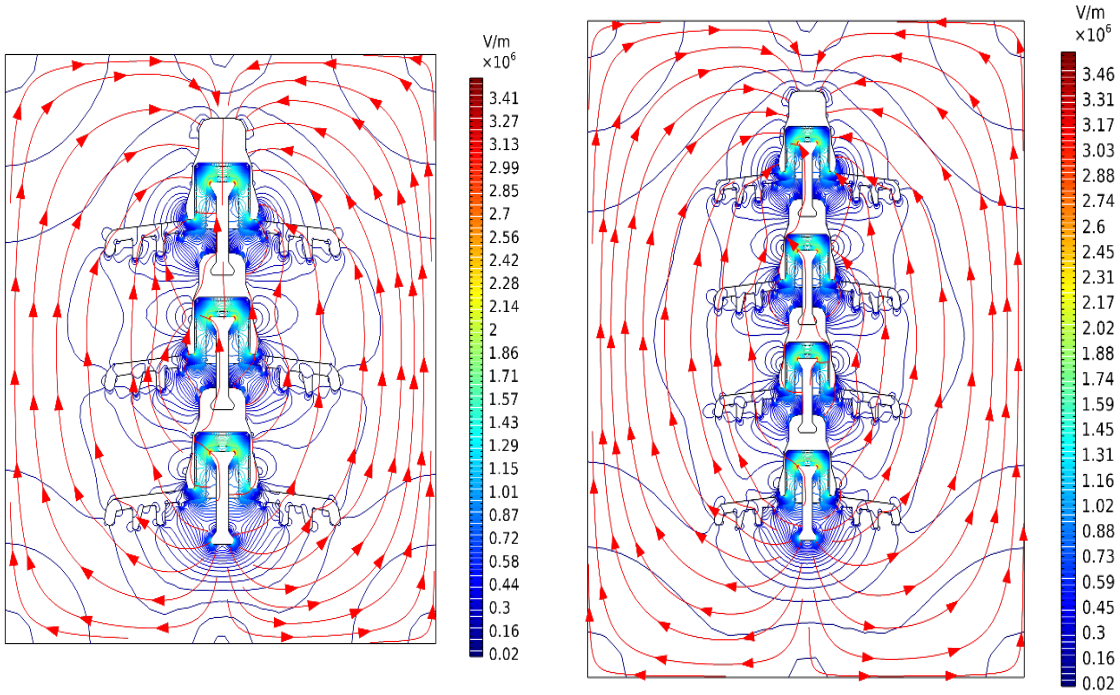

(a) (b)

Figure II.17: Electric field distribution and streamlines in the clean state for: (a) three insulators, (b) four insulators.

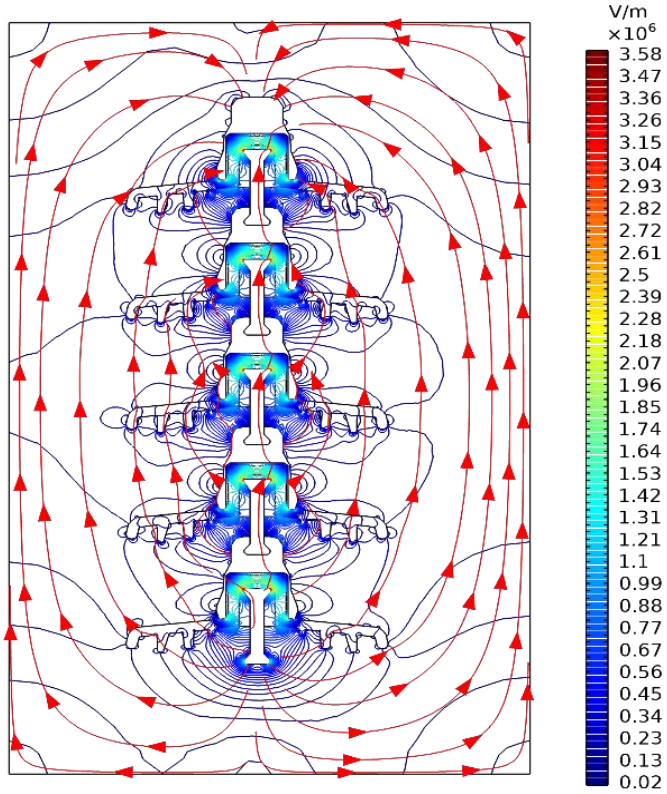

Figure II.18: Electric field distribution and streamlines in the clean state for five insulators.

Figures (II.19 to II.23) illustrate how pollution, in contrast to the beginning, causes the value at the end to climb dramatically.

Pollution causes the value at the start to decline and induces high value spikes of the electric field along the leakage distance.

The value at the end remains mostly unchanged in form in comparison to the clean condition when more insulators are added to the chain except they increase in value.

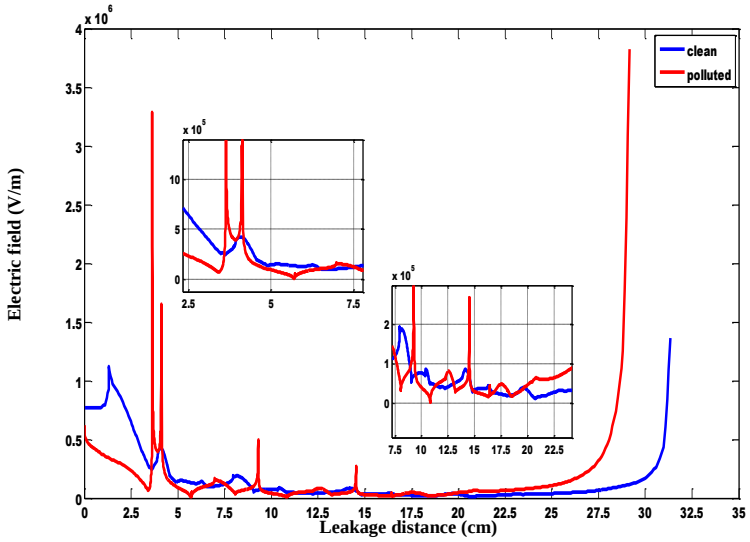

Figure II.19: Electric field-leakage distance across one insulators.

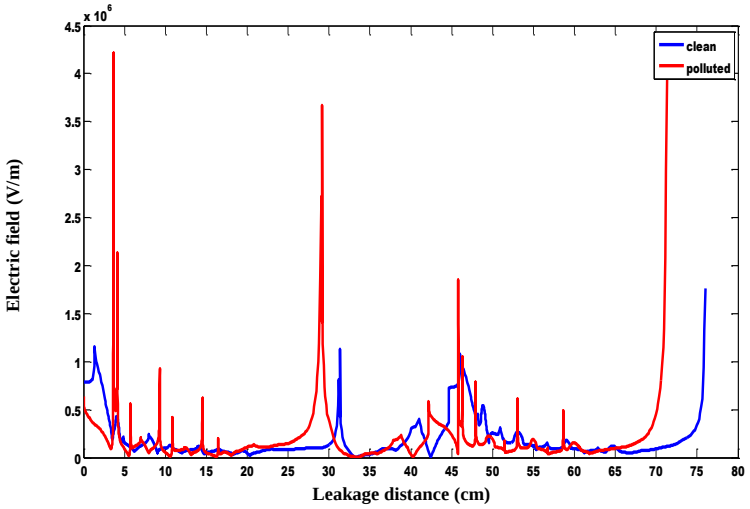

Figure II.20: Electric field-leakage distance across two insulators.

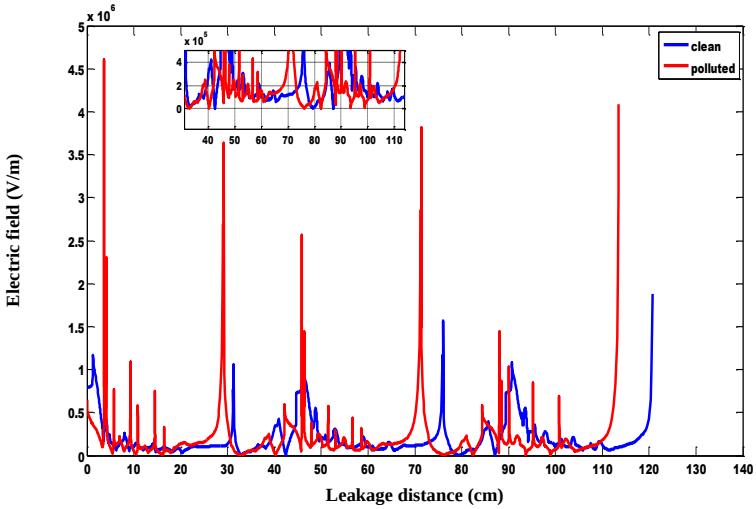

Figure II.21: Electric field-leakage distance across three insulators.

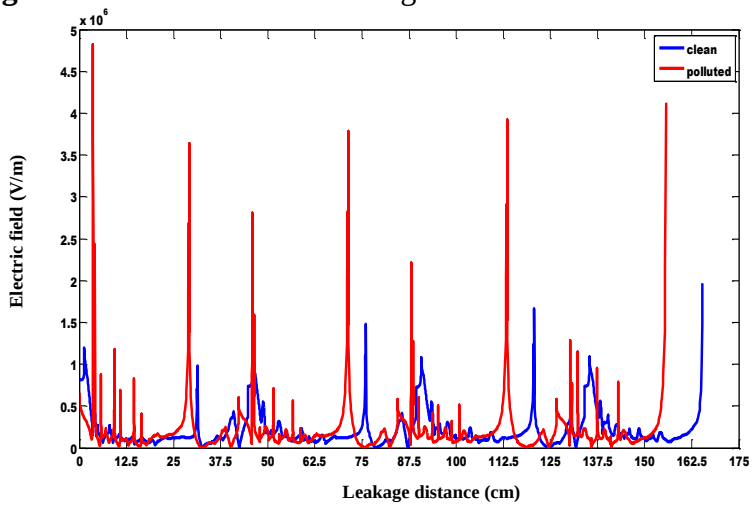

Figure II.22: Electric field-leakage distance across four insulators.

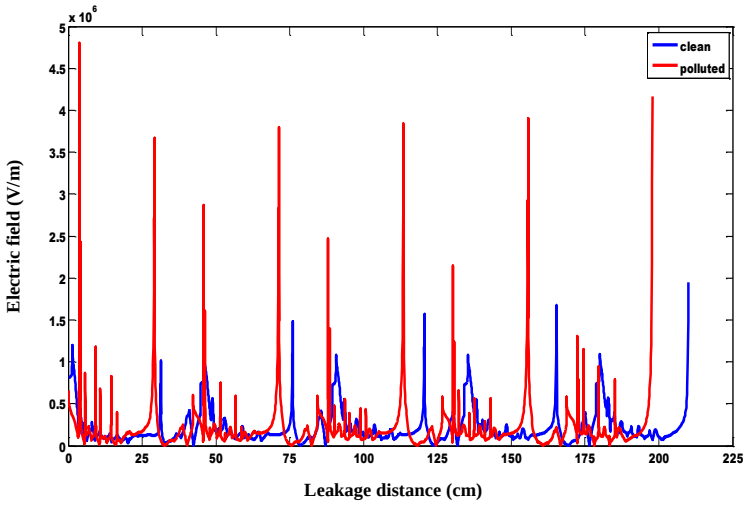

Figure II.23: Electric field-leakage distance across five insulators.

Every insulator in the chain starts with a spike, and each spike has a higher value than the one before it. On the pin side, the values at the beginning and end of the chain are always those where the electric field is at its strongest.

The arcs are most likely to begin at locations where the field values are high. The arcs in cap and pin insulators begin between the glass, just like they do in composite insulators, which start as sheds. The arcs in our insulator can also begin at the cap side, establishing a path to the pin from the cap to the glass.

II.7.3D simulation

The boundary condition for our model similar to the previous case, are two; the first one is the electric potential boundary, which is the pin of the first insulator in the chain with a voltage of 220 kV. The second boundary is the ground boundary, which is the cap of the last insulator.

II.7.1.The electric potential distribution

The pictures below shows a 3D volume plot and a 1D plot of the potential in the clean state. The 1D plot in figure II.25 enables a more detailed knowledge of how the values change along the leakage distance while the volume plot allows for a clearer picture of the potential.

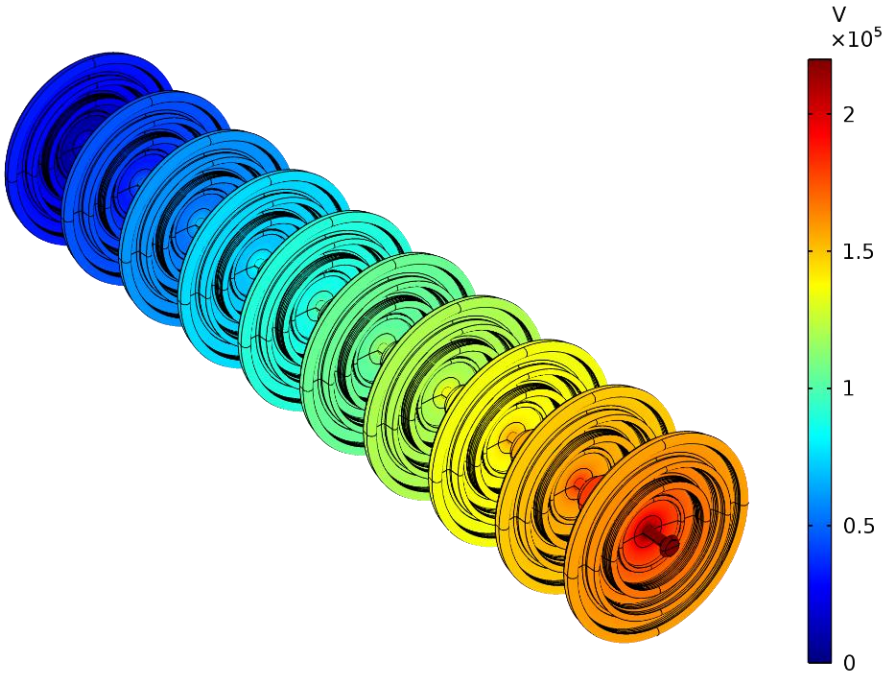

Figure II.24: Volume plot of the potential in the clean state

In order to see the effect of the quantity of pollution on the potential, a 1D plot of pollution in the surface shape (fully and partially) and in the droplet shape (fully and partially) is first drawn. In order to see how the shape of the pollution affects the potential, a second 1D plot of pollution is created in both the partially (surface and droplet) and fully (surface and droplet) situations.

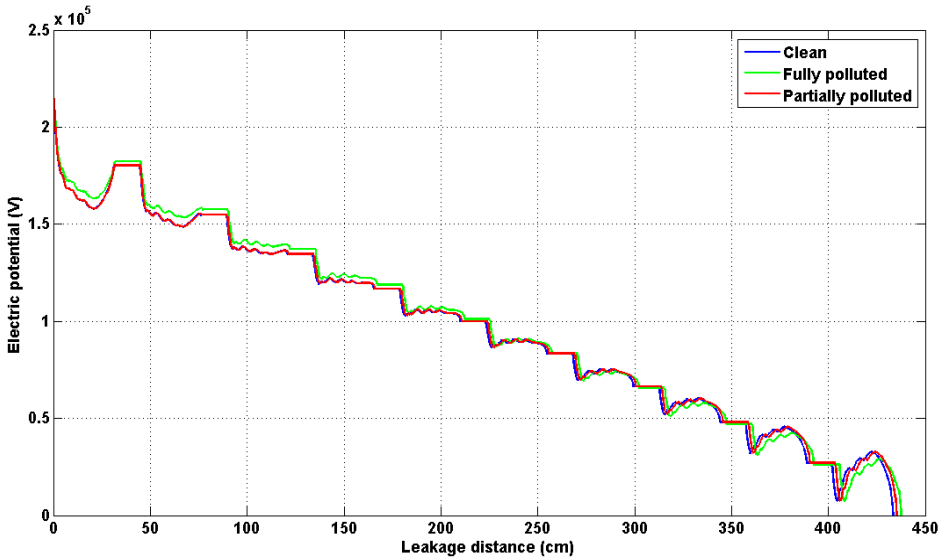

Figure II.25: Electric potential distribution of a clean and surface shape pollution on the insulators

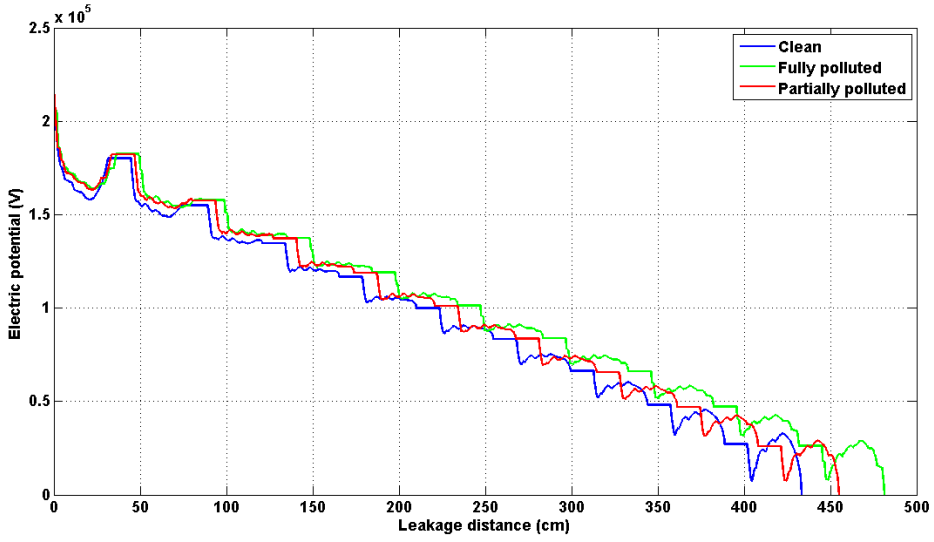

Figure II.26: Electric potential distribution of a clean and droplet shape pollution on the insulators

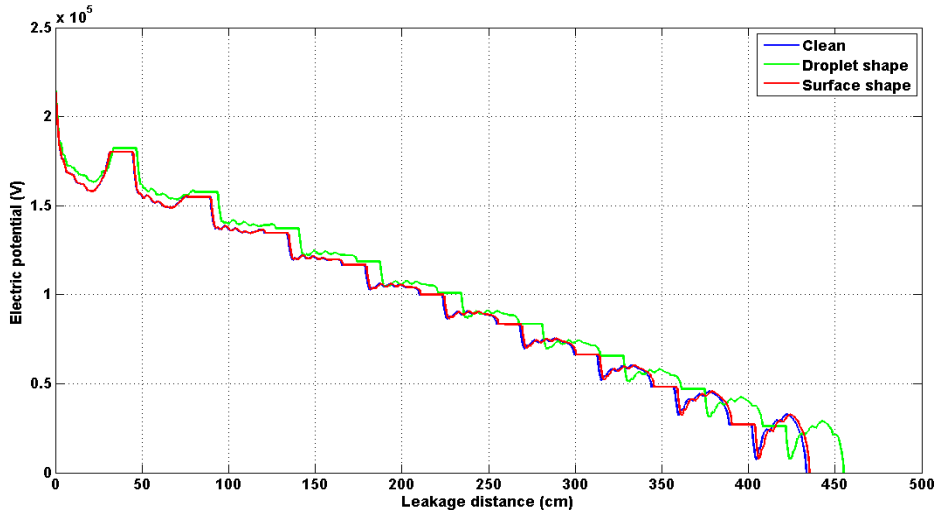

Figure II.27: Electric potential distribution of a clean and partially polluted insulator

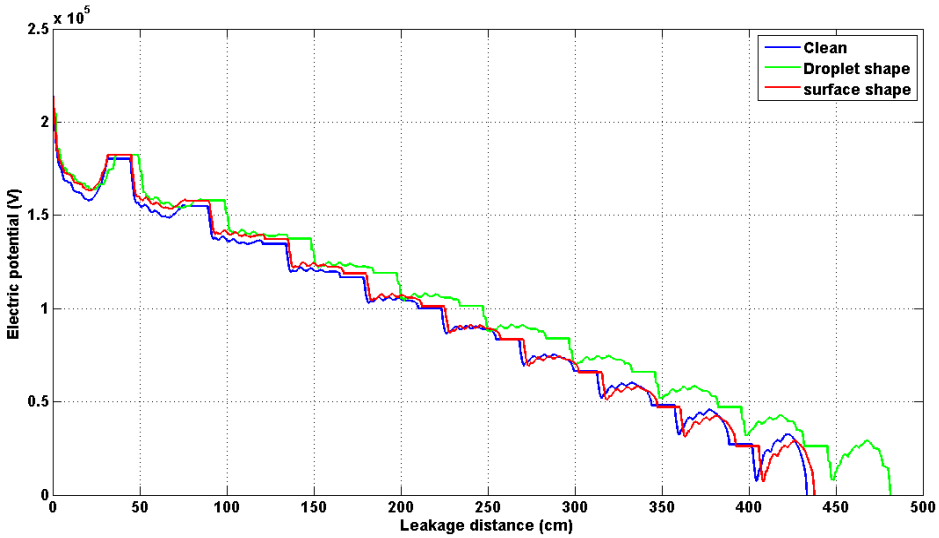

Figure II.28: Electric potential distribution of a clean and fully polluted insulator

Figure II.24 shows that when we get closer to the ground, the potential decreases, whereas When comparing figures (II.25 and II.26), the first and most noticeable difference is the length of the leaking distance between cases, which is a reasonable change given that the pollution has various shapes. The primary observation is that the potential does not significantly vary (as in its value) throughout the many scenarios discussed above. Even the biggest alterations, which are in the cases of the droplet-shaped pollutants (figures (II.27 and II.28)), only cause a little shift. While the other situations result in even more subtle alterations.

Secondly, to further understand the effect that the shape and location of pollution has on the potential, the plot of pollution in the surface and droplet cases is drawn on both the pin side and the groundside.

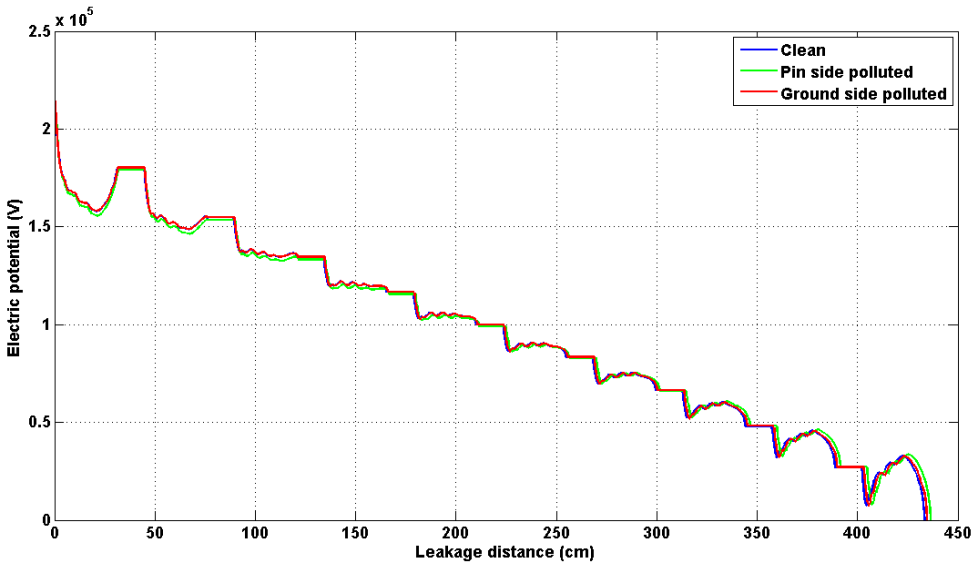

Figure II.29: Electric potential distribution of a clean, pin and groundside polluted insulator (surface shape)

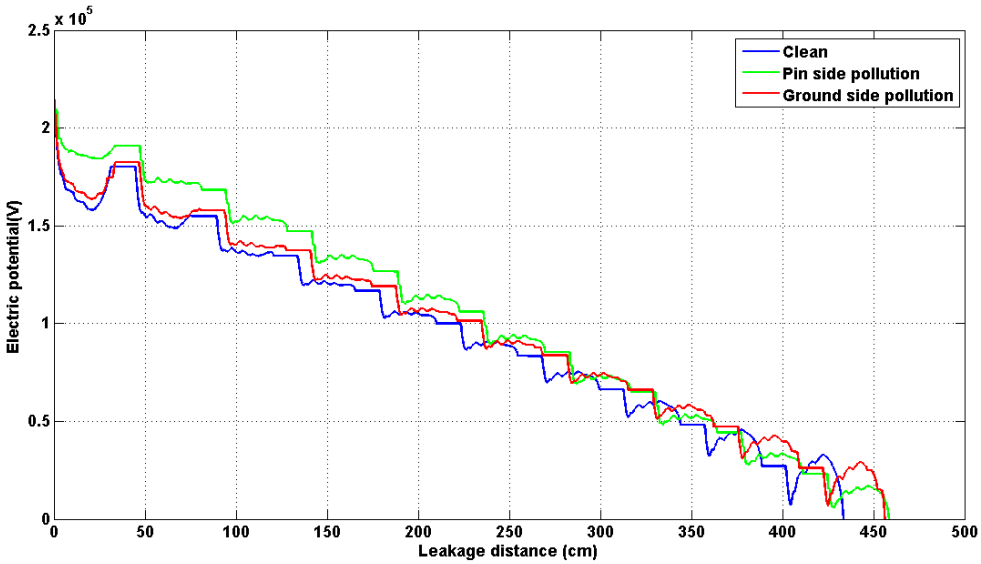

Figure II.30: Electric potential distribution of a clean, pin and groundside polluted insulator (droplets shape)

As shown in figure II.29, the distribution of the potential in the surface-shaped pollution scenario is similar to that in the prior cases in both the pin and groundsides. Figure II.30 illustrates a considerable shift in the shape of the droplets, which is the biggest change to have happened through all the combinations in these simulations. The potential begins higher than the other cases, only to catch up with them in the middle and then fall below them at the leakage distance's end. The main reason for the changes is that the pollution only appears on one side,

in contrast to the previous simulations (Figure II.28), where the droplets are present on both sides, where the pollution appears to calibrate the distribution changes and makes the changes appear much smaller than they actually are. The difference between the two situations in figure II.30 is that the pollution contributes to raise the potential value in the pin side scenario, which is the side of the insulator where the potential value really declines because the petticoats are covered. Because there aren't any obstructions on the groundside of the insulator like there are on the pin side, the potential growth in value is smaller there.

As a final comment, it is clear that pollution in these various quantities or shapes just alters the value of the pollutant.

II.7.2.The electric field distribution

The graphic below shows a 2D surface graph of the electric field in the clean state.

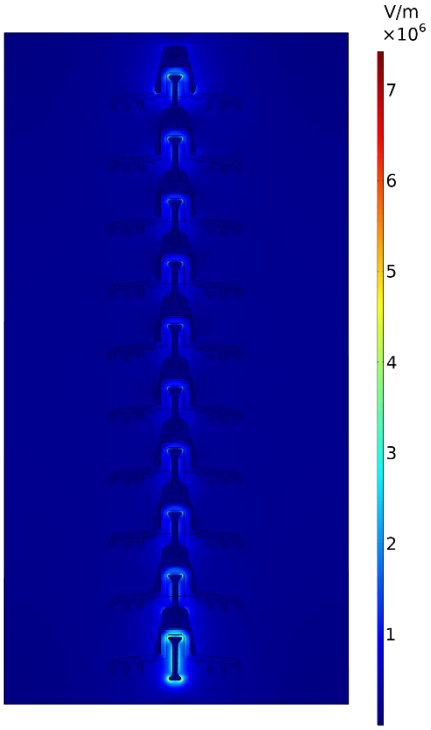

Figure II.31: Surface plot of the electric field in the clean case

According to figure II.31, between the pin and cap of each insulator are where the electric field experiences the biggest shifts. To see the differences between each instance and the clean state of the chain as well as between each other, a 1D plot of all the additional examples is created.

In order to determine how much pollution is there and how it affects field distribution, a plot of pollution in the shape of a surface (fully and partially) and a droplet (fully and partially) is first drawn.

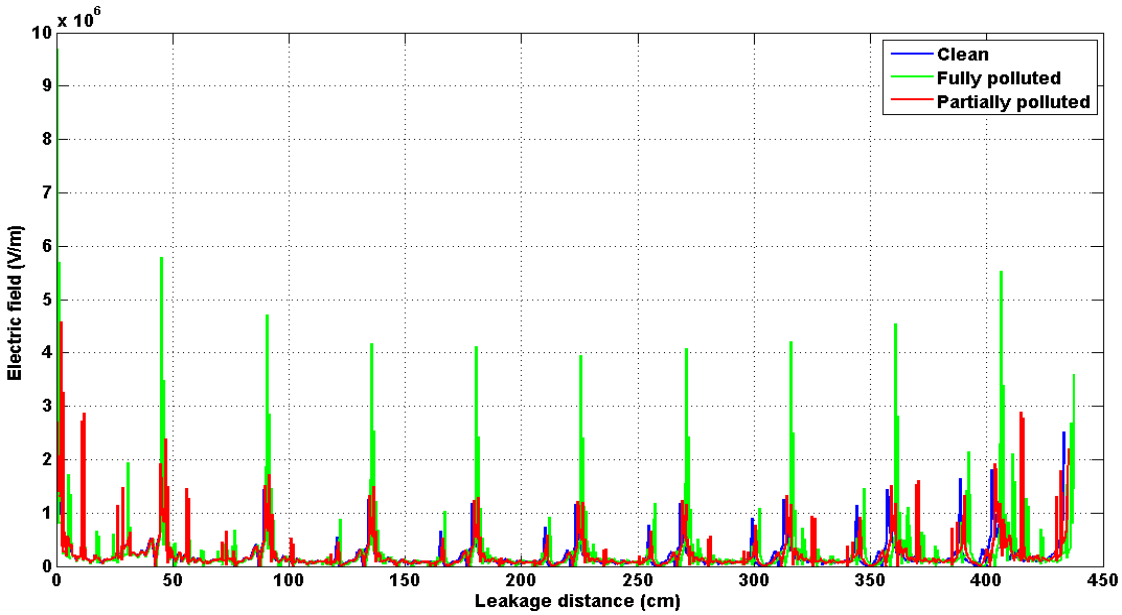

(a)

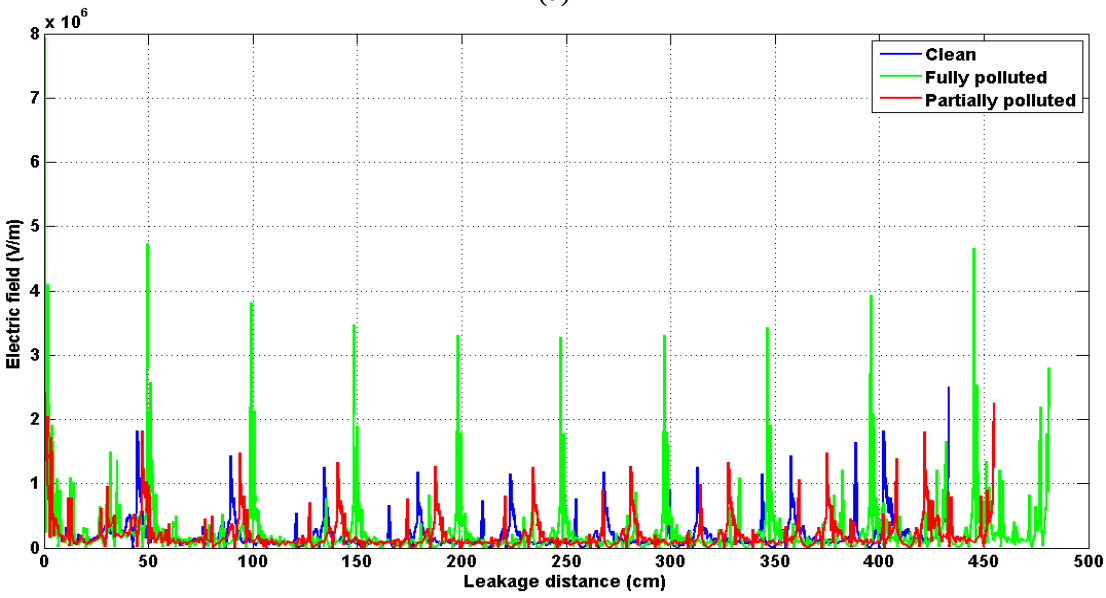

(b)

Figure II.32: Electric field of a clean, surface (a) and droplet (b) shape pollution on the insulators

Figures II.32(a) and II.32(b) show that the field distribution of either the surface shape pollution or the droplet shape pollution is substantially higher in the fully contaminated situation.

At the beginning and the end of the leaking distance, this elevation is projected to be three and two times higher, respectively. While there are no differences between the fields in the clean state and partially polluted case.

Second, a plot of pollution is created to show how it affects the field in both partial (surface and droplet) and full (surface and droplet) forms.

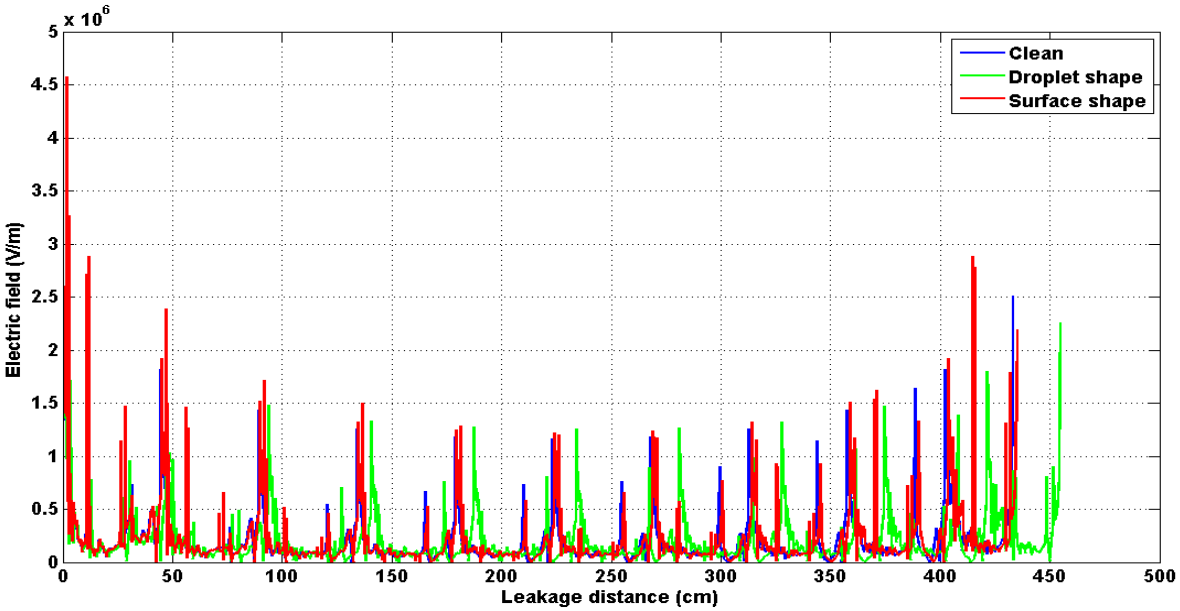

Figure II.33: Electric field distribution of a clean and partially polluted insulator

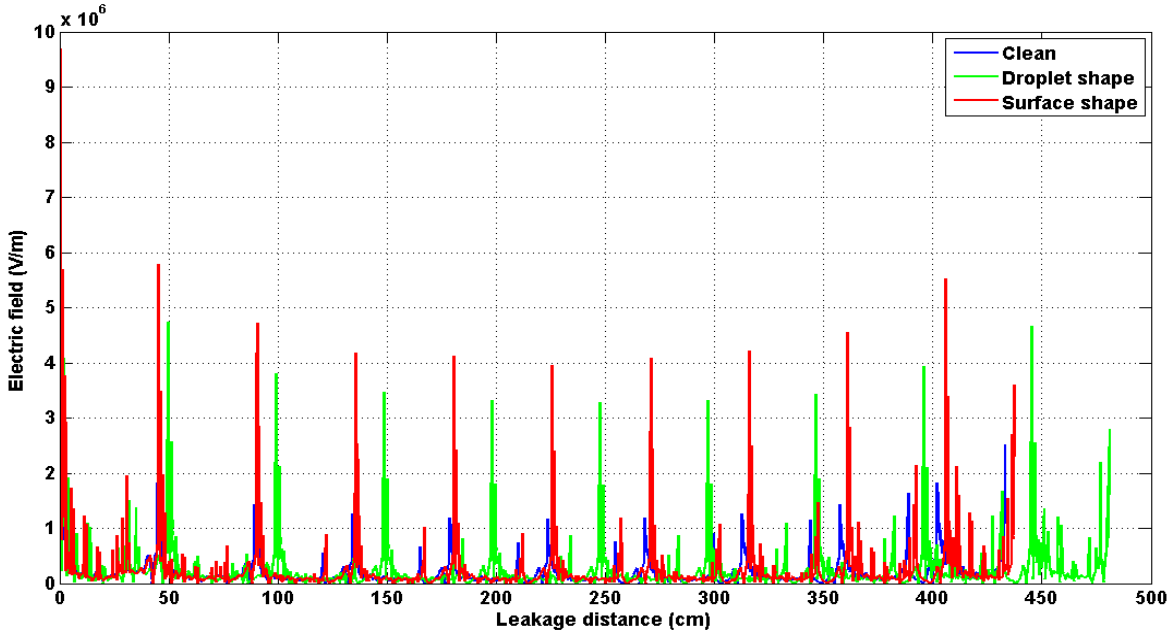

Figure II.34: Electric field distribution of a clean and fully polluted insulator

From figure II.33, it can be inferred that the field's general shape-in both value and shape-remains the same for both the droplet shape and the surface shape when the insulator is only partially contaminated.

This cannot be said for the totally polluted insulator, as seen in figure II.34. Although both pollution cases result in higher value spikes, the pollution caused by the surface shape case has a greater impact on the field values than the pollution caused by the droplet shape case. We can therefore conclude that under these situations, the quantity of pollution has a greater influence than the type of pollution.

In order to determine the effect the pollution's position and shape have on the field distribution, the full (surface and droplet) pollution plot is drawn on both the pin side and the groundside.

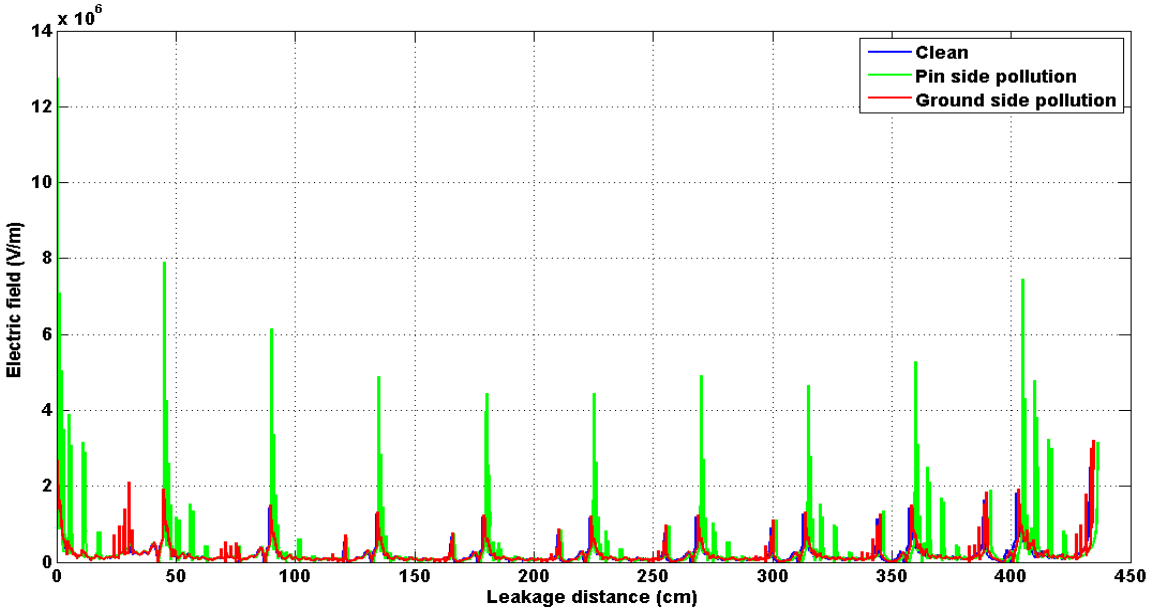

Figure II.35: Electric field distribution of a clean, pin and groundside polluted insulator (surface shape)

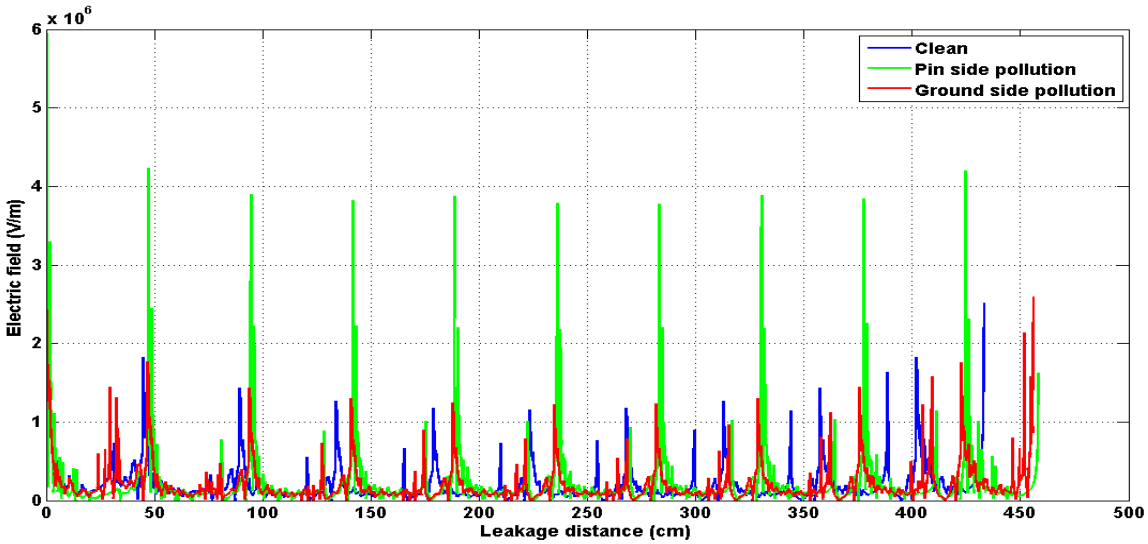

Figure II.36: Electric field distribution of a clean, pin and groundside polluted insulator (droplets shape)

The surface shape pollution on the pin side has the largest value at the beginning, as shown in figure II.35.

While the surface and droplet shape pollution on the groundside is depicted in each of the aforementioned examples, the field distribution remains mostly unchanged.

If we look at the pin side of figures 39 and 40, in addition to the rise in the spike values, we can also see that the spike of the field distribution in the surface-shaped pollution decreases as we approach the middle and increases once more as we approach the leakage distance's end.

Whereas the spike values in the droplet-shaped pollution remain constant the entire length of the leakage distance.

The change in values at the beginning, end, and especially at the beginning is another difficult-to-see alteration.

The values for each example at the beginning and end of the leaking distance are summarized in the table below.

Table II.2. The values of the electric field in each case at the start and the end of the leakage distance.

Pollution characteristics	Pollution shape	at the start (V/m)	at the end (V/m)
Fully polluted	Droplet	7.937128×10^6	2.803364×10^6
	Surface	9.692605×10^6	3.593068×10^6
Partially polluted	Droplet	3.001954×10^6	2.257312×10^6
	Surface	3.249824×10^6	2.196133×10^6
Pin side	Droplet	5.953113×10^6	1.625926×10^6
	Surface	12.766791×10^6	3.168915×10^6
Groundside	Droplet	2.918658×10^6	2.592762×10^6
	Surface	3.258763×10^6	3.206301×10^6

Table II.2 demonstrates that the electric field changes more when an insulator chain is completely contaminated. In other words, the more pollution, the greater the impact, but unlike the electric potential, the electric field changes more when the pollution is in the form of a surface than when it is in the form of a droplet. Contrary to the electric potential, the electric field with the highest value was found in the case of a surface-shaped pollution rather than a droplet-shaped pollution. The highest change occurred where the pollution is placed on the pin side and it is the highest value found across all the different simulations. These earlier observations demonstrate that the pollution's quantity, shape, and position all have an impact on the electric field, although the impact of quantity and position is more pronounced.

II.8.Conclusion

Our numerical models have produced insightful results for the performance of insulators under various pollution scenarios. Electric potential and field behavior patterns appear in the two-dimensional simulation, providing predicting capability for uniform contamination scenarios. Notably, the electric field shows irregular spikes, creating risks of early aging and flashover, whereas the electric potential shows virtually little change in form aside from minor deviations on the pin side.

We investigated the 1512L insulator chain in both clean and contaminated environments in the three-dimensional simulation. On the pin side, pollution in the form of droplets reacts significantly, with modest potential modifications in other circumstances. The electric field, on the other hand, exhibits considerable modifications in all pollution scenarios, with surface-shaped pollution in fully polluted insulators producing the most severe alterations.

This thorough understanding helps with insulator design optimization and knowing the best region placement for their function. This modeling approach should be quite useful for evaluating insulator performance and extending their operating life.

The following chapter would highlight the response surface methodology and the usage of the central composite design in the making of a tailored model for the prediction of a flashover voltage for the 1512L insulator.

CHAPTER III

Response Surface Methodology

III.1. Introduction

Artificial intelligence techniques have been used for the prediction and monitoring of transmission and distribution lines and more specifically for our purpose, the outdoor insulators to increase the continuity and reliability of power transmission and decrease the problems of flashover and breakdown of insulators throughout the whole process.

In research and scientific investigations, the Design of Experiments (DOE) is a systematic method used to optimize procedures, look into the connections between variables, and make data-driven judgments. DOE enables researchers to quickly obtain important data and develop meaningful conclusions by carefully organizing the experimental setup, managing variables, and randomizing treatments, thereby improving the reliability and effectiveness of their investigations [44].

The Response Surface Methodology (RSM) is a methodology that belongs to the design of experiments category it is used to model and optimize complicated systems with many variables. Using a chosen experimental design, a number of experimental runs are normally created using this process. It develops mathematical models defining the link between input elements and output reactions using experimental data. Particularly when the relationship between the variables is non-linear, RSM aids in the efficient discovery of optimal circumstances that maximize or reduce the response. It is frequently used for efficient testing and decision-making in engineering, chemistry, and product development [45].

The purpose of our study is to use the response surface methodology to get a mathematical model for the prediction of flashover voltage and to introduce an idea that the use of a tailored model for the prediction of the flashover voltage is way more accurate than a generalized model that predicts for any insulator so in other words models tailored for certain insulators that are widely used should be made to decrease the problem of flashover before going for a model that is made for any insulator.

In this chapter, an introduction to the response surface methodology is made and a more in depth study about one of its most popular types namely the central composite design is made. Finally, the desired model was made with different cases of the central composite design to better see the changes that occur on the model once different parameters of the central composite design are used.

III.2.RSM designs

The response surface methodology contains many designs but there are two major designs used namely the central composite design (CCD) and the box behnken design (BBD). CCD in figure III.1 contains the center points which are eventually augmented with the group of "star points" that allows estimation of curvature and additional points called cube points which are the high and low values for the factors [46].

BBD in figure III.2 have center points just like the CCD and unlike it, it has points situated on the center of each of the edges of the box called edge points rather than cube points [47]. One thing that is easily highlighted is the existence of the star points that BBD does not have. Star points also allow for more open field of factor values to be used if needed which the Box-Behnken design doesn't have since its point are constricted.

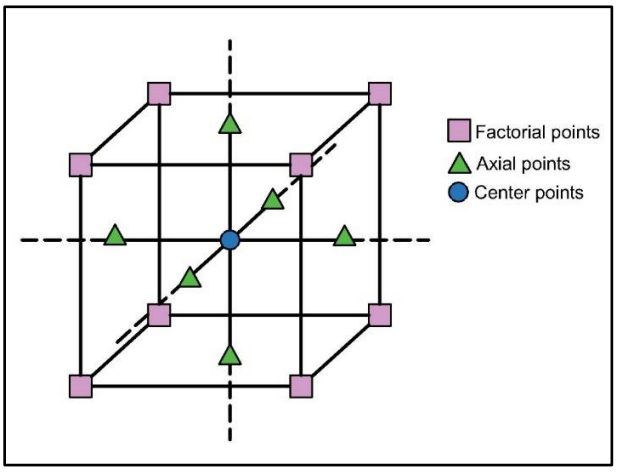

Figure III.1: Central composite design

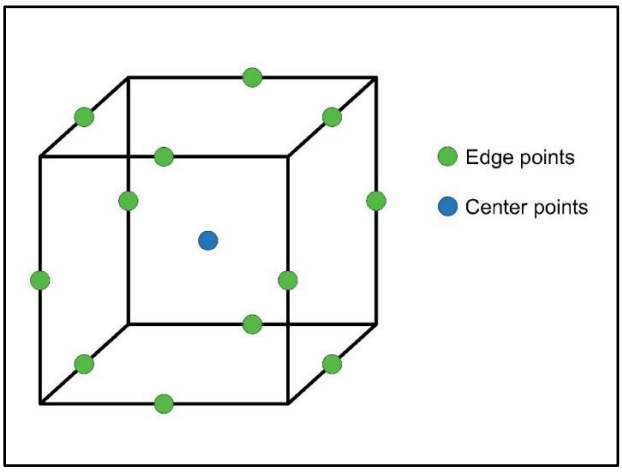

Figure III.2: Box-behnken design

III.3.Difference between BBD and CCD

BBD requires fewer runs than CCD, and it has a uniform variance across the design space. However, BBD also has some limitations. BBD design points steer clear of the extreme corners and are centered around the midpoint of the factor ranges. In the farthest parts of the experimental space, where the model might not be reliable. and it cannot handle categorical factors very well

- Having star points means that the points in most cases will be outside the cube, which may lead to values that cannot exist this shall be explained more in depth later.
- BBD has fewer runs as compared to CCD due to the existence of the star points.

- CCD requires at least two factors to create a model while BBD requires three factors.
- CCD is more dynamic due the star points while BBD is a more static design.

III.4. Steps of the central composite design

CCD and BBD have relatively the same steps except for the fact that BBD does not have the alpha (α) value so it is a pretty static design when that is concerned. In the rest of this work we will talk about the CCD design since they have almost the same steps. Any experiment using this method will go through the following steps

- Selection of the factors along with their levels and ranges
- Selection of the value of Alpha determining which type of design is going to be used
- Selection of the response variable
- Conducting the experiments needed
- Selection of the model
- getting the necessary analysis (ANOVA tests) to validate the model
- finally comes the optimization

The following are some terms found in RSM

Factors

Factors refer to the variables studied in the experiment and are also referred to as independent variables. There are two different types of factors

Continuous factors

In addition, referred to as experimental factors or quantitative factors are the type that can be assigned values (levels) and can be changed to have different values for example speed, temperature, etc.

Categorical factors

In addition, referred to as classification factors or qualitative factors are the type that come as categories or labels and cannot be changed such as the sex, brand, etc.

Responses

The response variable also known as the dependent variable and it is the outcome that we desire from doing the experiments and the variable that the optimization will be done for to get.

III.5. The Alpha (α) value

The Alpha (α) value is the distance between the center point and axial point in a coded value and defines the position of the axial point whether they are inside the cube, outside the cube or on the face of the cube. Should Alpha (α) have a value of less than one that means that the axial points will be positioned on the inside of the cube. Should Alpha (α) have a value of more than one that means that the axial points will be positioned on the outside of the cube. Should Alpha (α) have a value of '1' then that means that the axial points will be positioned on the face of the cube.

III.5.1. Calculations

The above mentioned cases of alpha (α) values create 5 factor levels namely the extremely high level, high level, center level, low level and extremely low level as seen in table III.1, except for when the value of alpha (α) is equal to 1 where the extremely high and extremely low levels do not exist meaning only 3 levels are left as seen in table III.2.

To get the values of the factors needed at the alpha value the following equations (III.1) and (III.2) are used. For the (+α) value we get

$$Factor(+\alpha) = (value(+\alpha) \times R) + C \quad \text{(III.1)}$$

For the (-α) value we get

$$Factor(-\alpha) = (value(-\alpha) \times R) + C \quad \text{(III.2)}$$

Where R and C are both expressed in their real units and R is the length in factor units between the center point and ± 1 factor level value

C is the factors center point value

Table III.1: Factor level values in the case of alpha higher than one

Factor level	Factor 1	Factor 2	…
-α(extremely low)	Lowest value	Lowest value	Lowest value
-1(low)	Low value	Low value	Low value
0(center)	Center point value	Center point value	Center point value
+1(high)	High value	High value	High value
+α(extremely high)	Highest value	Highest value	Highest value

Table III.2. Factor level values in the case of alpha equals to one

Factor level	Factor 1	Factor 2	…
-1(low)	Low value	Low value	Low value
0(center)	Center point value	Center point value	Center point value
+1(high)	High value	High value	High value

Note: when choosing the levels for a study the ± 1 levels need extra careful when choosing due to the existence of the ± α level. For example, we want to make a model that has a factor with 1 as the low value and 10 as a high value in this case the ± α of this factor may not exist as the – α will be a value under 0 which may not exist.

Depending on the number of factors as seen in table 3 the Alpha (α) value can be calculated using the following equation

$$\alpha = \left(2^k\right)^{1/4} \quad \text{(III.3)}$$

Where k is the number of factors in the study.

Table 3: Alpha values depending on the number of factors

Number of factors in a study	α value
2	±1.414
3	±1.682
4	±2
5	±2.378

III.5.2.Types of design in CCD

The Alpha (α) value is what determines the type of the CCD we are using and there is three types of CCD

III.5.2.1.Circumscribed design

The CCC design is the original design of CCD and what should be gotten through the normal calculation since this type is when the value of Alpha (α) is higher than one as seen in figure III.3.

A higher than one value of Alpha (α) will produce new extreme points for the original high and low values which in the end make for a 5 level in the factors.

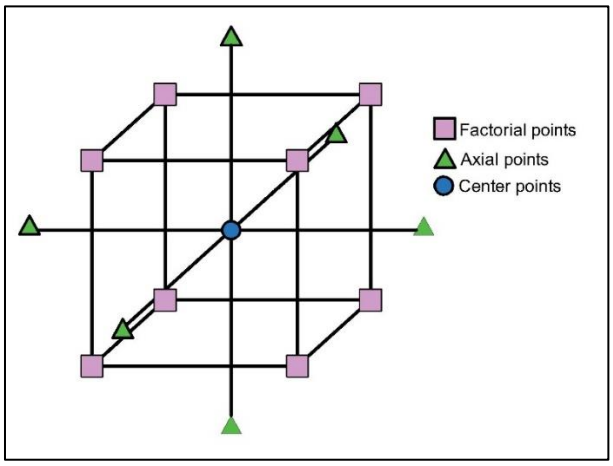

Figure III.3: Circumscribed design

III.5.2.2.Face centered design

CCF design occurs when the Alpha (α) value is equal to one, which means that the star points will be situated on the face of the cube as seen in figure III.4. This type of design requires only three levels of the factors the high, center and low levels.

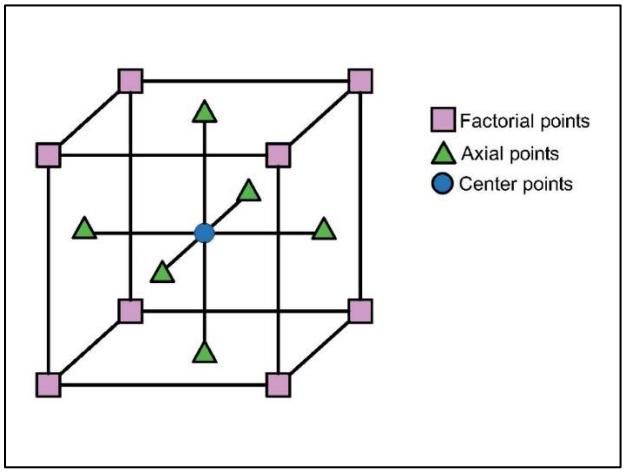

Figure III.4: Face centered design

III.5.2.3.Inscribed design

The CCI design is a design where the initial high and low value are the true limits for the factors as seen in figure III.5, in other words the value of Alpha (α) will be lower than one and so we get five levels for the factor still.

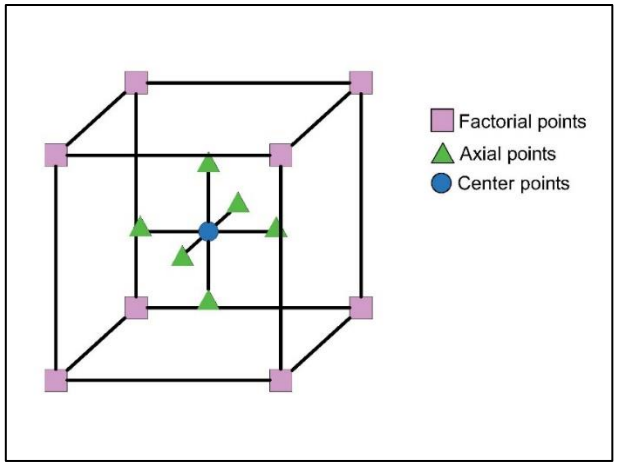

Figure III.5: Inscribed design

Both the inscribed and circumscribed designs are called rotatable design [48] because both the axial and cubic points have the same distance from the center as seen in figure III.6.

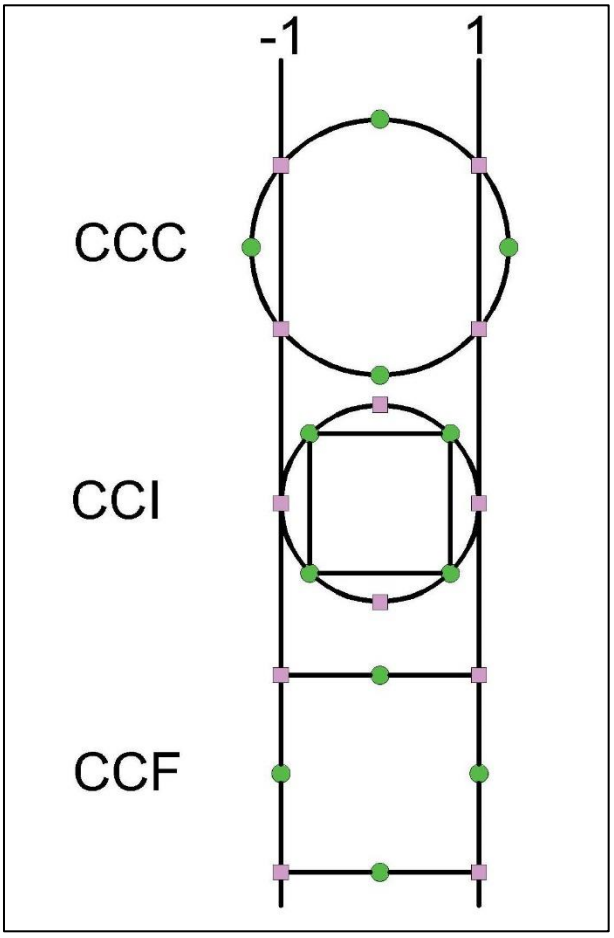

Figure III.6: Difference between the types of CCD

III.6. The experiments and choosing the model

In Minitab 19 after determining the alpha (α), you get the outline of the experiments needed for the study. The number of experiments can be calculated through the following equation:

$$N = k^2 + 2k + n \quad \text{(III.4)}$$

Where

k is the number of factors

n is number of center points

For a study with 2 factors and 3 factors, we get the following experimental setup as seen in tables (III.4 and III.5) respectively. These designs are made by Minitab in coded values and a coded value is for example speed of a car in figure III.7.

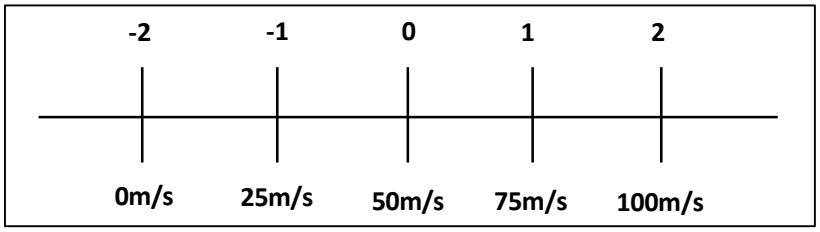

Figure III.7. Representation of coded values

Table III.4: Design plan for a two factors experiment

No.		Factor 1	Factor 2	Response
1	Factorial or cubic point runs = 4	-1	-1	The experimental outcome at each run
2		1	-1	
3		-1	1	
4		1	1	
5	Star points runs = 4	-1.414	0	
6		1.414	0	
7		0	-1.414	
8		0	1.414	
9	Center point	0	0	

Table 5: Design plan for a three factors experiment

No.		Factor 1	Factor 2	Factor 3	Response
1	Factorial or cubic point runs = 8	-1	-1	-1	The experimental outcome at each run
2		1	-1	-1	
3		-1	1	-1	
4		1	1	-1	
5		-1	-1	1	
6		1	-1	1	
7		-1	1	1	
8		1	1	1	
9	Star points runs = 8	-1.682	0	0	
10		1.682	0	0	
11		0	-1.682	0	
12		0	1.682	0	
13		0	0	-1.682	
14		0	0	1.682	
15	Center point	0	0	0	

To get the desired outcome from our experiment this design plan can be fitted into one of the following models

III.6.1.First order model

First order model when the responses lean more towards linearity meaning a less complicated outcome or a response that does not need that much of precision

$$y = \beta_0 + \sum_{i=1}^{k} \beta_i X_i \quad \text{(III.5)}$$

$$y = \beta_0 + \beta_1 X_1 + \beta_2 X_2 + ... + e \quad \text{(III.6)}$$

III.6.2.Linear and interaction response model

A bit more precise than the steepest response model the screening response model is the same with the addition of the interaction between the factors term

$$y = \beta_0 + \sum_{i=1}^{k} \beta_i X_i + \sum_{i=1}^{k-1} \sum_{j=i+1}^{k} \beta_{ij} X_i X_j + e \quad \text{(III.7)}$$

$$y = \beta_0 + \beta_1 X_1 + \beta_2 X_2 + ... + \beta_{12} X_1 X_2 + ... + e \quad \text{(III.8)}$$

III.6.3.Second order model

However, for better precision especially when nonlinearity is reported a second order or quadratic model should be used in the following form

$$y = \beta_0 + \sum_{i=1}^{k} \beta_i X_i + \sum_{i=1}^{k} \beta_{ii} X_i^2 + \sum_{i=1}^{k-1} \sum_{j=i+1}^{k} \beta_{ij} X_i X_j + e \quad \text{(III.9)}$$

$$y = \beta_0 + \beta_1 X_1 + \beta_2 X_2 + ... + \beta_{11} X_1^2 + \beta_{22} X_1^2 + ... + \beta_{12} X_1 X_2 + ... + e \quad \text{(III.10)}$$

Where

Y is the response

β_0 is the intercept constant or overall mean response

X_i is the main terms effect

X_iX_j is the interaction terms between the factors

X_i^2 are the squared terms

For example we have a 2 factor study and we want to put it in a first order model let's say the design in table III.4. Let's call factor 1 as A and factor 2 as B we get

$$y = \beta_0 + \sum_{i=1}^{k} \beta_i X_i + e \quad \text{(III.11)}$$

$$\left.\begin{aligned} y_1 &= \beta_0 + (-1\ \ value)\beta_A + (-1\ \ value)\beta_B + e \\ y_2 &= \beta_0 + (1\ \ value)\beta_A + (-1\ \ value)\beta_B + e \\ y_3 &= \beta_0 + (-1\ \ value)\beta_A + (1\ \ value)\beta_B + e \\ &\vdots \\ y_9 &= \beta_0 + (0\ \ value)\beta_A + (0\ \ value)\beta_B + e \end{aligned}\right\} \quad \text{(III.12)}$$

The set of equations (III.12) will be solved to get the constant coefficients and the same would be in the second order model or any model. Minitab uses matrices to solve these equations, one containing the responses, which is the matrix of the observed responses Y, one containing the factor values and one for the coefficients.

$$Y = \begin{bmatrix} y_1 \\ y_2 \\ \vdots \\ y_n \end{bmatrix}$$

$$X = \begin{bmatrix} 1 & x_{11} & x_{21} & x_{11}^2 & x_{21}^2 & x_{11}x_{21} \\ 1 & x_{12} & x_{22} & x_{12}^2 & x_{22}^2 & x_{12}x_{22} \\ \vdots & \vdots & \vdots & \vdots & \vdots & \vdots \\ 1 & x_{19} & x_{29} & x_{19}^2 & x_{29}^2 & x_{19}x_{29} \end{bmatrix}$$

$$\beta = \begin{bmatrix} \beta_0 \\ \beta_1 \\ \beta_2 \\ \beta_{11} \\ \beta_{22} \\ \beta_{12} \end{bmatrix}$$

The X and β matrices is how they should look like for second order models with 2 factors and 9 experiments.

In the end the equation coefficients are calculated through

$$\beta = \left(X^T X\right)^{-1} X^T Y \qquad \text{(III.13)}$$

Where X^T is the transposed matrix of the X matrix

Note that in the case where the number of variables is equal to the number of equations the degrees of freedom are non-existent meaning that we simply have no way to test the models term significance.

While choosing the model for the study, another option will be needed and that is the confidence interval. A confidence interval of a value of 95% is usually appropriate in any study,

this value helps Minitab in calculating the P-value, and this is on the terms we need to interpret for our model.

The P-value tells whether a term in our model is significant or not so a term above 0.05 is a non-significant term and can be erased from the model and a term below 0.05 is a significant term and is kept. It can be calculated using the degrees of freedom to get the value of the T-value and the get the P-value.

III.7. Analysis of variance (ANOVA)

ANOVA are statistical tests that we use for the confirmation of the model such as which factor has a higher influence on the response, which terms of the model are significant and which are not and other such tests.

Many terms help to identify whether a model is good or not so will talk about the major terms that are looked into the most and are more accurate and easy to interpret [49].

Minitab introduces the following statistical terms in numbers so the interpretation of the results is easier.

III.7.1. The standard deviation

It is denoted by S and is the standard deviation value of the difference between the experimental value and the fitted values.

It can be calculated through the following equation

$$S = \sqrt{\frac{\sum_{i=1}^{n} \left(y_i - y_{esti} \right)^2}{N-2}} \qquad \text{(III.14)}$$

Where

Y_i is the data

$Y_{est\ I}$ is the predicted values

N is the number of the data points

III.7.2. The R-sq. value

The R2 denotes the variation in percentage of the response given by the model, which basically means that it is a term that tells how much the model fits the data. It is calculated using the following equation

$$R^2 = 1 - \left(\frac{SS_{Error}}{SS_{Total}} \right) \quad \text{(III.15)}$$

Where

SS_{Error} is the sum of squares error and is calculated by

$$SS_{Error} = \sum_{i}^{n} \left(y_i - y_i \right)^2 \quad \text{(III.16)}$$

SS_{Total} is the total sum of squares and is calculated by

$$SS_{Total} = \sum_{i}^{n} \left(y_i - \bar{y} \right)^2 \quad \text{(III.17)}$$

III.7.3. The adjusted R-sq. value

The adjusted R2 tells whether the terms of the model are impactful on the model. Table 6 shows an example of three models that we added a new factor from the first model that had a single factor to the third model that has 3 factors. We see that at first an R2 and adjusted R2 of 60% and 55% respectively and after adding an additional factor to the model we 71% and 65% which is normal, but after we added a third factor we see that the R2 changes but the adjusted R2 doesn't change so we can consider removing the third factor for having no improvement on the model.

Table III.6. Example about the effect of an additional factor has on the R^2 and adjusted R^2

Model	Factor 1	Factor 2	Factor 3	R^2	Adjusted R^2
1	X			60%	55%
2	X	X		71%	65%
3	X	X	X	76%	65%

The adjusted R2 can also tell when having a very high value that the values all have an improvement on the model. It is calculated using the R2 value as seen in the following equations

$$adjusted\ R^2 = 1 - \left(\frac{\left(1 - R^2\right)\left(N - 1\right)}{N - k - 1} \right) \quad \text{(III.18)}$$

III.7.4. The predicted R-sq. value

The predicted R2 speaks more of the predictive ability of the model. Minitab calculates in the way of the systematically removing each data column than building a regression equation and seeing how well it is in predicting the data removed from the population.

A model that has a predicted R2 that is a lot less than R2 indicate that the model is over-fit. An over fit model occurs when there are terms that are not important in the model to population.

$$predicted\ R^2 = 1 - \left(\frac{PRESS}{SS_{Total}} \right) \tag{III.19}$$

PRESS is the prediction sum of squares and it is calculated by deleting a data point then the rest N-1 data points are used to make a regression equation to predict the value of the omitted response value (denoted by $y_{i(i)}$) so we get:

$$PRESS = \sum_{i=1}^{n} \left(y_i - y_{i(i)} \right)^2 \tag{III.20}$$

While the previously mentioned terms can greatly help in confirming a model, Minitab gives further confirmations in the form of plots for the residuals of the model. However, before that we need to define some terms.

III.7.5. Outliers

Outliers in residual plots is basically a point where the point deviate from the zero line meaning a high residual value.

III.7.6. Long tail and short tail distributions

We call a distribution having a long tail is when many of the values rest far away from the mean of the data meaning that the tail of the distribution does not hit the zero mark like the normal distribution. It tends to have many outliers with high values. While the short-tailed distribution is the reverse of that hitting the zero mark real quick compared to the normal distribution as seen in figure III.8.

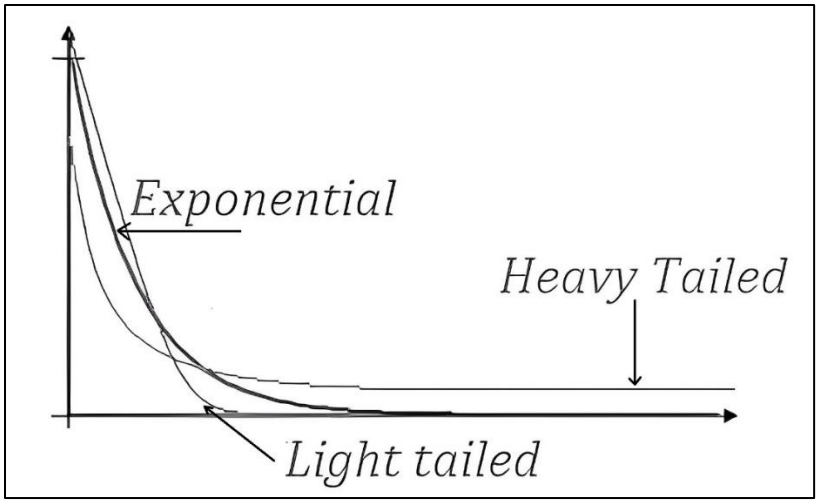

Figure III.8: Normal, long and light-tailed distributions.

III.7.7. Histogram of residuals

This histogram is made to show the distribution of the residuals of all the observations. It is used to determine whether there is skewness or outliners in the data. Therefore, we get three outcomes

- The first where there is a long tail in either direction left skew or right skew
- The second is when we get a bar so far removed from the others, which indicate an outlier
- The last is when the bars are at the center, which is the desirable outcome.

This plot is generally more accurate when there 20 or more observations in the data because you need more observations in the bars to pinpoint the skewness or outliers more accurately.

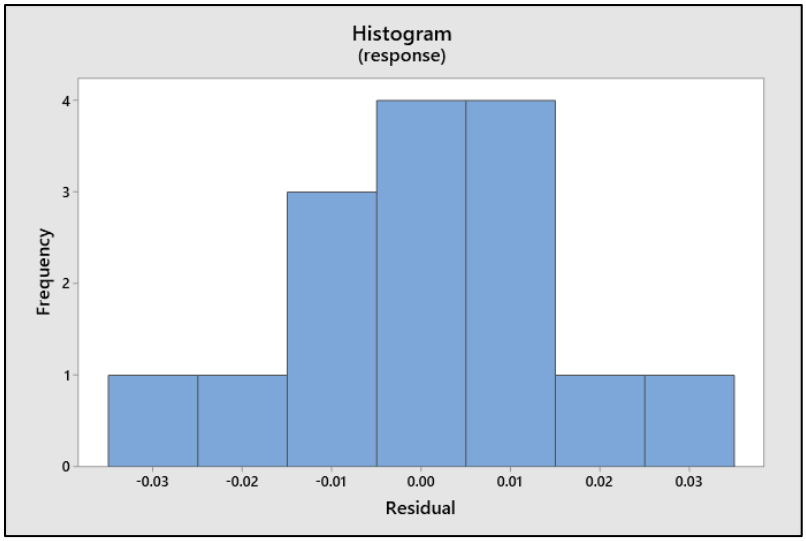

Figure III.9: Histogram of residuals.

III.7.8. Normal probability plot

This plot shows the residuals compared to their expected values when there is normal distribution. This plot should follow a straight line as seen in figure III.10 below. Any other pattern for this plot would need more study because it may indicate one the three problems either short or long tail distribution or an outlier.

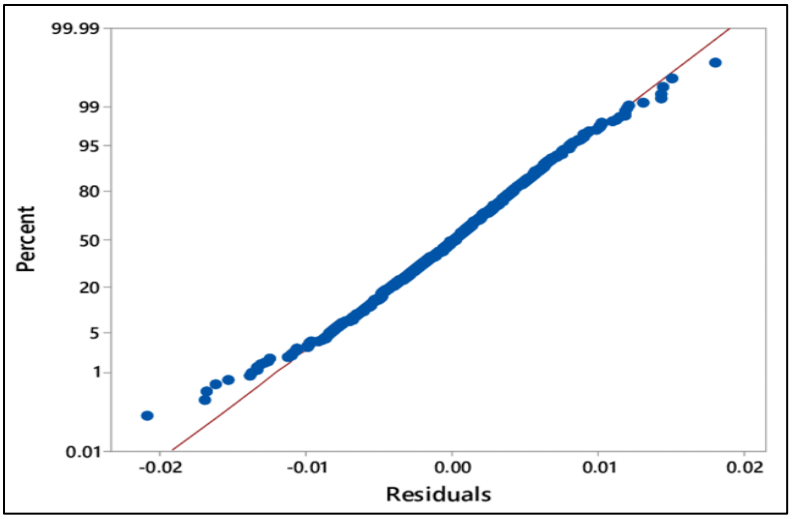

Figure III.10: Normal probability plot.

III.7.9. Residuals versus fits plot

It is a scatter plot of the residuals on the Y-axis and the predicted values on the X-axis. This plot helps in detecting the non-linearity and constant variance of the residuals. In the ideal case, the points should be placed randomly around the zero line with no recognizable pattern like in figure III.11.

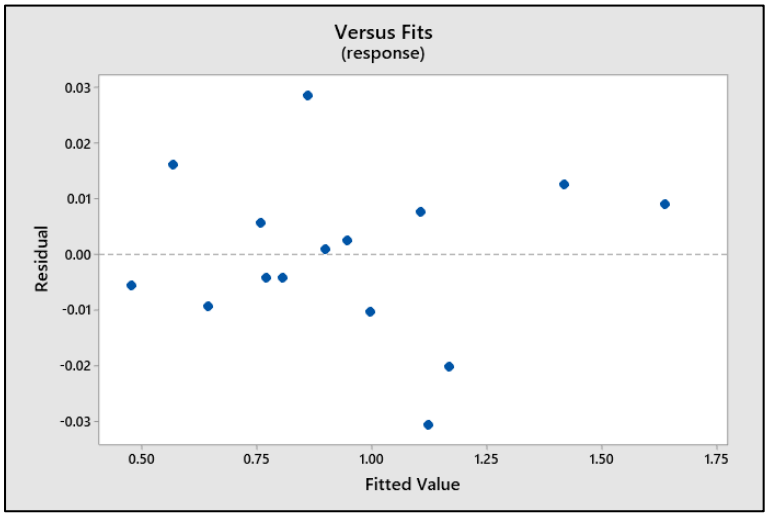

Figure III.11: Residual versus fits plot.

III.7.10.Surface and contour plots

The surface and contour plots are plots that helps in visualizing the response, while determining the trends in the variation of its values.

It is also useful in finding peaks for the response and where the lowest values would occur. While the surface is a 3D plot, the contour is a 2D plot so one is shown as a 3D surface and the other as a 2D surface.

III.8.Case study

The 1512L insulator is an insulator widely used in the Sahara desert regions in Algeria. Our objective is making a model for the prediction of the flashover voltage of this insulator in other words the end result would be a tailored made model for this insulator. We will use the Minitab 19 software and choose the central composite design under the response surface methodology to study this problem and create a prediction model.

First will take a look at the factors that effect this phenomenon and they are the conductivity and the level of pollution. There are many factors that affect the flashover voltage of the insulators but these two factors are the ones that have the highest effect.

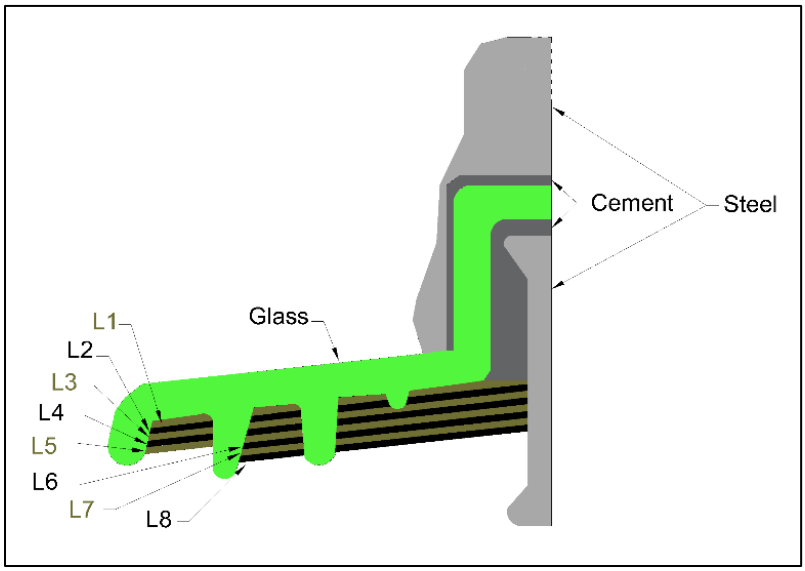

Figure III.12: 1512L Insulator with eight levels of pollution.

Secondly we define the factor levels, we have the conductivity to be between one and eight as the low and high level factors as for the conductivity we take it as zero as low level and the high level will be around 30 mS/cm.

Thirdly, we calculate the Alpha value and since we got two factors according to the previous equation, we get the following result

III.8.1.For a calculated alpha value

Following the traditional mathematical path for this method alpha would come out as presented in the calculation below

$$\alpha = \left(2^k\right)^{1/4} = \left(2^2\right)^{1/4} = 1.414$$

Therefore, the following table is created

Table III.7: Initial factor levels chosen

Factor level	Level of pollution	Conductivity (mS/cm)
-1.414(-α) (extremely low)	-1.65685	-6.31676
-1(low)	0	0
0(center)	4	15.2500
+1(high)	8	30
+1.414(+α) (extremely high)	9.65685	36.8168

The immediately problem we see and it has been talked about previously is the lowest and highest values. In this case, the highest values are acceptable while the lowest values are unacceptable since there is no negative values for our factors.

There is two ways to go about this from here either by changing the high and low values of the factors or changing a different design of CCD, making it face centered or inscribed design. We will first try changing the high and low values of the factors and we get

Table 8: Secondary factor levels chosen

Factor level	Level of pollution	Conductivity (mS/cm)
-1.414(-α) (extremely low)	2.1716	3.3642
-1(low)	3	8.02
0(center)	5	19.26
+1(high)	7	30.5
+1.414(+α) (extremely high)	7.8284	35.1558

After defining the factors, we get the following design plan

Table 9: Design plan for the experiment where the alpha is calculated

No.	Level of pollution	Conductivity (mS/cm)	Flashover voltage
1	-1	-1	55
2	1	-1	45.5
3	-1	1	50.8456
4	1	1	38.6
5	-1.414	0	54.1725
6	1.414	0	35.2660
7	0	-1.414	49.392
8	0	1.414	40.236
9	0	0	42.01

Fitting this design into a second order model we get the following quadratic model

$$U_p = 78.2 - 7.53L - 0.749\sigma + 0.509L^2 + 0.0165\sigma^2 - 0.0305L \cdot \sigma \quad \text{(III.22)}$$

The ANOVA tests for the quadratic model are shown in table III.10

Table 10: Terms and their coefficients and significance value for the second order model

Terms	Coefficients	P-value
Constant	78.2	0.000
L	-7.53	0.006
σ	-0.749	0.042
L · σ	-0.0305	0.618
L · L	0.509	0.255
σ · σ	0.0165	0.247

Table III.10 shows the terms of the model along with their coefficient and the P-value. As already explained about the P-value above we can tell whether a term is significant or not. Looking at the P-value in table III.10, we see that the constant, L and σ are all significant terms and the rest are above the 0.05 value so are insignificant.

By looking at the P-value results we see that other then the first order terms none of the others is significant enough to be in the model.

This also means that using the first order model would give close to the same results so we will try to fit the same data in a first order model and we get the following results

$$U_p = 65.96 - 3.03L - 0.2669\sigma \quad \text{(III.23)}$$

The ANOVA tests for the first order model are shown in table III.11.

Table III.11. Terms and their coefficients and significance value for the first order model

Terms	Coefficients	P-value
Constant	65.96	0.000
L	-3.03	0.000
σ	-0.2669	0.013

Comparing the two models we the obvious thing is that the linear model is less complicated and the P-value of the terms in the second model drops so they are more significant to the model so the more terms we add the higher the value goes and the less there are the more significant the terms become.

However, to compare models we need the summary table tests to get a better view of the capabilities of the models. (See table III.12).

Table III.12. The first order model tests

S	R^2	Adjusted R^2	Predicted R^2
2.42606	91.20%	88.26%	82.39%

Table III.13. The second order model tests

S	R^2	Adjusted R^2	Predicted R^2
2.47374	95.42%	87.80%	***

Both these models give almost the same results or close with minor differences and huge difference in the predicted R2 value.

The standard deviation value of the first order model in table III.12 is better but close with a difference of 0.04768 kV compared to the other, while the second model gives a better value for the R2 value but both are high enough to neglect this difference.

The real difference that we take a look at is the predicted R2 as seen in table III.13, Minitab doesn't give a value for the predicted R2 meaning that the model is over fit which means there are terms that are not important in the model and this would result in the bad predictive ability of the model compared to the first order model that has an 82.39% value. A little drop in the R2 compared to the predictive ability of the model would be better.

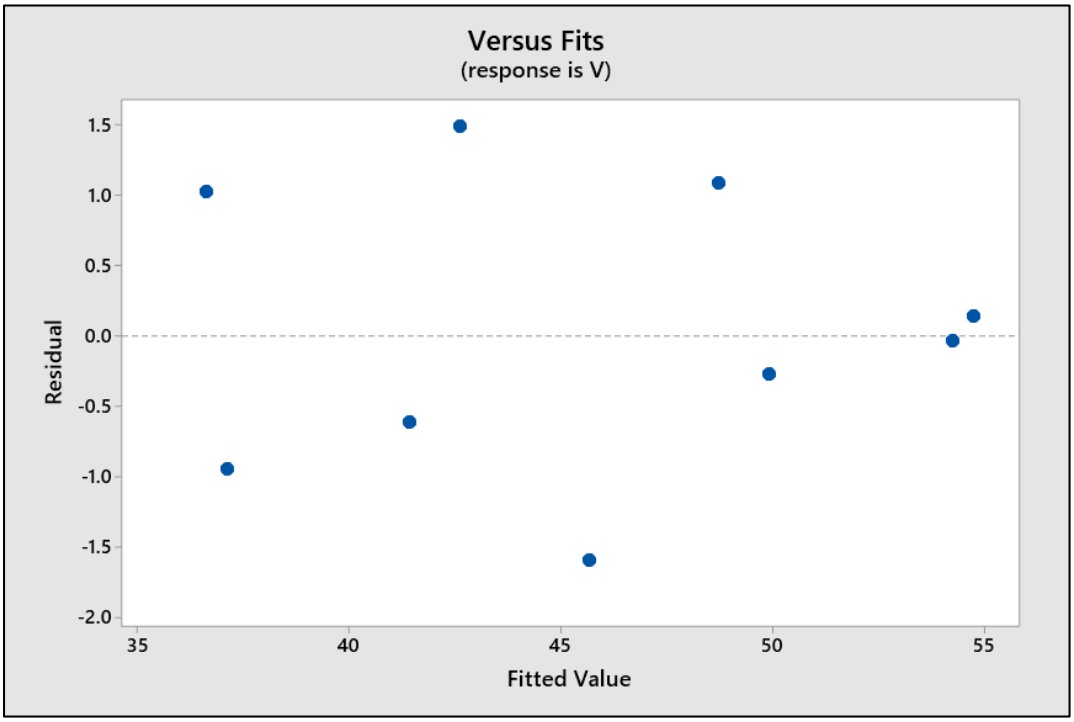

Figure III.13. Residuals versus fits plot of the first order model.

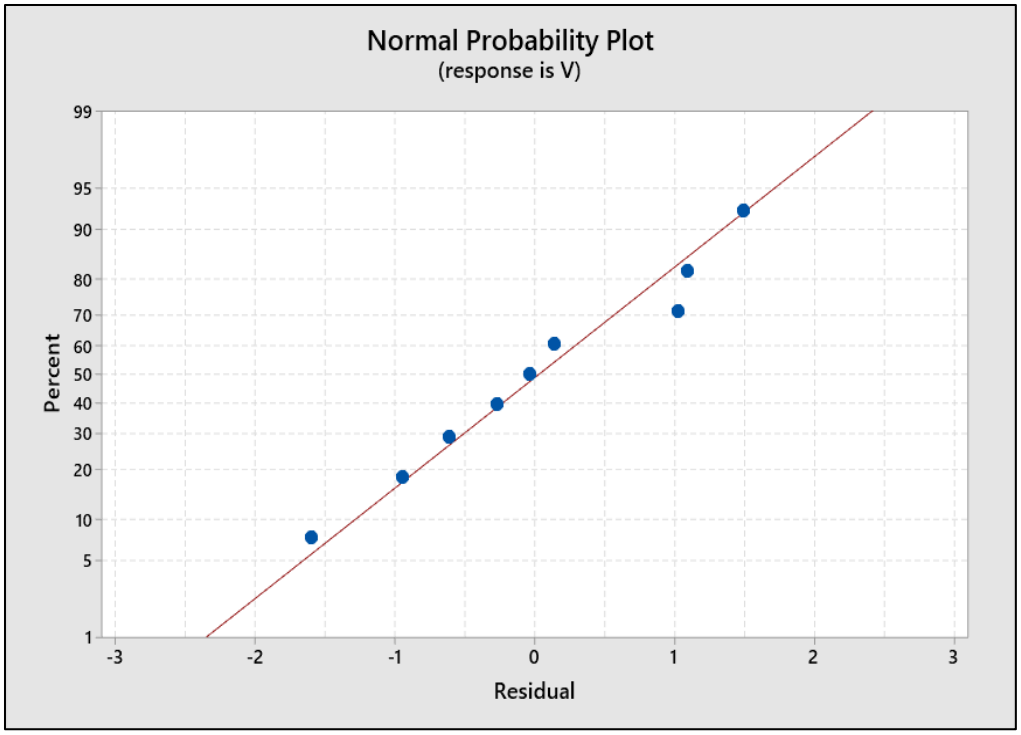

Figure III.14. Normal probability plot of the first order model.

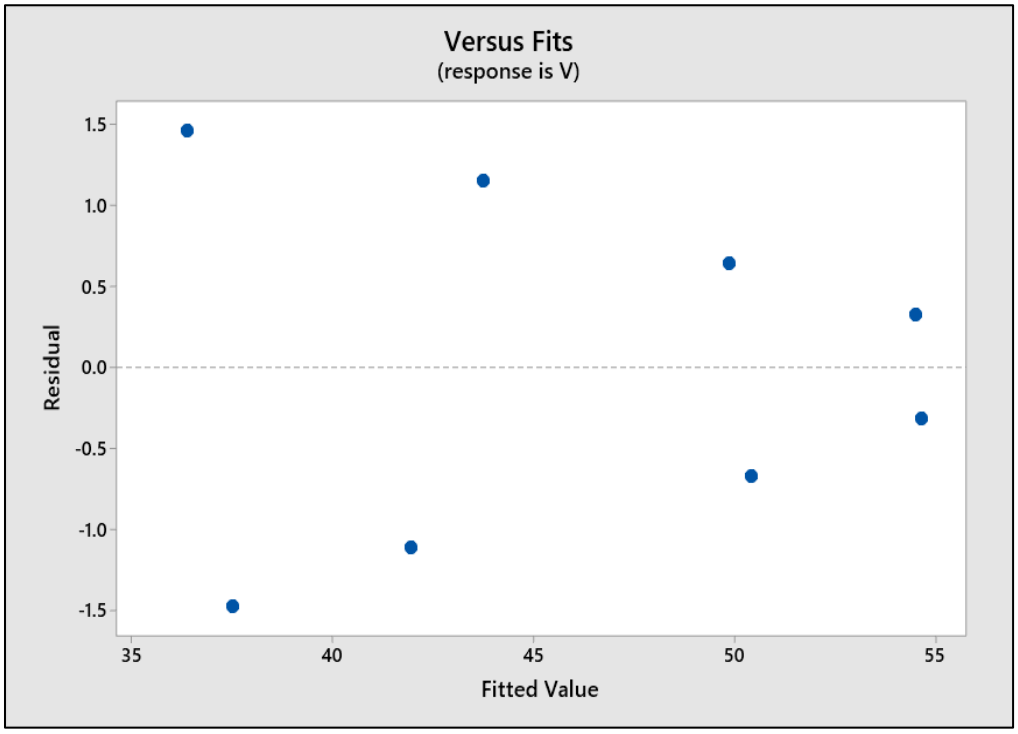

Figure III.15: Residuals versus fits plot of the second order model.

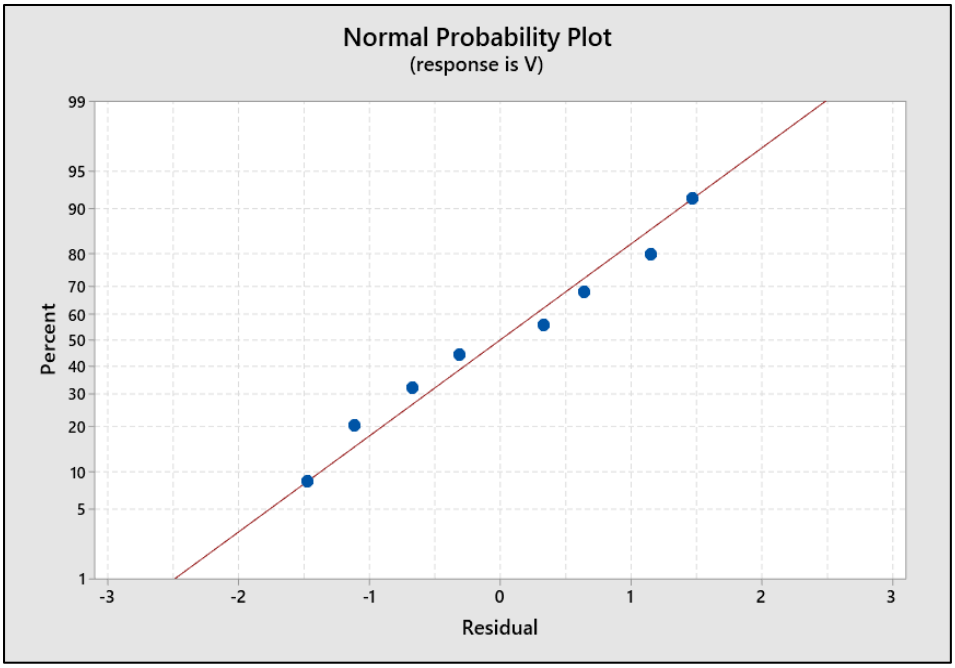

Figure III.16. Normal probability plot of the second order model.

We can conclude from the tests in table III.12 and table III.13 that the first model is better for this case and both figure III.13, Figure III.14 and figure III.15, figure III.16 do not contain any outliners or non-constant variance cases. As a last step we plot the contour and surface plots.

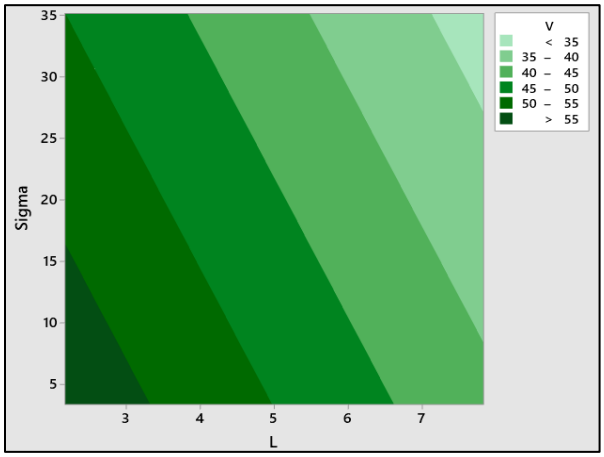

Figure III.17. First order model contour plot.

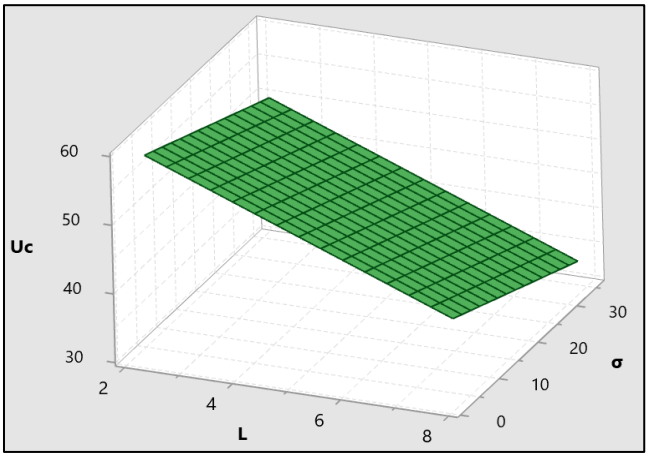

Figure III.18. First order model surface plot.

The first order surface and contour plots in figures (III.18 and III.17) respectively show the change in the response as surface with no curves so we see that the flashover voltage drops as we go further towards higher values of the level of pollution and the conductivity.

Model confirmation

After making the necessary steps and finding the model needed we get additional data not used in the model to do a test to see if the model can indeed predict the response or not.

Table III.14. Percentage error for the first order model**.**

N° Exp	Level of pollution (L)	Conductivity σ (mS/cm)	Flashover voltage (model) kV	Flashover voltage kV	Error (%)
1	3	1.823	56.3834	58	-2.787
2	6	30.5	39.6395	39.312	0.833
3	8	8.02	39.5795	42.672	-7.247

III.8.2.For a chosen alpha (α) = 1

For an alpha that equals one choosing a value from 0 to 8 for the levels of pollution and 0 to 30 for the conductivity would not work because the factorial points for the design plan would contain experiments where the conductivity is 0 and the level of pollution is 8 for instance and this can't happen.

In addition, we chose the levels so that no half a level should appear for example a middle level of four and a half, which would happen in the case where the levels are between one and eight. Therefor we chose the factor levels as seen in table III.15.

Table III.15. Factor levels of the design

Factor level	Level of pollution	Conductivity (mS/cm)
-1 (low)	2	1.8230
0 (center)	5	16.1615
+1 (high)	8	30.5000

Choosing the factor levels like this would give us the following results after putting the design plan seen in table III.16 and analyzing it

We get the following quadratic model

$$U_p = 73.206 - 5.551\,L - 0.5462\,\sigma - 0.03306\,L\sigma + 0.2693\,L^2 - 0.00054\,\sigma^2 \qquad \text{(III.23)}$$

Table III.16. Design plan for the experiment where the alpha is one

No.	Level of pollution	Conductivity (mS/cm)	Flashover voltage
1	-1	-1	62.2000
2	1	-1	45.8000
3	-1	1	47.7120
4	1	1	37.0000
5	-1	0	55.7078
6	1	0	40.9802
7	0	-1	51.3000
8	0	1	40.3200
9	0	0	45.8099

The ANOVA tests are represented in the following table 17 and table 18

Table III.17. Terms coefficients and significance value

Terms	Coefficients	P-value
Constant	73.206	0.000
L	-5.551	0.000
σ	-0.5462	0.000
L · σ	0.03306	0.008
L · L	0.2693	0.004
σ · σ	-0.00054	0.752

That has the following model statistics

Table III.18. The second order model test

S	R^2	Adjusted R^2	Predicted R^2
0.453433	99.88%	99.68%	98.53%

So far looking at table 18 we can see that this is the best model so far with a standard deviation of less than 0.5kV and a high predictive ability stated by the Predicted R2. With as high a value as the R2 and the adjusted R2 in the table this model fits the data very well as well as having the perfect model terms.

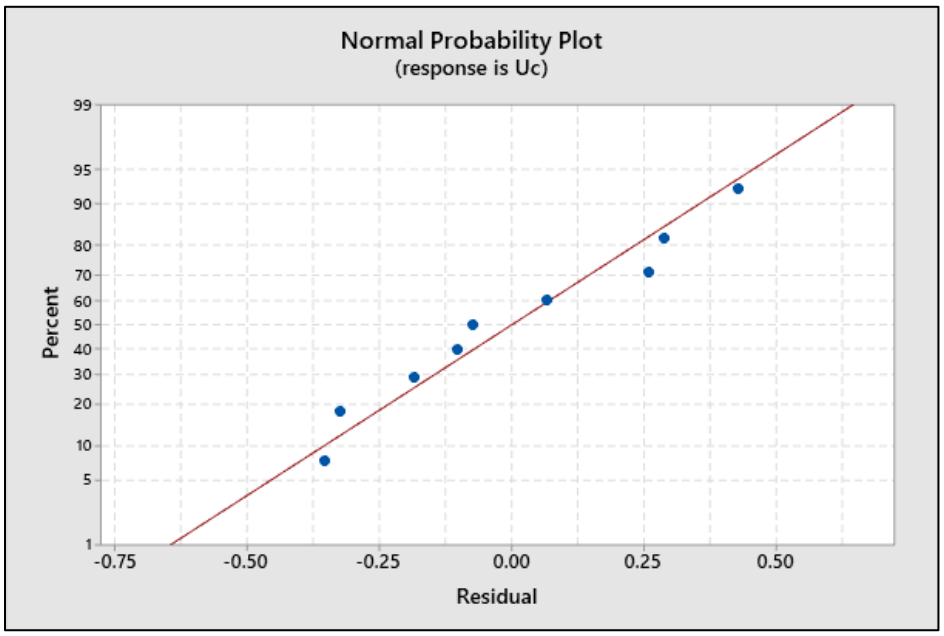

Figure III.19. Normal probability plot of the second model (Alpha=1)

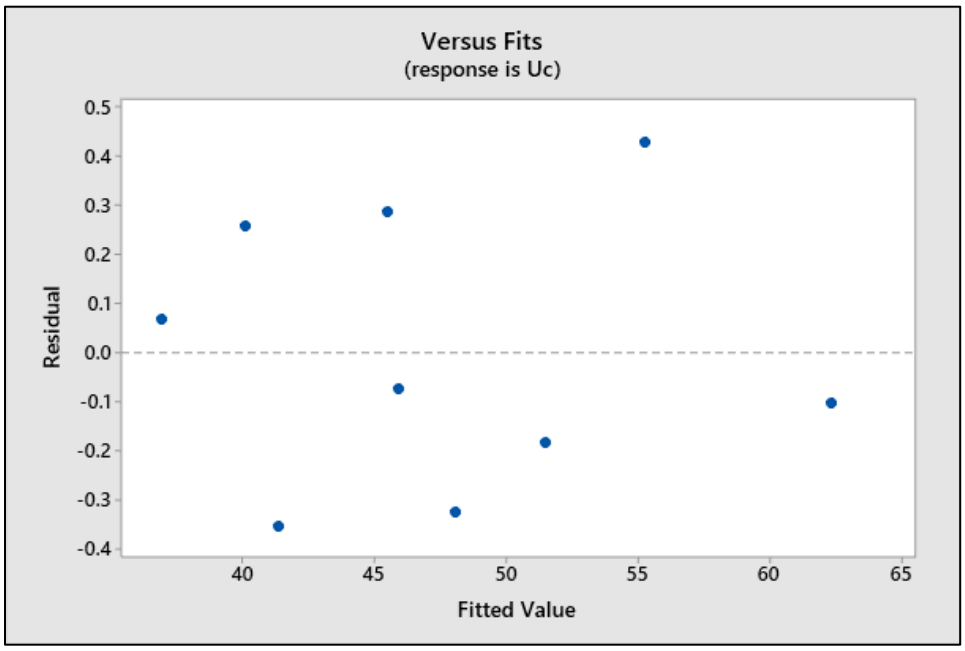

Figure III.20. Residuals versus fits plot of the second model (Alpha =1)

For the residual plots both the normal probability plot and the residuals versus fits plot do not show any kind of pattern or any types of problem which then concludes that this model fits perfectly the data given.

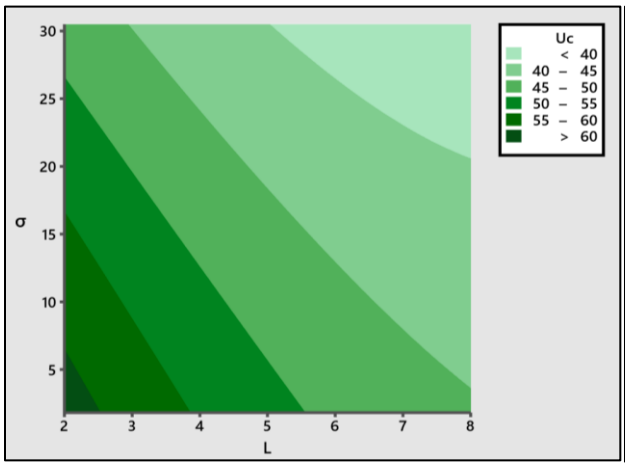

Figure III.21. Second order model (alpha= 1) contour plot

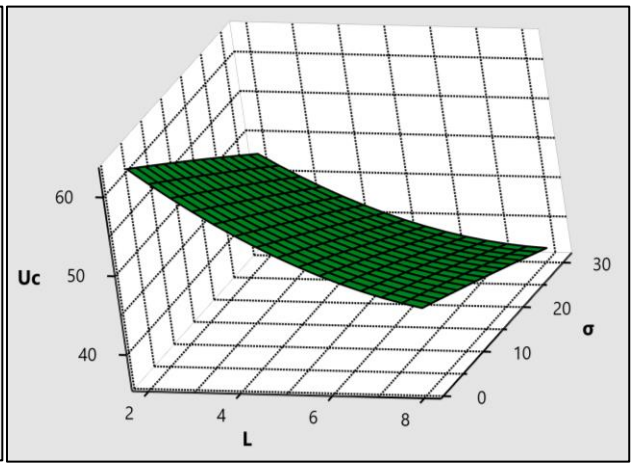

Figure III.22. Second order model (alpha= 1) surface plot

The surface and contour plots in figures 22 and 21 of this model shows the same results as the previous one only with more precision and the surface has a curve so this model represents the voltage better especially since it gave better ANOVA results.

Model confirmation

Again, we proceed to make the necessary steps to confirm whether the model predicts for unknown data points as seen in the form of the error in table III.19.

Table III.19. Percentage error for the second order model (alpha= 1)

N° Exp	Level of pollution (L)	Conductivity σ(mS/cm)	Flashover voltage (model) kV	Flashover voltage kV	Error (%)
1	3	1.823	58.162	58	0.28
2	6	30.5	38.986	39.312	-0.83
3	8	8.02	43.773	42.672	2.58

This model can help with the prediction of the flashover voltage of this insulator so an estimate of the voltage can be made we can first calculate how much the insulator holds through the following estimation equation

$$N = V_{L-L} / (\sqrt{3} \cdot C) \quad \text{(III.25)}$$

Where:

N is the number of discs in an insulator

V_{L-L} is the complex line voltage

C is the voltage a single insulator can hold

Like this, we can compare where the flashover voltage is at compared to the voltage it has been placed to work at.

Another way to use this model is by the producers of this insulator in the case of trying to make improvement on the insulator and such.

III.9. Conclusion

In this chapter, a powerful technique that offers a methodical approach to optimizing complicated systems is the Response Surface Methodology (RSM).

The Central Composite Design (CCD), a strategic procedure with distinct steps that direct experimentation, is a key tool within RSM. These actions include the purposeful choice of factor levels and the insertion of various alpha values to explore the experimental environment. The process continues with selecting mathematical models that are adapted to the needs of the study, then using various ANOVA tests and plots to judge the model's validity.

A case study where we combined RSM and CCD to construct a model that predicts insulator flashover voltage is one of the interesting applications of these methods. This model accounts for variables such as conductivity and pollutant levels. Through this study, we demonstrate how these techniques can be applied in actual situations, providing useful answers to engineering problems. Finally, a good model for the prediction of the flashover voltage was created.

A comparison between the difference of choosing an Alpha equal or higher than one can generate. Usually going through the usual way to find a model that would best work on the factors that you chose and your problem would work but that may not be the very best of models that would represent your study and problem. Going through RSM the regular way would be better compared to taking a chance at different model that may or may not even work. Therefore, one should study the problem very well and make a model with he’s own predictions even before making the experiment that would give an idea about the model that would come out at the end.

This may not be optimal, as it may not work for every model since as the number of factors increase the harder it gets to make assumption or prediction for certain responses but it is still better to do this before you finalize the factor levels and do the experiments.

CHAPTER IV

Artificial Neural Network

IV.1.Introduction

Traveling into the world of ANNs is like entering the center of a transforming force. The foundation of contemporary AI, these networks have evolved beyond their theoretical roots. Their far-reaching consequences range from unraveling the most fundamental principles of intelligence to finding solutions to real-world problems. They are the minds behind driverless vehicles, picture classifiers, recommendation engines, speech recognition systems, and more [50]–[53]. Healthcare [54], finance [55], manufacturing [56] and countless other industries have the potential to be completely transformed by ANNs.

Our investigation starts with a look in the past—a look at the historical background that propelled ANNs to the fore. Following their development reveals a timeline dotted with significant innovations, from the groundbreaking work of Warren McCulloch and Walter Pitts in the 1940s to the revival of neural networks in the 21st century with Geoffrey Hinton's deep learning algorithms [57], [58]. This trek is proof of the tenacity of a thought whose time has arrived.

Our mission's central question is: Why are ANNs important? We look at their inner workings and applications, and the answer emerges. With their capacity to generalize patterns from data and adjust to changing environments, ANNs have a distinct advantage [50]. They are the key component in the world of complicated, data-driven challenges because they excel in situations where traditional rule-based programming fails [53].

The fundamental components of ANNs are explored as we progress through this chapter, demystifying their architecture, training approaches, and practical applications. Each segment on our tour serves as a stepping-stone, illuminating the extraordinary development of these artificial networks from conception to reality.

IV.2.Artificial neural network

The capacity of ANNs to learn from data is one of its distinguishing characteristics. ANNs may identify underlying patterns, correlations, and characteristics in datasets through a process called training, which enables them to make predictions, classify objects, or make optimized solutions [59]. An optimization algorithm that aims to reduce the discrepancy between the network's output and the actual target values directs this learning process. ANNs have found use

in a variety of industries, from speech and picture identification [60]–[62] to autonomous cars and natural language processing [63], [64]. They are crucial in the age of big data because they are excellent at jobs involving complicated, non-linear relationships and massive datasets.

An artificial neural network seeks to mathematically simulate the human brain in order to replicate some of its characteristics, such as memory, learning ability, capacity for partial information processing. [65]

ANNs have been incredibly successful in many different fields, but they are not without difficulties. When using ANNs, practitioners must take into account a number of factors, including architectural design, overfitting, and the requirement for large volumes of data. Additionally, as ANNs frequently operate as "black boxes" that make it difficult to explain their decisions, it is still a research topic to better understand how these models operate internally.

IV.3. Working principle of ANN

Artificial neural networks (ANNs) are computer models that draw inspiration from how the human brain is organized and functions as seen in figure IV.1. They are made up of interconnected nodes, which are frequently referred to as neurons or units and are arranged into layers: an input layer, one or more hidden layers, and an output layer. The following are the main ideas that guide how ANNs function:

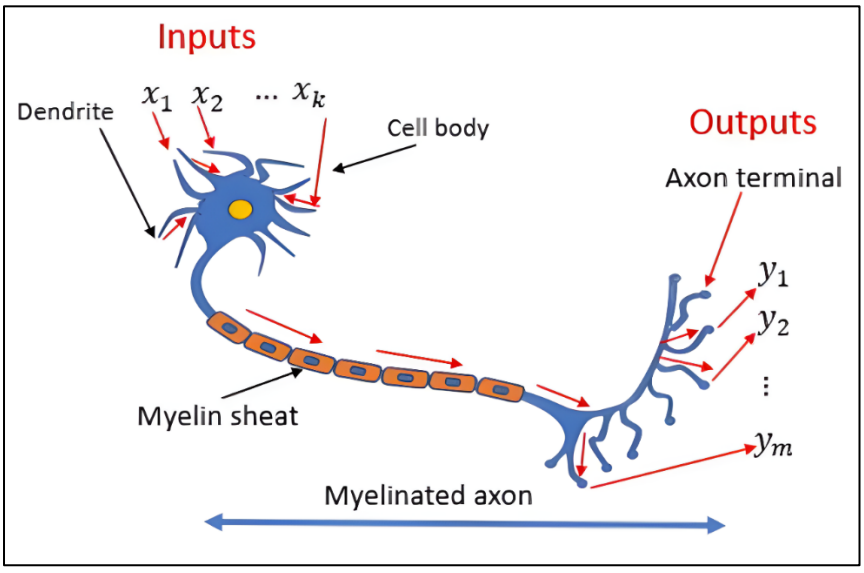

Figure IV.1. similarities between ANN structure and the human brain.[66]

IV.4. Differences between ANN and BNN

Although they share many of the same fundamental building blocks, biological neural networks (BNNs) and artificial neural networks (ANNs) have some distinctions.

Neurons are the fundamental components that process and transfer information in both ANNs and BNNs. However, compared to ANNs, BNN neurons are more complex and diversified. In BNNs, neurons are more complex and typically only have one output while in ANNs, neurons are more straightforward and typically have many dendrites that receive input from multiple sources.
Synapses are the locations of connection between neurons in BNNs and ANNs where information is conveyed.

Although the connections between neurons in ANNs are typically fixed and the strength of the connections is determined by a set of weights, the connections between neurons in BNNs are more flexible and the strength of the connections can be altered by a variety of factors, including learning and experience.

Neural pathways are the connections between neurons in both BNNs and ANNs that enable information to be transported across the network.

The neurological connections between the neurons can be changed by experience and learning in BNNs, where the neural pathways are extremely complex and diverse. Neural pathways in ANNs are typically simpler and established by the network's architecture.

IV.5. Structure of ANN

ANN generally contains different types of layers connected together by connection that have weights and biases that shape it. we mention the following

IV.5.1. The input layer:

The input layer is where the outside world sends its information or features. In this layer, each neuron corresponds to a certain input characteristic.

IV.5.2. The hidden layer:

The term "hidden layer" refers to a layer that is between the input and output layers. Through a sequence of weighted connections and activation functions, these layers change the input data to get the output data.

IV.5.3. The output layer:

The final outcome or prediction is generated by the output layer. The amount of neurons in this layer varies depending on the type of task.

IV.5.4. Weighted Connections

Each neuronal connection has a weight attached to it. To improve the performance of the network, these weights are a learnable parameter and are changed and adjusted during training.

The weights control how strongly one neuron influences another. The signal is amplified by larger weights while being attenuated by lesser weights.

IV.5.5. Activation function

In artificial neural networks (ANNs), activation functions are an essential element. They give the network non-linearity, enabling it to model intricate data connections. These functions decide a neuron's output based on its input.

The activation functions are what allow the network to learn and represent intricate features and patterns in data, making it capable of handling a variety of tasks, from image recognition to natural language processing.

Without activation functions, the entire network would behave like a linear model, limiting its ability to capture complex patterns and relationships in data. [67]

The Identity function, the Logistic Sigmoid function, the Hyperbolic Tangent function and the Rectified Linear Unit (ReLU) are four of the most frequently utilized activation functions in ANNs.

IV.5.5.1. The identity function

The simplest activation function is the Identity function, which is written as $y = x$ and ranges from $\left[-\infty\ ,\ +\infty\right]$ as seen in figure IV.2. Since it is a linear function, the relationship is seen, as the output is directly proportional to the input this means that the input is maintained as it is making desirable in the cases where the linearity is desirable. This comes with lack of non-linearity required for complex function approximation. [68]

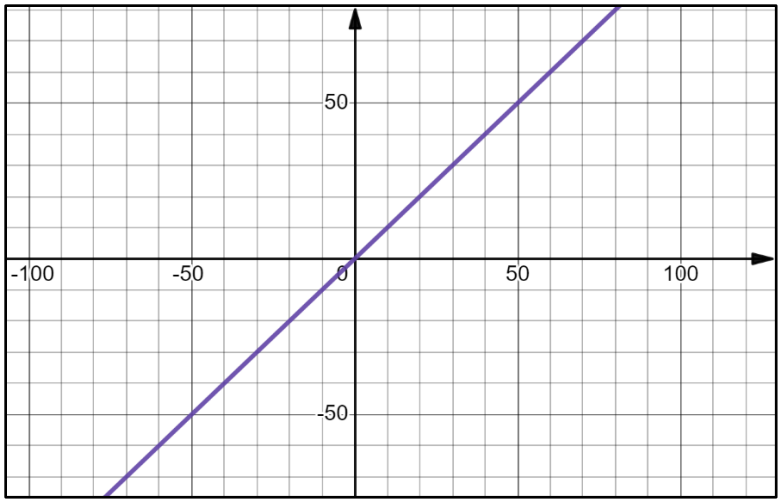

Figure IV.2: The identity function

IV.5.5.2.The sigmoid function

One of the classical approximation functions used in ANN the sigmoid function or often called the logistic sigmoid function expressed as $f(x) = \frac{1}{1+e^{-x}}$. Unlike the identity function, this function introduces non-linearity to the network and is particularly useful for binary classification and estimating probabilities since it squashes the output into a value between $\left[0\ ,\ 1\right]$ as seen in figure IV.3. It is suitable for gradient-based optimization techniques since its derivative is simple to calculate. It may experience the vanishing gradient problem, especially for high input values as well as small gradients that are produced by outputs that are near to 0 or 1, which slows learning. [69], [70]

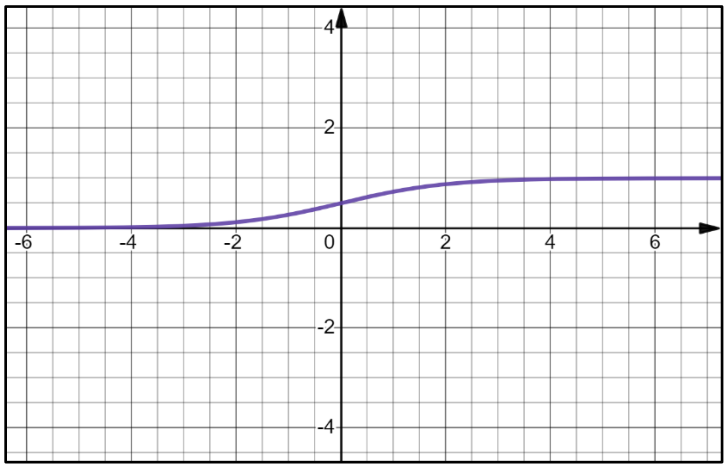

Figure IV.3: the sigmoid function

IV.5.5.3.The hyperbolic tangent function

The hyperbolic tangent function (tanh) denoted as $f(x)=\frac{e^{x}-e^{-x}}{e^{x}+e^{-x}}$ is another popular activation function as seen in figure IV.4. It gives the output as a value that ranges between $\left[-1\ ,\ 1\right]$ meaning that it is a zero-centered function. Compared to the sigmoid function, it has fewer vanishing gradient issues and just like the sigmoid function, it introduces the non-linearity to the network. It can still experience the vanishing gradient problem, much like the Sigmoid, especially for extremely high or low input values. [71], [72]

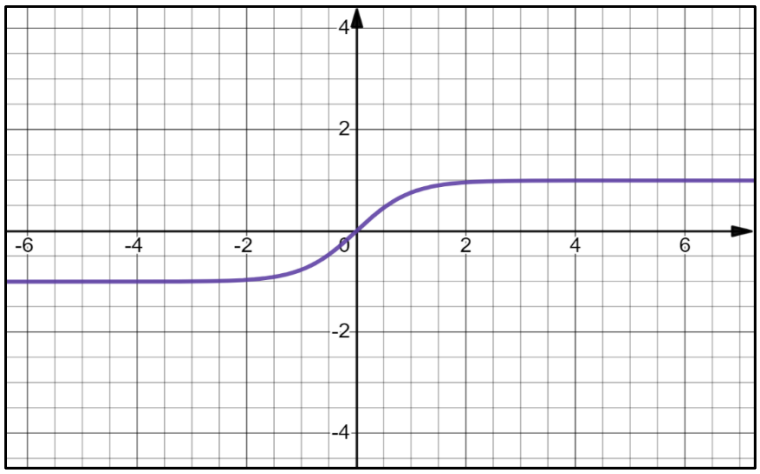

Figure IV.4: the hyperbolic tangent function

IV.5.5.4.The rectified linear unit (ReLU)

Denoted as $ReLU\left(x\right)=\left(0,x\right)$ is another popular activation function. The ReLU function behaves in two different ways, it outputs a 0 when the output is either 0 or a negative value and it outputs the inputs value itself when the input given to it is a positive value. In essence, it allows positive values to pass through unmodified while replacing any negative values with zero.

ReLU is a favored option in many neural network topologies since it is computationally effective and simple to compute. ReLU's constant non-vanishing gradient, especially when compared to other functions like Sigmoid and tanh, helps to alleviate the vanishing gradient issue. It gives the network non-linearity, allowing it to mimic complicated functions. Although is better in some aspects then other functions it has the potential for "dying ReLU neurons," which prevent learning by causing neurons to become stuck and persistently output zero for specific inputs.

This problem is addressed by variants like Leaky ReLU and Parametric ReLU (PReLU). [71], [72]

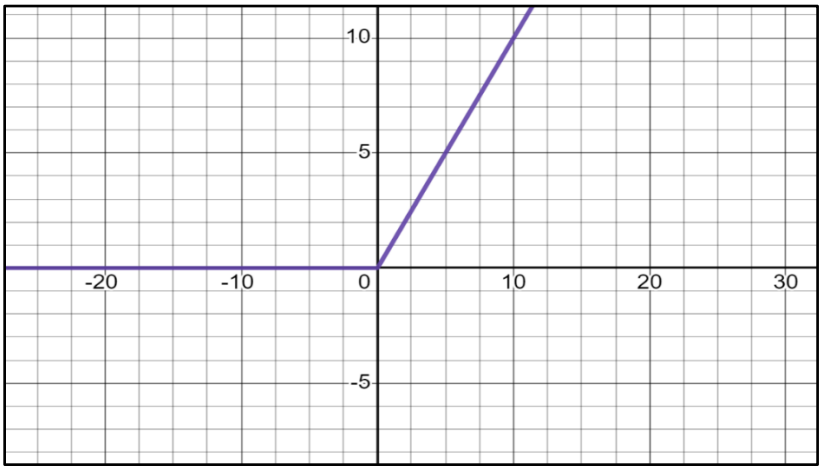

Figure IV.5: the rectified linear unit function

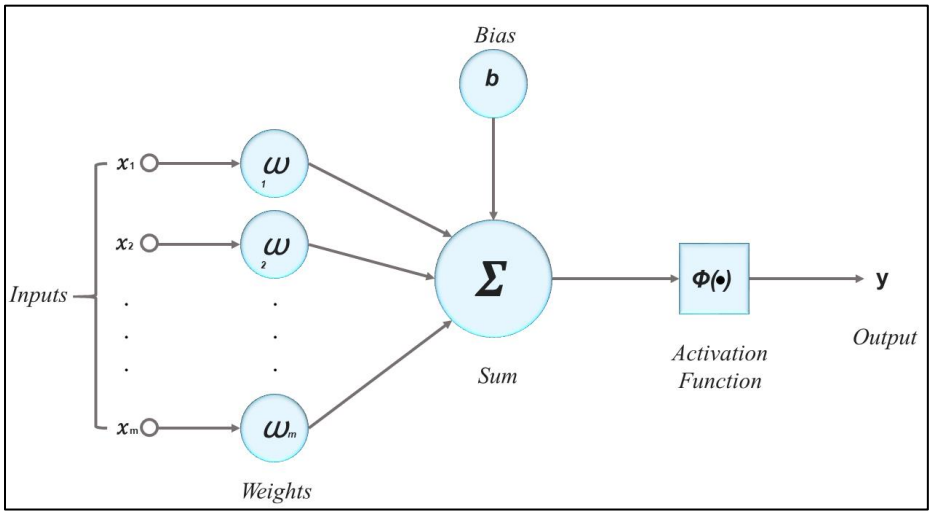

Figure IV.6: Basic ANN structure

IV.6. Working principle of an ANN

Let us consider a simple neural network with one hidden layer and this network would take a vector X with an 'm' size as an input and produces Y as an output.

The output of the neuron in the hidden layer would come out in the following form

$$z_i^1 = \sum_{j=1}^{m} w_{ij}^1 x_j + b_i^1 \qquad \text{(IV.1)}$$

Where:

z_i^1: is the weighted sum of inputs to neuron i in the hidden layer.

w_{ij}^1: is the weight assigned for connection between j^{th} neuron in the input layer and the i^{th} neuron on the hidden layer.

b_i^1: is the bias term for the i^{th} neuron in the hidden layer.

m: is the number of input features.

Now we pass the output of each neuron in the hidden layer through an activation function as follows

$$a_i = \sigma(z_i) \tag{IV.2}$$

Where

a_i: is the activation of the i^{th} neuron in the hidden layer.

σ: is the activation function for the hidden layer.

Next, similarly we calculate the output of each neuron in the output layer

$$z_j^2 = \sum_{i=1}^{k} w_{ji}^2 a_i + b_j^2 \tag{IV.3}$$

Where

z_j^2: is the weighted sum of inputs to neuron i in the hidden layer.

w_{ji}^2: is the weight assigned for connection between i^{th} neuron in the hidden layer and the j^{th} neuron in the output layer.

b_j^2: is the bias term for the j^{th} neuron in the output layer.

k: is the number of neurons in the hidden layer.

The final output of this network would then be found by passing the weighted sum of inputs to neuron i in the hidden layer (z_j^2) through an appropriate activation function, which depends the nature of the problem.

$$y_i = \sigma(z_j^2) \tag{IV.4}$$

Where

y_i: is the output of the j^{th} neuron in the output layer.

σ: is the activation function of the output layer.

IV.7.Training an Artificial neural network

There are two main types of propagation in Artificial Neural Networks (ANNs): forward propagation (also known as feedforward propagation) and backward propagation (also known as backpropagation).

These two procedures are crucial to the training and development of ANNs but before we delve into them we need to define some terms first:

IV.7.1.Types of learning in an ANN

In ANN there are different types of learning that are different in the way they handle or generate information. These differences allow for these different types of learning to be used under different situations. Some of the learning types of ANN are:

IV.7.1.1.Supervised learning

In supervised learning, the algorithm is taught from a labeled dataset, meaning the input data has labels that correspond to the desired outcomes. In order to effectively recreate the link between inputs and known outputs, the main objective is to learn a mapping from input data to output labels. [73], [74]

During training, input data are given to the ANN, which then predicts the outputs and modifies its parameters (weights and biases) to reduce the error between its predictions and the actual labels.

IV.7.1.2.Unsupervised learning

Unsupervised learning entails training ANNs on datasets without target outputs because the input data is not tagged. Without having a specific target in mind, the main goal is to find patterns, structures, or relationships in the data. [73], [75]

In unsupervised learning, ANNs frequently use methods like clustering (grouping similar data points).

IV.7.1.3.Reinforcement learning

The concept of reinforcement learning involves ANNs interacting with their surroundings and learning by getting feedback in the form of rewards or penalties based on their activities.

The environment does not provide feedback on what the intended outcome should be or if it is correct or incorrect. As a result, in this sort of learning, the network itself must identify the patterns, characteristics, and relationships between the input and output data through trials and error. They act in a setting, get their feedback, and use this input to adjust their approaches. [73], [76]

IV.7.2.The cost and loss functions

Any neural network's primary objective is to produce precise predictions. How far the neural network's predictions differ from the actual values can be expressed using a cost function. It serves as a gauge for the discrepancy between expected and actual results. The cost function spans the complete training set, whereas the loss function is for a single training point. There are many types of cost functions and some of the popular ones are

IV.7.2.1.Mean absolute error (MAE) / L1 loss function

MSE is a function that is commonly used for problems of regression. The absolute difference between the values that were predicted and the actual values are averaged. MAE regards each error equally. In other words, it doesn't penalize bigger errors more severely than little ones, which can be useful in circumstances when every error should be given the same significance [77]. The function is written as follows

$$MAE = \frac{1}{n}\sum_{i=1}^{n}\left|y_i - y_i\right| \tag{IV.5}$$

Where

n : is the number of data points

y_i : are the input values

y_i : are the predicted values

IV.7.2.2.Mean squared error (MSE) / L2 loss function

MSE is another function that is frequently used to solve regression problems. The average of the squared difference between the expected and actual values is computed.

Due to squaring, MSE significantly penalizes larger errors, making it sensitive to outliers. [78]

The function is written as follows:

$$MSE = \frac{1}{n}\sum_{i=1}^{n}\left(y_i - y_i\right)^2 \tag{IV.6}$$

IV.7.2.3.Cross-entropy loss function

Especially in logistic regression and neural networks, cross-entropy loss is frequently employed for classification issues. It assesses how differently actual class labels and anticipated class probability differ. The model is encouraged to produce a high probability for the right class by this loss function. [79]

The function is written as follows

$$L\left(y, y\right) = -\left(y\log\left(y\right) + \left(1-y\right)\log\left(1-y\right)\right) \tag{IV.7}$$

Where

y : is the true label (either 0 or 1)

y : is the predicted probability

IV.7.2.4.The Huber loss function

The MSE and MAE's greatest qualities are combined in the Huber loss. While approaching MSE close to the prediction, it is less sensitive to outliers like MAE. [80]

The function is defined as follows

$$L\left(y, y\right) = \begin{cases} \frac{1}{2}\left(y-y\right)^2 & if \quad \left|y-y\right| \le \delta \\ \delta\left|y-y\right| - \frac{1}{2}\delta^2 & if \quad \left|y-y\right| > \delta \end{cases} \tag{IV.8}$$

The parameter δ (delta) in the Huber Loss function is a user-defined hyperparameter that establishes the point at which the loss changes from being quadratic (like Mean Squared Error or L2 loss) to linear (like Mean Absolute Error or L1 loss).

It's a crucial Huber Loss parameter, and its value regulates the trade-off between the loss function's resistance against outliers and its ability to fit the data.

The kind of cost function to utilize depends on the kind of problem being solved. For instance, a different cost function is needed for classification tasks than regression problems.

IV.7.3. The gradient

The gradient is a vector that depicts how quickly a function changes in relation to its parameters in the context of artificial neural networks. It indicates the direction of the function's steepest ascent. Typically, when we discuss training an ANN, we are referring to the process of minimizing a loss or cost function by altering the network's parameters (weights and biases). In this optimization procedure, the gradient is critical. In mathematics, a vector of partial derivatives is used to express the gradient of a loss function with respect to a vector of parameters, such as the weights and biases of a neural network, which is written as follows:

$$\nabla L = \left[\frac{\partial L}{\partial \theta_1}, \frac{\partial L}{\partial \theta_2}, \cdots, \frac{\partial L}{\partial \theta_n} \right] \tag{IV.9}$$

Where:

∇L : is the loss function L's gradient vector

$\frac{\partial L}{\partial \theta_i}$: is the partial derivative of the loss function with respect the parameter vector of the i^{th} place.

In conclusion, when training ANNs, the gradient is utilized to update the weights and biases of the network in a way that minimizes the loss function. The gradient describes the rate of change of a function with regard to its parameters. In ANNs, it is calculated using the chain rule and backpropagation, and several optimization techniques use the gradient to change the training parameters.

IV.7.4. Optimization methods

In order to minimize the error or loss function, optimization techniques are essential for training ANNs. Some of the commonly used optimization methods include.

IV.7.4.1. Gradient decent optimization

The gradient descent is an important optimization approach used in machine learning, specifically when training artificial neural networks (ANNs). Its main goal is to identify the ideal set of model parameters (weights and biases) that minimizes a particular loss function and enables accurate prediction [81]. Gradient Descent's main principle is to iteratively adjust model parameters in a way that lowers the loss function. The approach calculates the gradient of the loss function with respect to the model parameters at each iteration [82], [83]. We can summarize this method in a total of 5 steps

- The model parameters (weights and biases) for Gradient Descent are initially estimated. These settings are initialized when the network starts training.
- Using the parameters of the present model, the program produces predictions. It calculates the loss, a metric that expresses how closely the predictions match with the actual target values.
- The gradient of the loss is calculated with regard to each model parameter. This is accomplished by using the chain rule of calculus to propagate gradients backward through the network with the process of backpropagation.
- The model's parameters are updated in the gradient's negative direction in order to minimize the loss. For each parameter θ, the update is carried out using the following for

$$\theta_{new} = \theta_{old} - \gamma \cdot gradient(\theta_{old}) \quad \text{(IV.10)}$$

Where γ is the learning rate. The size of each step during parameter updates depends on the learning rate. It is important to pick the right learning rate; a high learning rate can cause overshooting of the ideal solution, whereas a low learning rate can cause slower convergence.

- Up until a stopping requirement is satisfied, steps 2 through 4 are iteratively repeated. A limit number of repetitions or when the change in the loss function becomes insignificant are two common termination criteria.

IV.7.4.2.Levenberg-Marquardt

The Levenberg-Marquardt (LM) algorithm is an optimization strategy used for training artificial neural networks (ANNs). It is a variant of the standard gradient descent method that seeks to identify the ideal weights and biases to reduce the loss function of the network. Non-linear optimization issues, which are frequent in neural network training, benefit greatly from Levenberg-Marquardt algorithm. It provides effective convergence and enhanced stability by combining elements of both the gradient descent and the Gauss-Newton approach. By changing the parameters in the steepest descent direction, the gradient descent method reduces the sum of the squared errors.

By assuming that the least squares function is locally quadratic in the parameters and locating the minimum of this quadratic, the total of the squared errors is decreased in the Gauss-Newton technique. When the parameters are far from their optimal value, the Levenberg-Marquardt technique behaves more like a gradient descent approach, and when the parameters are near their optimal value, the method behaves more like the Gauss-Newton method [84], [85]. We can summarize this method in a total of 5 steps

- Just like the gradient decent method, the initialization of the model parameters is made (the initial weights and biases when training the network)
- Determine the difference between the output that was expected and the final prediction made by the network (often using a loss function like Mean Square Error).
- Calculate the Jacobian matrix, which shows the partial derivatives of the output of the network with respect to its biases and weights. This matrix offers details on how slight adjustments to the parameters alter the output of the network.
- Analyze the algorithm to see if it has converged. This can be achieved by keeping an eye on changes in the error and the LM parameter values. The training process is terminated if convergence requirements are satisfied.
- Iteratively repeat steps 2 through 6 if convergence has not yet been attained. To balance between Gauss-Newton and gradient descent updates, dynamically adjust the LM parameter.

The Levenberg-Marquardt algorithm's update rule is as follows:

$$\Delta\theta = \left(J^T \cdot J + \lambda \cdot I\right)^{-1} \cdot J \cdot e \qquad \text{(IV.11)}$$

$\Delta\theta$: is the addition and change to the model parameter

J : is the Jacobian matrix

J^T : is the transpose of the Jacobian matrix

λ : is the damping factor

I : is the identity matrix

e : is the error vector

IV.7.5. Overfitting and regularization techniques

Regularization and overfitting are two important concepts in artificial neural network (ANN) training.

IV.7.5.1. Overfitting

When an ANN learns to perform remarkably well on the training data but is unable to generalize successfully to unknown or new data, this is known as overfitting [86].

In essence, the network does not detect the underlying patterns but rather fits the noise or oscillations in the training data. Overfit models perform poorly on real-world data because they are unable to generalize [87]. When the ANN is extremely complex in comparison to the amount of training data available, it can occur. It might also happen if the network has too many epochs in its training.

IV.7.5.2. Regularization techniques

In order to combat overfitting and improve the generalization of ANNs, regularization techniques are used. These regularization methods reduce overfitting, reduce ANN complexity, and produce more accurate models that generalize well to new data [88]. Regularization method selection is frequently influenced by the particular dataset and task at hand [89]. Some of the popular regularization techniques used include the L1 and L2 regularization techniques, the early stopping technique, the data augmentation technique and the dropout technique.

IV.7.6. Forward Propagation:

Forward propagation is the process of deriving the network's output from its input data. Up until the final output is generated, input values are multiplied by weights, activation functions

are applied, and the altered data are passed to subsequent layers. So to say, it works through the following steps [90], [91]

- The input layer of the network receives the input data.
- The input is multiplied by the weights and each neuron in the hidden layers, as well as those in the output layer, is then given an activation function.
- The process continues until the final output is produced, with the output of one layer acting as the input for the next.
- The network's prediction for the input is shown in the final output.

The objective of forward propagation is to provide an output for the given input that is as close as possible to the actual target.

IV.7.7. Backpropagation:

This method is a fundamental algorithm in artificial intelligence. It is created specifically for ANN training, enabling them to learn from data and gradually enhance their predicting abilities. It works through the following steps [81], [92]

- **Forward pass:** The process is kicked off by a forward pass through the network which is like the forward propagation, where input data is processed layer by layer to yield predictions. Each neuron adds up its inputs in a weighted manner, applies an activation function, and sends the output to the following layer. The prediction of the output for the supplied input is produced by this forward pass.
- **Error calculations:** The output of the network is compared to the actual output values following the forward pass, and the error is determined. Mean Squared Error (MSE) for regression tasks and Cross-Entropy for classification tasks are two common error-measuring methods.
- **Gradient calculation:** Calculating the gradient of the error with respect to the weights and biases of the network is the fundamental concept of backpropagation. This gradient shows how responsive each parameter is to changes in the error. These gradients are computed layer by layer, starting with the output layer and working backwards through the network, using the chain rule from calculus.
- **Weight updates:** The weights and biases of the network are updated using an optimization approach, such as gradient descent, after the gradients are known. The direction in which these

updates are made minimizes the error calculated. The step size during weight updates is controlled by the learning rate hyper parameter.

The main goal of backpropagation is to iteratively modify the weights and biases of the network to reduce the error between expected and actual outputs. The network learns to recognize intricate links and patterns in the training data through repeated iterations, enabling it to make precise predictions on brand-new, unforeseen data.

IV.8. Data management and splitting in the ANN training

The network would split the data provided into 3 different datasets with each one having a different purpose

IV.8.1. The training dataset

This is and should be the biggest chunk of the dataset, and it's what the ANN gets trained on. In order to produce accurate predictions, the model adapts its parameters (weights and biases) based on this data during training.

IV.8.2. The validation dataset

a portion of the information that is independent of the training set. It is used to keep track of the model's performance as it is being trained.

The validation set offers an impartial assessment of the model, assisting in preventing overfitting. Based on the results of the validation, you change the hyperparameters.

IV.8.3. The test dataset

The training and validation data are kept entirely apart from this dataset. It is employed to assess the model's performance following training and tuning.

The test dataset offers an objective evaluation of the model's ability to generalize to new data.

So in summery by exposing the model to a substantial amount of labeled data, the training dataset is utilized to teach the model.

While the Validation Dataset is used during training to evaluate the model's performance on unseen data and to fine-tune hyperparameters, the model learns from the patterns and correlations in the training dataset. It also aids in early stopping if the model begins to overfit.

Finally, the Test Dataset is held back until the model is fully trained and the hyperparameters are determined.

It provides an unbiased evaluation of how well the model generalizes to fresh, untested data.

IV.9.Types of artificial neural network

ANN contains many types and what follows are some its types

IV.9.1.Feedforward artificial neural network

The fundamental deep learning models are deep feedforward networks, commonly known as feedforward neural networks or multilayer perceptrons (MLPs). Data is passed in a unidirectional flow from the input layer through hidden layers, then to the output layer, to make it work. Every neuron in a layer connects to every neuron in the layer above it, computing a weighted sum of inputs that is then sent via an activation function. Layer by layer, this procedure continues until the desired product is produced. Because information goes from the function being evaluated from x through the calculations necessary to define f, to the output y, these models are called feedforward models. The model's outputs cannot be fed back into it because there are no feedback connections [93].

A feedforward network's objective is to approximate some function f. For instance, y = f(x) for a classifier transfers an input x to a category y. A feedforward network establishes the mapping y = f(x; θ) and discovers the value of θ that yields the best function approximation.

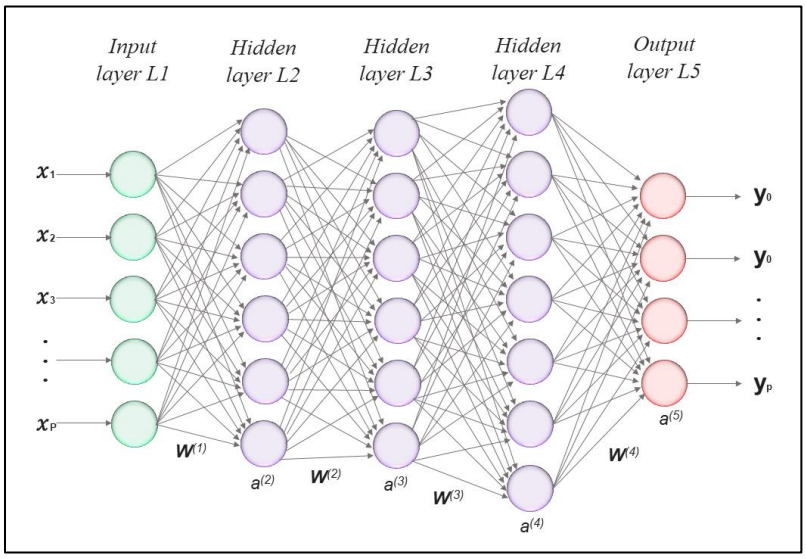

Figure IV.7. FNN structure with 3 hidden layers.

FNNs are often depicted by piecing together a variety of functions, they are also known as networks. A directed acyclic graph illustrating the relationship between the functions is attached to the model. For instance, we may chain together the three functions f(1), f(2), and f(3) to form f(x) = f(3)(f(2)(f(1)(x))).

The most typical neural network architectures are these chain structures. In this instance, f(1) is referred to as the network's first layer, f(2) as its second layer, and so on. The depth of the model is determined by the chain's overall length. The output layer is the last layer of a feedforward network.

IV.9.2. Recurrent Neural Networks

RNNs differ from FNNs in that they can sustain feedback loops and memory. Each neuron receives input from prior time steps in addition to the current time step, enabling it to recognize temporal connections in data. [94], [95]

$$h_t = f_W\left(h_{t-1}, x_t\right) \tag{IV.12}$$

The function will depend on some weights W and will take the previous state of the model ht-1 along with the input at the current state xt and update it and as we pass into the next state this new output will become the previous and be passed through this function and so on as seen in figure IV.8.

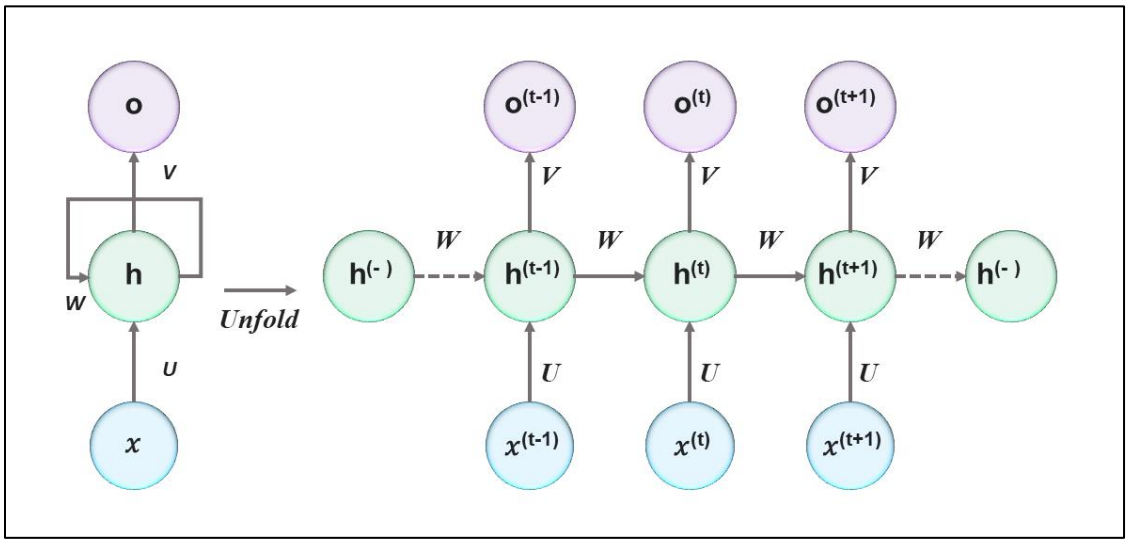

Figure IV.8. RNN structure and unfolded structure.

IV.9.3. Convolutional Neural Networks

Since convolutional neural networks were found they have become a game-changer in the field of artificial intelligence, notably in the processing of images and videos. These specialized artificial neural networks have demonstrated outstanding effectiveness in tasks including picture identification, object detection, and even medical image analysis. They are created to emulate the human visual system. Convolutional layers are the foundation of CNNs, they learn spatial feature hierarchies from incoming data automatically and adaptively. These layers slide over the input image while recognizing local patterns like edges, corners, and textures using tiny, trainable filters called kernels. Convolutional layers with multiple iterations extract increasingly complicated characteristics. Convolutional layers are followed by pooling layers, which aid in making the feature maps less dimensional. The most popular pooling operation, known as max pooling, chooses the highest value possible within a given local area. The most crucial data is kept while the computational complexity is decreased by this downsampling procedure [94], [96].

CNNs frequently incorporate one or more fully connected layers following feature extraction using convolutional and pooling layers. These layers carry out conventional neural network operations and can be employed for tasks like regression, analysis or classification. [96], [97]

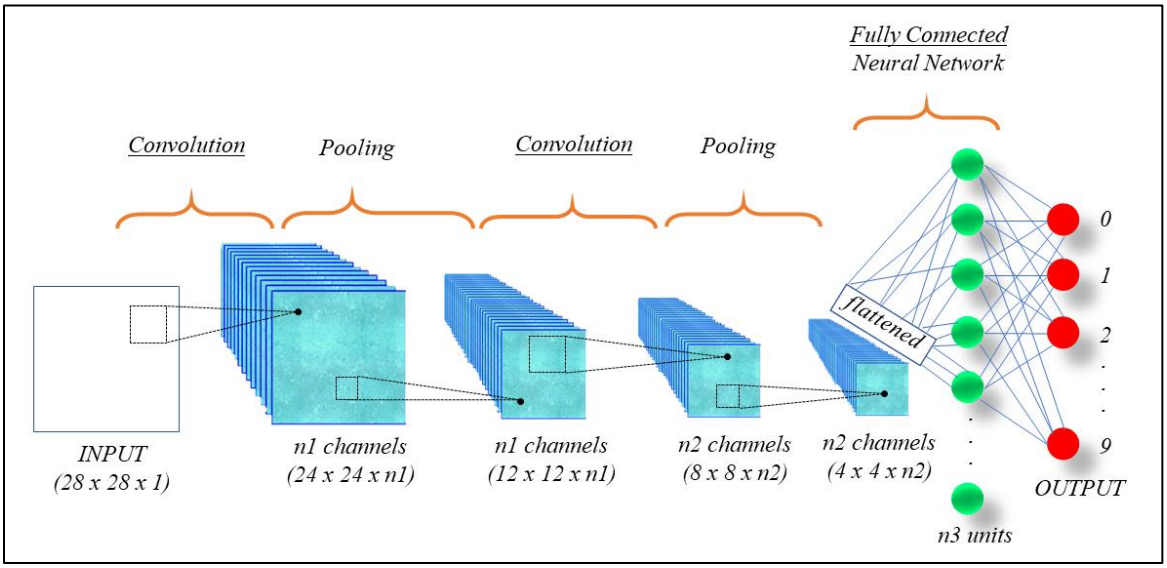

Figure IV.9. Convolutional neural networks structure

IV.9.4.Radial Basis Function Network

RBF network typically only makes use of an input layer that does no computation and works as a data carrier just like in FNN, one hidden layer filled with radial basis functions centered around chosen data points, and an output layer. [98]

These networks' little depth and common use of only two layers is one constraint. While the second layer is trained using supervised techniques, the first layer is built in an unsupervised manner. These networks, which differ fundamentally from feed-forward networks in that they have more nodes in the unsupervised layer, are more powerful. They work by computing the similarity between input data and selected centers, with outputs getting smaller as data get farther away from centers. [94]

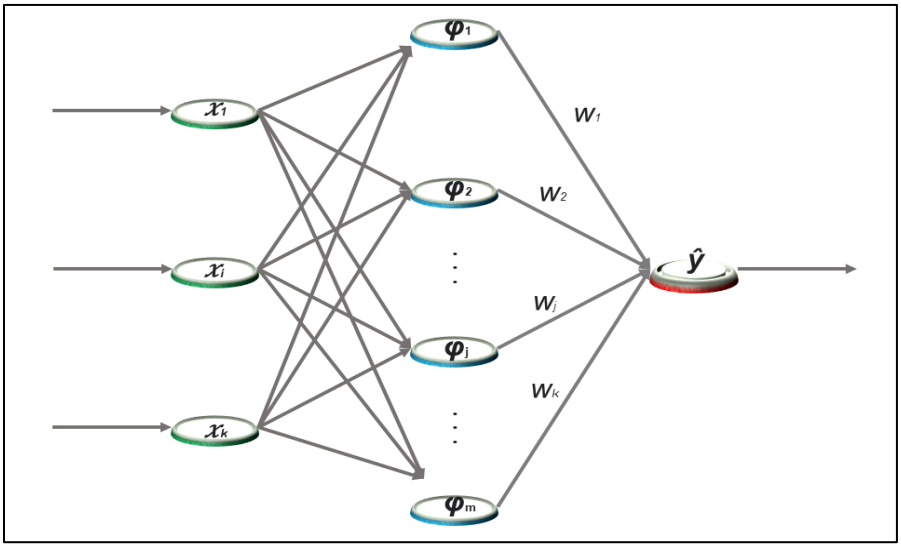

Figure IV.10. Radial basis function network structure

IV.10.Case study

We will try to create a feedforward neural network with the MATLAB software that can predict the flashover voltage of the 1512L insulator.

Just like in the previous chapter, the network would have two inputs as in the level of pollution and the conductivity of pollution. MATLAB contains a neural network-fitting app, which creates a feedforward network that has two layers, a hidden layer producing its output through the sigmoid function and an output layer that produces its output through the identity function meaning a linear output neuron as seen in the figures (IV.11 and IV.12) bellow.

We will make two different model just to make a comparison between this method and the previous method used. Therefore, at first, we will make a model with lesser data points and see the models prediction for these points then we will make another model but feed for it enough input data points to see how well its predictions can get.

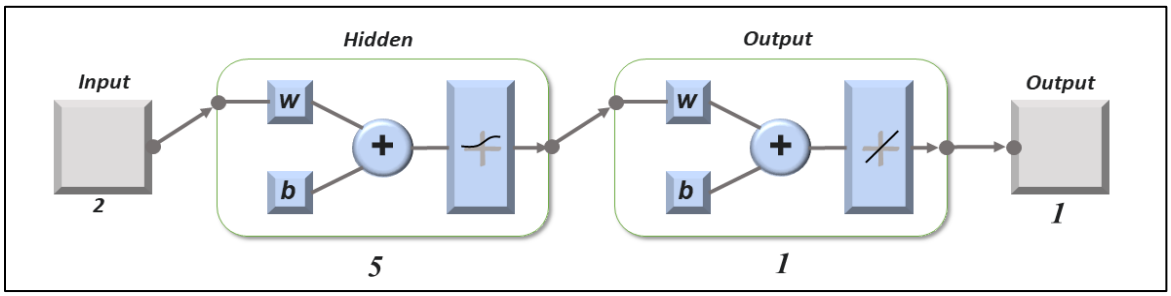

Figure IV.11. FFN structure for the first network

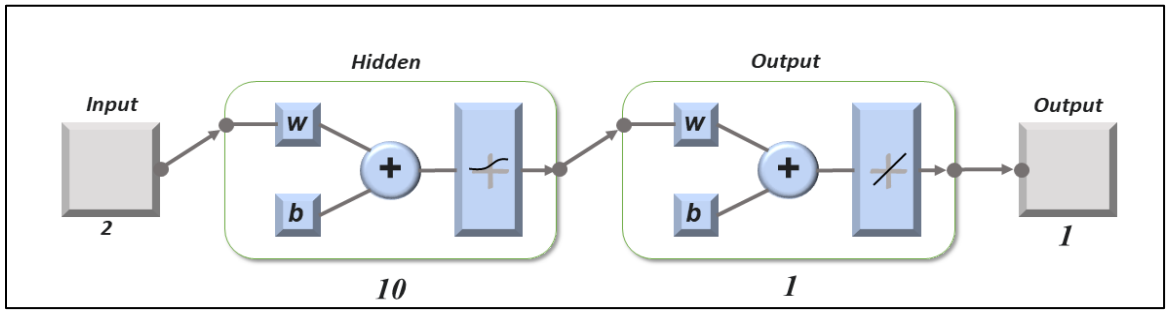

Figure IV.12. FFN structure for the second network

IV.10.1.First model

In this model, we will feed 9 data points as inputs for the model. The data points will have a varied set of inputs through the levels of pollution and values of conductivity in other words we will take 8 levels of pollution while repeating 1 and on each level, we put a different conductivity level while repeating 2 compared to the others. The end result will be 9 by 2 matrix for the inputs and 9 by 1 matrix for the output. This model is made so we can compare the model made by the central composite design of the response surface methodology and the FFN studied in this chapter.

After that, the data fed to the model is divided into three categories the training dataset, the validation dataset and test dataset. The data is randomly divided between these three categories with the training dataset taking 60% of the total data and the validation and test datasets each taking 20%.

These percentages are not predefined by MATLAB or anything else the user is given the choice for the validation and test datasets but generally a 10% or 15% would be enough for the network.

The number of hidden layers chosen for this network is 5 layers and should be change to a different number should the results be undesirable or not good enough, until the network is good enough for the prediction.

After defining everything needed, the Levenberg-Marquardt algorithm is chosen to be used for the network training along with Mean Squared Error function. After training the model for 7 iterations, we are given the following results in table IV.1.

Table IV.1. MSE and R-value results for the first network

Dataset	Samples	MSE	R
Training	5	26.51383	0.897438
Validation	2	474.23221	0.99999
Testing	2	116.58793	1

Where

MSE: is the average squared difference between outputs and predictions so the lower it is the better the network is.

R: is the value that measures the correlation between the outputs and the predictions. A value of 1 would mean a very close relationship and a 0 value would mean a random relationship.

Looking at the MSE values and taking into account that the lesser they are the better we can tell that this model contains a high error and its prediction is way off the mark. While seeing that the R –values for this network are good we can't say for sure that this network is good this might be an indication that the model is simply overfit so we can look at the error histogram and the regression plots to better confirm both these results.

- **Error histogram**

The error histogram in figure IV.13 shows the number of sample of the data as instances and the error that correspond to each of the datasets as well as where the zero error is located in the form of the orange line as seen in figure IV.13.

We can see that three of the training data sample are located close to the zero line while the rest of the sample are far away.

The highest error is found in the validation dataset with a value of 25.57 kV, which is very high. Even the lowest error found in the test dataset is high with a value of 7.619 kV.

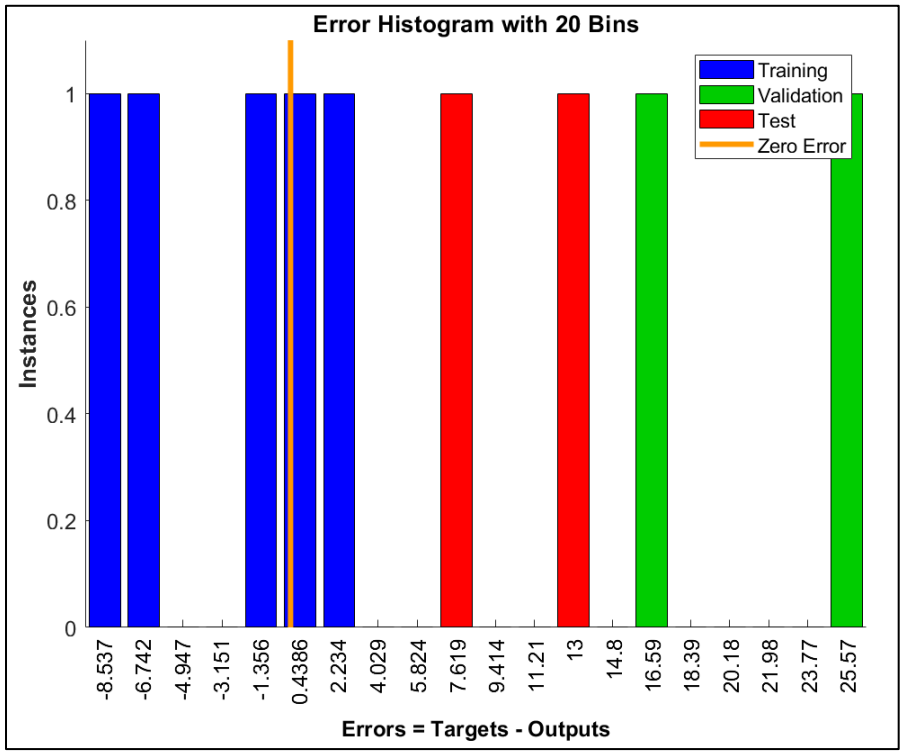

Figure IV.13. Error histogram of the first network

Regression plots

The regression plots in figure 14 graph the regression plot for each dataset and then for all of them together.

We can see that the reason for the high R-value in the validation and test results is the lack of sample data.

Even though the training dataset has a good R value it still is not good enough to offset the problem of lack of data and we can see that through the last regression plot that has a value of 0.52629.

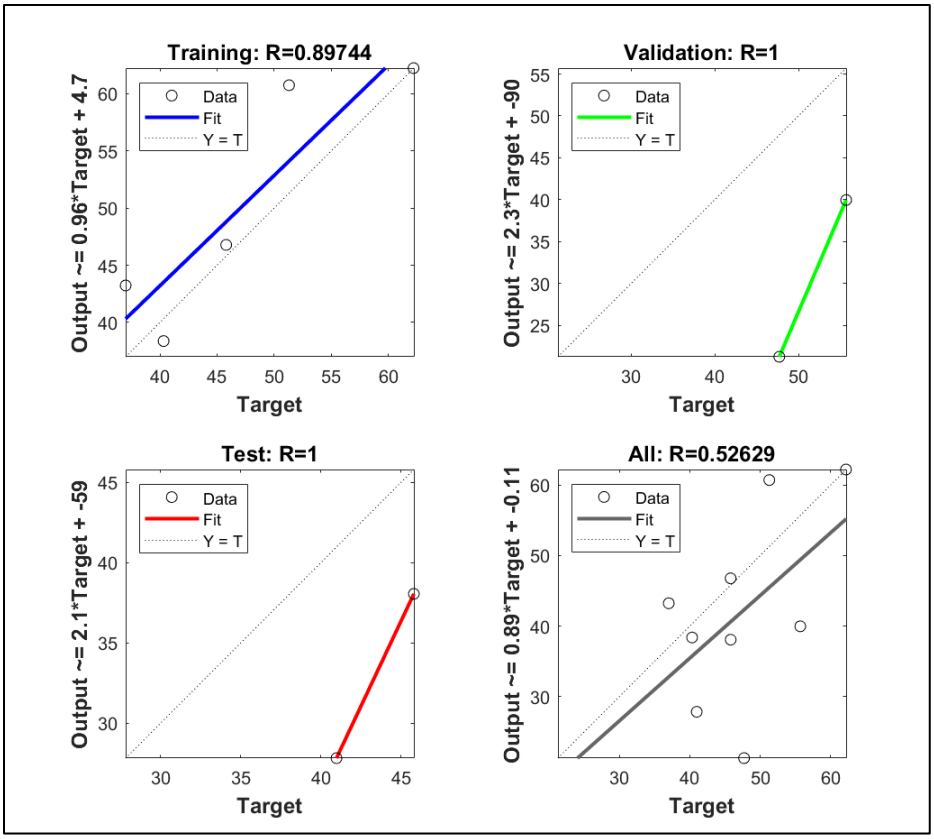

Figure IV.14: Regression plots of the first network

IV.10.2.Second model

In this network, we will feed all our data points as inputs for the model. Unlike the previous network, it will have a 45 by 2 matrix for the inputs and a 45 by 1 matrix for the outputs.

Using a 30% portion of the data for the validation and test datasets 15% for each one leaves us with 70% of the data or 31 samples of data for the training dataset. After training the network with Levenberg-Marquardt algorithm in 13 iterations, we get the following results.

Table IV.2. MSE and R-value results for the second network

Dataset	Samples	MSE	R
Training	31	0.07182	0.999490
Validation	7	1.55307	0.994680
Testing	7	3.36325	0.964507

This network represent a good result as seen in table 3 with the MSE values under 3.5 indicating that the error is very low and an R-value of above 0.96 for all datasets meaning that there is a good correlation between the outputs and predictions and this should indicate that the network predicts very well.

Error histogram

Drawing of the histogram in figure 15 shows that the majority of the data sample is close to the zero line. The bars closest to the zero line contain 20 data samples, which close to half the entire data with the rest closely stacked close to it. The highest error recorded was found in the test dataset with a 4.409 value.

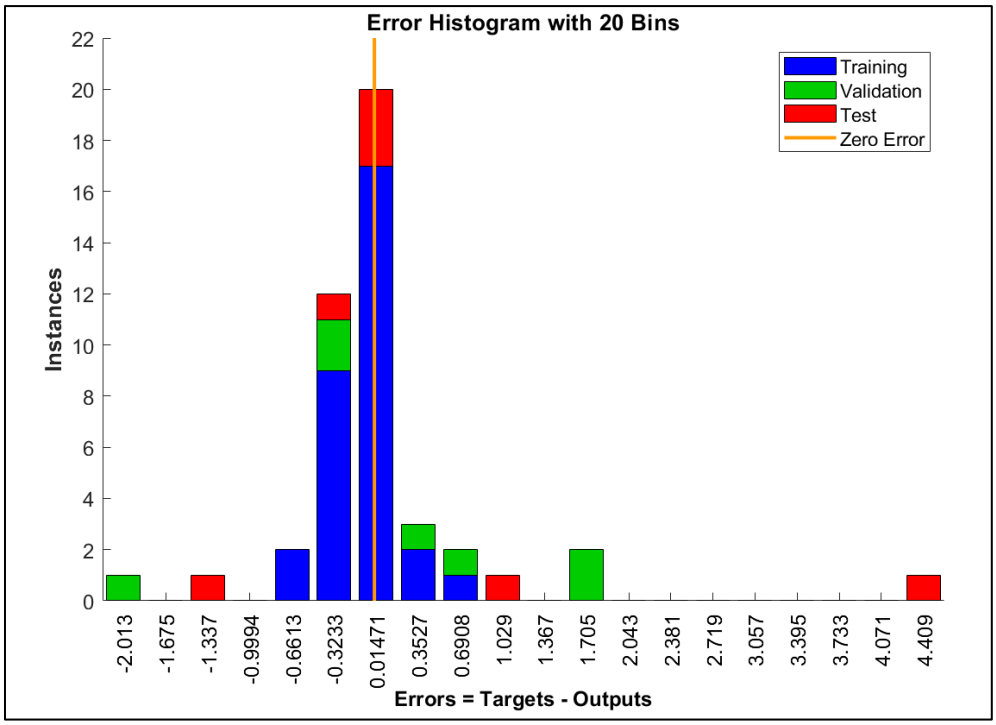

Figure IV.15. Error histogram of the second network

Regression results

The regression plots in figure 16 show that the data in all three datasets follow a straight line more or less so the networks overall R-value is 0.9937, which is a very good result and should make precise prediction.

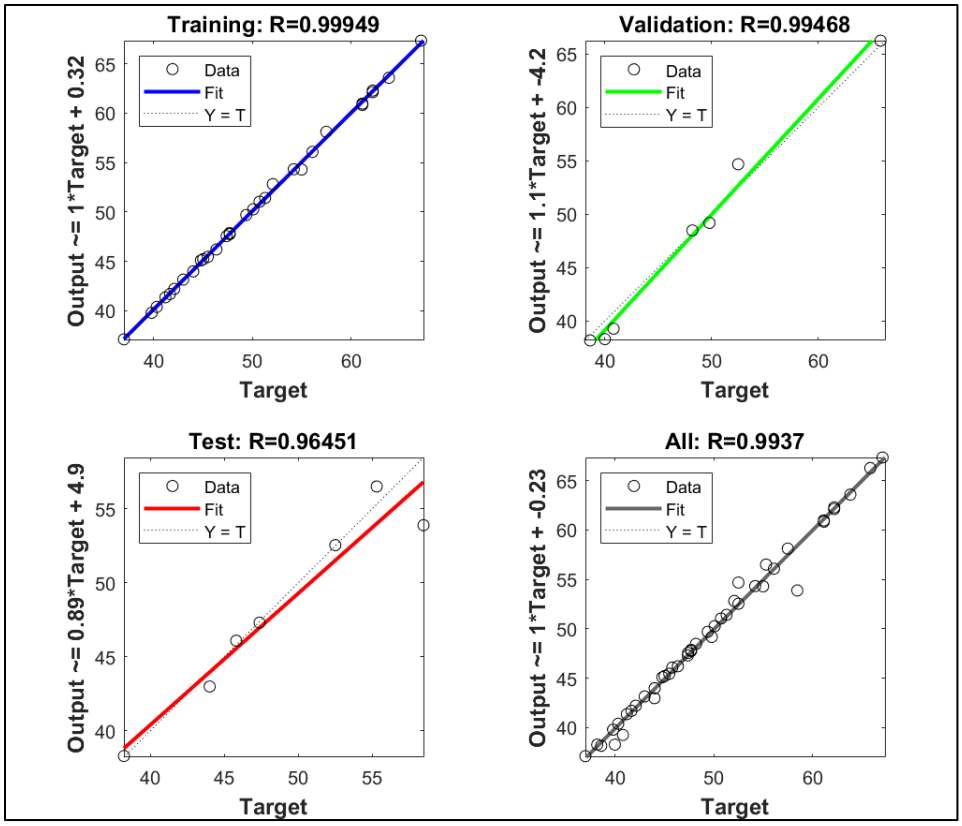

Figure IV.16. Regression plots of the second network

IV.11.Conclusion

As this chapter ends, it is clear that ANNs are an essential tool in the field of modern data science. Real-world problems can be solved in a variety of ways thanks to their ability to model complex relationships in data and generate predictions based on observed patterns.

ANNs are a powerful ally for both researchers and practitioners, whether they are working with tiny, controlled datasets or huge, complex material. Extensive analysis of Artificial Neural Networks (ANNs) has been offered in this chapter, illuminating their underlying theories and some of its various types. Finally, a case study to make a prediction model for the flashover voltage of the 1512L insulator has been made in two different cases.

The first case, which is made to compare ANN with the RSM. ANN was given a small sample of data point to see how well it will fair in its predictions. The RSM created a model that is of higher prediction capability than ANN in this case.

The second case was made with a larger sample data to get the precise predictions needed. While the prediction capability of this network is not that high compared to the RSM model it is still better.

In conclusion RSM should be the first method engineers or researchers should go for first because even when it does not produce the desired results switching to ANN would have no problems. RSM should be the first to go to method due to the small amount of data it needs to generate a model compared to ANN.

GENERAL CONCLUSION

General conclusion

The present thesis aims at the contribution to the study of the behavior of high voltage insulators polluted by different methods. Use of a two and three dimensional simulations to visualize the electric potential and electric field around an insulator. The use of the response surface methodology and artificial neural network to create a model and a network respectively for the prediction of the flashover voltage.

In the first chapter, a thorough investigation of high voltage insulators at the start of our thesis revealed their enormous significance for the transfer of electrical energy. We explored the various types of insulators that provide both mechanical support and electrical insulation, acting as the separator of the line and ground in power systems. After that, we looked into the difficulties these insulators have, discovering that pollution has a big impact on how well they perform. The reliability and functioning of overhead electrical energy transmission lines could be compromised by these pollution-related disruptions in electrical insulation. In the chapters that follow, we will examine how pollution affects insulator performance and identify creative solutions to these problems.

In the second chapter, the potential and electric field distributions were examined in the 1512L insulator chain's clean and contaminated states in a two and three dimensional simulations. While the electric potential barely varies, the electric field experiences the biggest variations.

Through the two dimensional simulations, it is clear that after two insulators, the electric potential and electric field begin to follow a particular pattern, which makes it easier to predict how they would behave in the presence of uniform pollution. Additionally, it is clear that the presence of pollution in this form only affects the value of the electric potential distribution on the pin side, while the value of the potential on the metal components of the insulator, beginning with the cap of the first one, remains constant. The same cannot be true for the distribution of the electric field because pollution, despite having a uniform shape, causes significant value spikes that cause a number of issues that eventually cause flashover and premature aging.

Through the three dimensional simulations, the electric potential shows the greatest change in the case of the droplet shaped pollution on the pin side only, meaning that both the shape and position of the pollution has an effect on the potential. Although in the other cases studied the

potential shows some changes they are very small. While the potential shows the change in the droplet shaped pollution on the pin side only, the electric field does not. Through all the cases, the electric field value rises a lot especially at the start. Additionally looking at the results at the start of the leakage distance, the highest value of the field is found with the surface shape and the highest value at the end are all found in the case of a surface shape in the different cases.

Comparing the many cases investigated, it can be shown that the electric field exhibits an obvious difference in each situation, whereas the potential exhibits an apparent change only in the case of the droplet shape on the pin side pollution. In contrast to the potential, the electric field exhibits the greatest variations in a totally contaminated insulator when the surface shape is polluted. We may state that this insulator is better positioned in regions with greater precipitation rates, meaning that desert places are a little more damaging to the insulator. This is because the positions where the field spikes are high are potential places where an arc will develop.

Lastly, this simulation method can very well be used for the making of the insulator designs needed and additionally for finding of the insulators working region before setting it up on the towers to get the maximum of the insulator life.

In the third chapter, the response surface methodology was used to study the breakdown voltage of the 1512L insulator. For the purpose of creating a model that links the components, the level of pollution, and its conductivity value, the central composite design technique was used. Two different models were created. The first model was created by following the traditional mathematical way using the central composite design equation. The second model was created using a customized design by choosing a different alpha value. For a total of 9 runs the results were as follows

In the first model, the model was fitted into a first order model and then into a second order model. This was done to get the best desirable results since a second order model should have the best results in terms of prediction and data fitness. For the first order model correlation value (R2 = 91.20%) and a value of (R2 = 95.42%) in the second order model. The predicted R2 was found to be (predicted R2 = 82.39%) for the first order model while the second order model had indicated that the model might be over fit. The standard deviation coefficient were found to be S = 2.42606 and S = 2.47374 for the first and second order models respectively. The models had an adjusted R2 equal to 88.26% and 87.80% for the first and second order model respectively.

While these last two result, look pretty much the same the P-value the second order model indicated a factor was not needed in the model. All These results show that the first order model is better.

In the second model, a second order model was made. The results show a strong correlation value (R2 = 99.88%), the predicted R2 (predicted R2 = 98.53%), and a very low standard deviation coefficient (S = 0.453433) were all found after the model is done demonstrating how well the model fit the data. The verification data revealed that the model was actually very close to the prediction of the insulator's flashover voltage. The model had an adjusted R2 comparable to 99.68%, showing that no irrelevant influences were present with some terms being omitted due to the P-value only.

In the last chapter, two feed forward artificial neural networks were created for the prediction of the 1512L insulator flashover voltage. Both networks make use of the level of pollution and conductivity to predict the voltage. The hidden layer would make use of the sigmoid function while the output layer uses the identity function and the Levenberg-Marquardt backpropagation algorithm is used for the training.

The first network would make use of 9 data points as inputs. The correlation value for the whole network is very low with a value of 0.52629. The error for this model hits as high as 25.57 kV in the validation data set.

For the second network, 45 data points are fed to the network as inputs. The correlation value for the whole network is very high with a value of 0.9937. The error for this model hits as high as 4.409 kV in the test data set.

Even though the network created by the feedforward neural network is great tool for the prediction, it is still a data consuming method. On the other hand, the response surface methodology is a systematic method that make use of too few runs to create a model all the while making at the very least decent models. When working on a model the response surface methodology should be the first to go to method because even when it does not work it is still possible to transfer back to the neural network while the reverse cannot really be said.

Some recommendation that follow this work can be as follows

To ensure that the simulation results are proper, carry out more experimental research. Testing in the real world can improve the suggested models' applicability and dependability.

Extend the study's reach to evaluate the effects of other environmental variables on insulator performance, such as changes in temperature and humidity.

Extend the number of models to other types of insulators used by the Algerian electricity company and apply these models on real world line insulators.

It is advised to create an improved experimental model that carefully takes into account the height variations of insulator sheds in light of the gaps in current models. The inclusion of the sheds' height dimension enhances the model's ability to replicate the effects of external conditions on the flashover performance of the insulator. This improvement will help create a more thorough understanding of how insulators behave in various situations, which will eventually boost prediction accuracy and produce more accurate depictions of real-world situations. This improvement will play a crucial role in improving the accuracy and consistency of experimental models used to evaluate insulator performance and direct future design decisions.

REFERENCES

References

[1] L. Shu, Y. Liu, Q. Hu, G. He, Z. Yu, L. Xiao, “Three-dimensional electric field simulation and flashover path analysis of ice-covered suspension insulators,” High Volt., vol. 5, no. 3, pp. 327–333, Jun. 2020,

[2] X. Qiao, Z. Zhang, X. Jiang, R. Sundararajan, and J. You, “DC pollution flashover performance of HVDC composite insulator under different non-uniform pollution conditions,” Electr. Power Syst. Res., vol. 185, Aug. 2020.

[3] H. Terrab and A. Bayadi, “Experimental study using design of experiment of pollution layer effect on insulator performance taking into account the presence of dry bands,” IEEE Trans. Dielectr. Electr. Insul., vol. 21, no. 6, pp. 2486–2495, 2014.

[4] M. Tahir Khan Niazi, Arshad, J. Ahmad, F. Alqahtani, F. A. B. Baotham, and F. Abu-Amara, “Prediction of critical flashover voltage of high voltage insulators leveraging bootstrap neural network,” Electron., vol. 9, no. 10, pp. 1–21, Oct. 2020.

[5] M. Ghayedi, R. Shariatinasab, and M. Mirzaie, “AC flashover dynamic theoretical and experimental model under fan-shaped and longitudinal pollution on silicone rubber insulator,” IET Sci. Meas. Technol., vol. 15, no. 9, pp. 719–729, Nov. 2021.

[6] A. A. Salem, R. Abd-Rahman, S. A. Al-Gailani, M. S. Kamarudin, H. Ahmad, and Z. Salam, “The Leakage Current Components as a Diagnostic Tool to Estimate Contamination Level on High Voltage Insulators,” IEEE Access, vol. 8, pp. 92514–92528, 2020.

[7] S. Gopal and Y. Narayana Rao, “Flashover Phenomena of Polluted Insulators,” IEE Proc. - Gener. Transm. Distrib., vol. 131, no. 4, pp. 140–143, 1984.

[8] Z. Guan and R. Zhang, “Calculation of DC and AC flashover voltage of polluted insulators,” IEEE Trans. Electr. Insul., vol. 25, no. 4, pp. 723–729, 1990.

[9] M. T. Gençoglu and M. Cebeci, “The pollution flashover on high voltage insulators,” Electr. Power Syst. Res., vol. 78, no. 11, pp. 1914–1921, 2008.

[10] S. Khatoon, A. A. Khan, and S. Singh, “A review of the flashover performance of high voltage insulators constructed with modern insulating materials,” Trans. Electr. Electron. Mater., vol. 18, no. 5, pp. 246–249, 2017.

[11] F. A. M. Rizk and A. Q. Rezazada, “Modeling of altitude effects on AC flashover of polluted high voltage insulators,” IEEE Trans. power Deliv., vol. 12, no. 2, pp. 810–822, 1997.

[12] K. Siderakis, D. Pylarinos, E. Thalassinakis, I. Vitellas, and E. Pyrgioti, “Pollution Maintenance Techniques in Coastal High Voltage Installations,” Eng. Technol. & Appl. Sci. Res., vol. 1, no. 1, pp. 1–7, 2011.

[13] B. Zelalem and M. Mamo, “Assessment of external insulation problems related to pollution and climatic conditions in Ethiopia,” IEEE Electr. Insul. Mag., vol. 36, no. 4, pp. 36–46, 2020.

[14] M. T. Gençoğlu and M. Cebeci, “The pollution flashover on high voltage insulators,” Electr. Power Syst. Res., vol. 78, no. 11, pp. 1914–1921, Nov. 2008.

[15] A. Kara, “Contribution à l’étude d’un modèle dynamique de contournement d’un isolateur pollué,” Mémoire de Magister, SETIF1 (UFAS), Algérie, 2013.

[16] M. Mohamed, “Validation de nouvelles méthodes de modélisation du contournement des isolateurs pollués,” Thèse de doctorat, USTO - MB, Algérie, 2018.

[17] A. A. Salem and R. Abd-Rahman, “A Review of the Dynamic Modelling of Pollution Flashover on High Voltage Outdoor Insulators,” in Journal of Physics: Conference Series, Jul. 2018, vol. 1049, no. 1, 2018.

[18] A. M. Rahal and C. Huraux, “Flashover Mechanism of High Voltage Insulators,” IEEE Trans. Power Appar. Syst., vol. PAS-98, no. 6, pp. 2223–2231, 1979.

[19] D. Dyhia, “Dimensionnement par optimisation d’isolateurs capot et tige pour lignes Haut tension,” Thèse de doctorat, USTHB, Algérie, 2019.

[20] B. Amel, “Etude d’un isolateur à haute tension par l’intelligence artificielle,” Thèse de doctorat, Kasdi Merbah Ouargla, Algérie, 2022.

[21] S. M. A. Dhalaan and M. A. Elhirbawy, “Simulation of voltage distribution calculation methods over a string of suspension insulators,” in 2003 IEEE PES Transmission and Distribution Conference and Exposition (IEEE Cat. No. 03CH37495), 2003, vol. 3, pp. 909–914.

[22] C. Nyamupangedengu, L. P. Luhlanga, and T. Letlape, “Acoustic and HF detection of defects on porcelain pin insulators,” in 2007 IEEE Power Engineering Society Conference and Exposition in Africa-PowerAfrica, 2007, pp. 1–5.

[23] M. W. Adou, H. Xu, and G. Chen, “Insulator faults detection based on deep learning,” in 2019 IEEE 13th International Conference on Anti-counterfeiting, Security, and Identification (ASID), 2019, pp. 173–177.

[24] International standard norme internationale Insulators for overhead lines with a nominal voltage above 1 000 V-Ceramic or glass insulator units for AC systems-Characteristics of insulator units of the cap and pin type. 2021.

[25] O. Lyamine, “Contribution à l’étude et à l’analyse du comportement des isolateurs des lignes de transmission sous contraintes de tension,” Thèse de doctorat, Université Ferhat Abbas, Algérie, 2020.

[26] R. Boudissa, A. Bayadi, and R. Baersch, “Effect of pollution distribution class on

insulators flashover under AC voltage," Electr. Power Syst. Res., vol. 104, pp. 176–182, 2013.

[27] R. Matsuoka, S. Ito, K. Sakanishi, and K. Naito, "Flashover on contaminated insulators with different diameters," IEEE Trans. Electr. Insul., vol. 26, no. 6, pp. 1140–1146, 1991.

[28] L. Maraaba, Z. Alhamouz, and H. Alduwaish, "A neural network-based estimation of the level of contamination on high-voltage porcelain and glass insulators," Electr. Eng., vol. 100, no. 3, pp. 1545–1554, 2018.

[29] R. Boudissa, T. Belhoul, K. D. Haim, and S. Kornhuber, "Effect of inclination angle of hydrophobic silicone insulation covered by water drops on its DC performance," IEEE Trans. Dielectr. Electr. Insul., vol. 24, no. 5, pp. 2890–2900, 2017.

[30] J. L. Goudie, "Silicones for outdoor insulator maintenance," in Conference Record of the the 2002 IEEE International Symposium on Electrical Insulation (Cat. No.02CH37316), 2002, pp. 256–259.

[31] W. Que, S. A. Sebo, and R. J. Hill, "Practical Cases of Electric Field Distribution Along Dry and Clean Nonceramic Insulators of High-Voltage Power Lines," IEEE Trans. Power Deliv., vol. 22, no. 2, pp. 1070–1078, 2007.

[32] B. Zhang, J. He, X. Cui, S. Han, and J. Zou, "Electric field calculation for HV insulators on the head of transmission tower by coupling CSM with BEM," IEEE Trans. Magn., vol. 42, no. 4, pp. 543–546, 2006.

[33] L. Cui and M. Ramesh, "Prediction of flashover voltage using electric field measurement on clean and polluted insulators," Int. J. Electr. Power Energy Syst., vol. 116, Mar. 2020.

[34] S. A. Bessedik and H. Hadi, "Prediction of flashover voltage of insulators using least squares support vector machine with particle swarm optimisation," Electr. Power Syst. Res., vol. 104, pp. 87–92, 2013.

[35] S. F. Stefenon et al., "Classification of insulators using neural network based on computer vision," IET Gener. Transm. Distrib., vol. 16, no. 6, pp. 1096–1107, 2022.

[36] R. S. H. Mah and D. M. Himmelblau, "Role and impact of computers in engineering education," Chem. Eng. Educ., vol. 29, no. 1, pp. 46–49, 1995.

[37] C. Muniraj and S. Chandrasekar, "Finite element modeling for electric field and voltage distribution along the polluted polymeric insulator," World J. Model. Simul., vol. 8, no. 4, pp. 310–320, 2012.

[38] E. Akbari, M. Mirzaie, A. Rahimnejad, and M. B. Asadpoor, "Finite element analysis of disc insulator type and corona ring effect on electric field distribution over 230-kV

insulator strings," Int. J. Eng. Technol., vol. 1, no. 4, pp. 407–419, 2012.

[39] O. Ghermoul, H. Benguesmia, and L. Benyettou, "Electric Potential and Field Distributions Simulation on a Barrier Separating Two Electrodes Under Different Constraints," in 2022 International Conference of Advanced Technology in Electronic and Electrical Engineering (ICATEEE), 2022, pp. 1–5.

[40] O. Ghermoul, H. Benguesmia, and L. Benyettou, "3D Simulation of the Electric Field of Cap and PinInsulatorusingComsolMultiphysics," in 2022 International Conference of Advanced Technology in Electronic and Electrical Engineering (ICATEEE), 2022, pp. 1– 4.

[41] N. M'ziou, H. Benguesmia, and H. Rahali, "Modeling Electric Field and Potential Distribution of an Model of Insulator in Two Dimensions by the Finite Modeling Electric Field and Potential Distribution of an Model of Insulator in Two Dimensions by the Finite Element Method," International Journal of Energetica, vol. 3, no 1, p. 1-5, 2018.

[42] H. Benguesmia, N. M'Ziou, and A. Boubakeur, "Simulation of the potential and electric field distribution on high voltage insulator using the finite element method," Diagnostyka, vol. 19, no. 2, pp. 41–52, 2018.

[43] H. Benguesmia, B. Bakri, S. Khadar, F. Hamrit, and N. M'ziou, "Experimental study of pollution and simulation on insulators using comsol® under AC voltage," Diagnostyka, vol. 20, no. 3, pp. 21–29, 2019.

[44] F. F. Liu, C. Y. W. Ang, and D. Springer, "Optimization of extraction conditions for active components in Hypericum perforatum using response surface methodology," J. Agric. Food Chem., vol. 48, no. 8, pp. 3364–3371, 2000.

[45] E. Donkoh, J. Degenstein, M. Tucker, and Y. Ji, "Optimization of Enzymatic Hydrolysis of Dilute Acid Pretreated Sugar Beet Pulp Using Response Surface Design," J. Sugarbeet Res., vol. 49, no. 1, pp. 26–38, Apr. 2012.

[46] O. Ghermoul, H. Benguesmia, and L. Benyettou, "Development of a Flashover Voltage Prediction Model with the Pollution and Conductivity as Factors Using the Response Surface Methodology," Energies, vol. 15, no. 19, 2022.

[47] D. R. Pinheiro, R. de F. Neves, and S. P. A. Paz, "A sequential Box-Behnken Design (BBD) and Response Surface Methodology (RSM) to optimize SAPO-34 synthesis from kaolin waste," Microporous Mesoporous Mater., vol. 323, p. 111250, 2021.

[48] S. Bhattacharya, "Central composite design for response surface methodology and its application in pharmacy," in Response surface methodology in engineering science, IntechOpen, 2021.

[49] M. Demirel and B. Kayan, “Application of response surface methodology and central composite design for the optimization of textile dye degradation by wet air oxidation,” Int. J. Ind. Chem., vol. 3, no. 1, pp. 1–10, Dec. 2012.

[50] Y. Lecun, Y. Bengio, and G. Hinton, “Deep learning,” Nature, vol. 521, no. 7553, pp. 436–444, 2015.

[51] A. Krizhevsky, I. Sutskever, and G. E. Hinton, “ImageNet Classification with Deep Convolutional Neural Networks,” in Proceedings of the 25th International Conference on Neural Information Processing Systems - Volume 1, 2012, pp. 1097–1105.

[52] K. He, X. Zhang, S. Ren, and J. Sun, “Deep Residual Learning for Image Recognition,” in 2016 IEEE Conference on Computer Vision and Pattern Recognition (CVPR), 2016, pp. 770–778.

[53] D. Silver, A. Huang, C.Maddison, et al., “Mastering the game of Go with deep neural networks and tree search,” Nature, vol. 529, no. 7587, pp. 484–489, 2016, doi: 10.1038/nature16961.

[54] A. Esteva, B. Kuprel, R. Novoa, et al. “Dermatologist-level classification of skin cancer with deep neural networks.,” Nature, vol. 542, no. 7639, pp. 115–118, Feb. 2017.

[55] J. Huang, J. Chai, and S. Cho, “Deep learning in finance and banking: A literature review and classification,” Front. Bus. Res. China, vol. 14, no. 1, p. 13, 2020.

[56] O. Fink, Q. Wang, M. Svensén, P. Dersin, W.-J. Lee, and M. Ducoffe, “Potential, challenges and future directions for deep learning in prognostics and health management applications,” Eng. Appl. Artif. Intell., vol. 92, p. 103678, 2020.

[57] W. S. McCulloch and W. Pitts, “A logical calculus of the ideas immanent in nervous activity,” Bull. Math. Biophys., vol. 5, no. 4, pp. 115–133, 1943.

[58] G. E. Hinton, S. Osindero, and Y.-W. Teh, “A fast learning algorithm for deep belief nets.,” Neural Comput., vol. 18, no. 7, pp. 1527–1554, Jul. 2006.

[59] W. Wu, G. C. Dandy, and H. R. Maier, “Protocol for developing ANN models and its application to the assessment of the quality of the ANN model development process in drinking water quality modelling,” Environ. Model. Softw., vol. 54, pp. 108–127, 2014.

[60] J. Neto, L. Almeida, M. Hochberg, Ciro Martins, Luís Nunes, S. Renals, T. Robinson, “Speaker-adaptation for hybrid HMM-ANN continuous speech recognition system,” 1995.

[61] D. W. Massaro, J. Beskow, M. M. Cohen, C. L. Fry, and T. Rodgriguez, “Picture my voice: Audio to visual speech synthesis using artificial neural networks,” in AVSP’99-International Conference on Auditory-Visual Speech Processing, 1999.

[62] H. E. Kocer and K. K. Cevik, “Artificial neural networks based vehicle license plate

recognition," Procedia Comput. Sci., vol. 3, pp. 1033–1037, 2011.

[63] N. A. Spielberg, M. Brown, N. R. Kapania, J. C. Kegelman, and J. C. Gerdes, "Neural network vehicle models for high-performance automated driving," Sci. Robot., vol. 4, no. 28, p. eaaw1975, 2019.

[64] Y. Liu and M. Zhang, "Neural network methods for natural language processing." MIT Press One Rogers Street, Cambridge, MA 02142-1209, USA journals-info~…, 2018.

[65] S. Agatonovic-Kustrin and R. Beresford, "Basic concepts of artificial neural network (ANN) modeling and its application in pharmaceutical research," J. Pharm. Biomed. Anal., vol. 22, no. 5, pp. 717–727, 2000.

[66] Fukuchi, Tomohide, Ikechukwu, Mark Ogbodo, and Ben Abdallah, Abderazek, "Design and Optimization of a Deep Neural Network Architecture for Traffic Light Detection," SHS Web Conf., vol. 77, p. 1002, 2020.

[67] S. Sharma, S. Sharma, and A. Athaiya, "Activation functions in neural networks," Towar. Data Sci, vol. 6, no. 12, pp. 310–316, 2017.

[68] A. Wanto, A. P. Windarto, D. Hartama, and I. Parlina, "Use of binary sigmoid function and linear identity in artificial neural networks for forecasting population density," IJISTECH (International J. Inf. Syst. Technol., vol. 1, no. 1, pp. 43–54, 2017.

[69] S. A. Balaji and K. Baskaran, "Design and development of artificial neural networking (ANN) system using sigmoid activation function to predict annual rice production in Tamilnadu," arXiv Prepr. arXiv1303.1913, 2013.

[70] M. Rezaeian Zadeh, S. Amin, D. Khalili, and V. P. Singh, "Daily outflow prediction by multi layer perceptron with logistic sigmoid and tangent sigmoid activation functions," Water Resour. Manag., vol. 24, pp. 2673–2688, 2010.

[71] A. D. Rasamoelina, F. Adjailia, and P. Sinčák, "A review of activation function for artificial neural network," in 2020 IEEE 18th World Symposium on Applied Machine Intelligence and Informatics (SAMI), 2020, pp. 281–286.

[72] C. Bircano\uglu and N. Ar\ica, "A comparison of activation functions in artificial neural networks," in 2018 26th signal processing and communications applications conference (SIU), 2018, pp. 1–4.

[73] H. U. Dike, Y. Zhou, K. K. Deveerasetty, and Q. Wu, "Unsupervised learning based on artificial neural network: A review," in 2018 IEEE International Conference on Cyborg and Bionic Systems (CBS), 2018, pp. 322–327.

[74] D. K. Chaturvedi, "Artificial neural network and supervised learning," Soft Comput. Tech. its Appl. Electr. Eng., pp. 23–50, 2008.

[75] J. Corchado, C. Fyfe, and B. Lees, "Unsupervised learning for financial forecasting," in

Proceedings of the IEEE/ IAFE/ INFORMS 1998 Conference on Computational Intelligence for Financial Engineering (CIFEr) (Cat. No. 98TH8367), 1998, pp. 259–263.

[76] M. M. Noel and B. J. Pandian, "Control of a nonlinear liquid level system using a new artificial neural network based reinforcement learning approach," Appl. Soft Comput., vol. 23, pp. 444–451, 2014.

[77] J. Qi, J. Du, S. M. Siniscalchi, X. Ma, and C.-H. Lee, "Analyzing upper bounds on mean absolute errors for deep neural network-based vector-to-vector regression," IEEE Trans. Signal Process., vol. 68, pp. 3411–3422, 2020.

[78] X. Chen, R. Yu, S. Ullah, D. Wu, Z. Li, Q. Li, H. Qi, J. Liu , M. Liu, Y. Zhang, "A novel loss function of deep learning in wind speed forecasting," Energy, vol. 238, p. 121808, 2022.

[79] K Hu, Z. Zhang, X. Niu, Y. Zhang, C. Cao, F. Xiao, X. Gao, "Retinal vessel segmentation of color fundus images using multiscale convolutional neural network with an improved cross-entropy loss function," Neurocomputing, vol. 309, pp. 179–191, 2018.

[80] J. R. Dwaram and R. K. Madapuri, "Crop yield forecasting by long short-term memory network with Adam optimizer and Huber loss function in Andhra Pradesh, India," Concurr. Comput. Pract. Exp., vol. 34, no. 27, p. e7310, 2022.

[81] M. Ekman, Learning Deep Learning: Theory and Practice of Neural Networks, Computer Vision, Natural Language Processing, and Transformers Using TensorFlow. Addison- Wesley Professional, 2021.

[82] Y. Goldberg, Neural network methods for natural language processing. Springer Nature, 2022.

[83] J. M. Cohen, S. Kaur, Y. Li, J. Z. Kolter, and A. Talwalkar, "Gradient descent on neural networks typically occurs at the edge of stability," arXiv Prepr. arXiv2103.00065, 2021.

[84] H. P. Gavin, "The Levenberg-Marquardt algorithm for nonlinear least squares curve-fitting problems," Dep. Civ. Environ. Eng. Duke Univ., vol. 19, 2019.

[85] H. Yu and B. M. Wilamowski, "Levenberg--marquardt training," in Intelligent systems, CRC Press, 2018, pp. 11–12.

[86] I. V Tetko, D. J. Livingstone, and A. I. Luik, "Neural network studies. 1. Comparison of overfitting and overtraining," J. Chem. Inf. Comput. Sci., vol. 35, no. 5, pp. 826–833, 1995.

[87] L. Jin, X. Kuang, H. Huang, Z. Qin, and Y. Wang, "Study on the overfitting of the artificial neural network forecasting model," ACTA Meteorol. Sin. Ed., vol. 19, no. 2,

p. 216, 2005.

[88] S. Gupta, R. Gupta, M. Ojha, and K. P. Singh, “A comparative analysis of various regularization techniques to solve overfitting problem in artificial neural network,” in Data Science and Analytics: 4th International Conference on Recent Developments in Science, Engineering and Technology, REDSET 2017, Gurgaon, India, October 13-14, 2017, Revised Selected Papers 4, 2018, pp. 363–371.

[89] I. Nusrat and S.-B. Jang, “A comparison of regularization techniques in deep neural networks,” Symmetry (Basel)., vol. 10, no. 11, p. 648, 2018.

[90] K. Hirasawa, M. Ohbayashi, M. Koga, and M. Harada, “Forward propagation universal learning network,” in Proceedings of international conference on neural networks (ICNN’96), 1996, vol. 1, pp. 353–358.

[91] X. Zhou, W. Zhang, Z. Chen, S. Diao, and T. Zhang, “Efficient neural network training via forward and backward propagation sparsification,” Adv. Neural Inf. Process. Syst., vol. 34, pp. 15216–15229, 2021.

[92] S. Sapna, A. Tamilarasi, M. P. Kumar, and others, “Backpropagation learning algorithm based on Levenberg Marquardt Algorithm,” Comp Sci Inf. Technol (CS IT), vol. 2, pp. 393–398, 2012.

[93] I. Goodfellow, Y. Bengio, and A. Courville, Deep learning. MIT press, 2016.

[94] C. C. Aggarwal and others, “Neural networks and deep learning,” Springer, vol. 10, no. 978, p. 3, 2018.

[95] J. Nowak, A. Taspinar, and R. Scherer, “LSTM Recurrent Neural Networks for Short Text and Sentiment Classification BT - Artificial Intelligence and Soft Computing,” 2017, pp. 553–562.

[96] L. Zhang, S. Wang, and B. Liu, “Deep learning for sentiment analysis: A survey,” Wiley Interdiscip. Rev. Data Min. Knowl. Discov., vol. 8, no. 4, p. e1253, 2018.

[97] J. Chung, C. Gulcehre, K. Cho, and Y. Bengio, “Empirical evaluation of gated recurrent neural networks on sequence modeling,” arXiv Prepr. arXiv1412.3555, 2014.

[98] P. Huang, H. Wang, and W. Ma, “Stochastic Ranking for Offline Data-Driven Evolutionary Optimization Using Radial Basis Function Networks with Multiple Kernels,” in 2019 IEEE Symposium Series on Computational Intelligence (SSCI), 2019, pp. 2050–2057.